The IgCAM CAR regulates calcium homeostasis in the developing heart

Inaugural Dissertation to obtain the academic degree
Doctor rerum naturalium (Dr. rer. nat.)

Submitted to the Department of Biology, Chemistry and Pharmacy
of Freie Universität Berlin

Christina Claudia Matthäus

November 30, 2015

This thesis was prepared between February 2012 and September 2015 at the Max-Delbrueck-Center for Molecular Medicine at the Department of Developmental Neurobiology under the supervision of Prof. Dr. Fritz G. Rathjen.

1. Reviewer: Prof. Dr. Fritz G. Rathjen, Department of Developmental Neurobiology, Max-Delbrueck-Center for Molecular Medicine

2. Reviewer: Prof. Dr. Michael Gotthardt, Department of Neuromuscular and Cardiovascular Cell Biology, Max-Delbrueck-Center for Molecular Medicine

Disputation: 26.11.2015

Contents

List of Figures

Abbreviations

µm	micrometer
µM	micromolar
ACSF	artificial cerebrospinal fluid
AKT	Protein kinase B (PKB)
APS	ammonium persulphate
AV	atrioventricular
bp	base pairs
BSA	bovine serum albumin
CAM	cell adhesion molecule
CAR	coxsackievirus and adenovirus
cDNA	complementary desoxyribonucleic acid
CHAPS	3-[(3-cholamidopropyl)dimethylammonio]-1-propanesulfonate
Cx	Connexin
Da	Dalton
DAPI	4-6-diamidino-2-phenylindole
DIV	days in vitro
DMEM	Dulbeccos modified Eagles medium
DMSO	Dimethyl sulfoxide
DNA	Desoxyribonucleic acid
E10.5	Embryonic day 10.5
EDTA	Ethylendiaminetetraacetic acid
EGTA	Ethylene glycol tetraacetic acid
FCS	fetal calf serum
fig	figure
GAPDH	Glyceraldehyde 3-phosphate dehydrogenase
GSK3β	Glycogen synthase kinase 3 beta
h	hour(s)
HCN	hyperpolarization-activated cyclic nucleotide- gated cation channel
HRP	Horseradish peroxidase
hz	heterozygous

Ig	immuno globulin
ICC	Immunocytochemistry
IP3	Inositol trisphosphate
IP3R	Inositol trisphosphate receptor
kb	kilo base
KO	knock out
m	milli
M	molar
mCU	mitochondrial calcium uniporter
min	minutes
mRNA	messenger RNA
n	nano
NCX	Sodium calcium exchanger
n.s.	not significant
NTP	nucleoside triphosphate
PBS	phosphate-buffered saline
PCR	Polimerase chain reaction
PFA	Paraformaldehyde
PI3K	Phosphatidylinositol-4,5-bisphosphat 3-kinase
PKC	protein kinase C
PLB	Phospholamban
PLC	Phospholipase C
PMCA	Plasma membrane Ca^{2+} ATPase
RNA	ribonucleic acid
ROI	Region of interest
RyR	Ryanodine receptor
SDS	Sodium dodecyl sulfate
SEM	Standard error of the mean
SERCA	Sarcoplasmic/endoplasmic reticulum calcium ATPase
SR	sarcoplasmic reticulum
TAE	Tris base, acetic acid and EDTA
TBS	Tris-buffered saline
TBS-T	Tris-buffered saline with Tween-20
TEMED	Tetramethylethylenediamine
wt	wild type
ZO-1	zona occuldens 1

1 Introduction

1.1 Heart development

The heart is a highly specialised organ which consists of many different cell types: atrial and ventricular cardiomyocytes, endocardial cells, valvular components, connective tissue, as well as smooth muscle and endothelial cells of arteries and veins (Brade et al., 2013). Therefore correct development of the cardiac cell types and the heart is required to maintain the constant pumping and circulation of blood. During embryonic development the heart is the first functional organ which is formed whereby this process can be dived into distinct phases: specification of cardiac progenitors, formation of the linear heart tube, cardiac looping, chamber formation, septation and maturation (Gessert & Kühl, 2010).

Initially, the cells which later form the heart have a mesodermal origin and express the transcription factor *Eomes* that induce cardiac development (Chaudhry et al., 2014). *Eomes* induces expression of *Mesp1*, a transcription factor which itself triggers the expression of the specific cardiac genes *Nkx2.5* and *Gata5*. These two genes are required for the specification and migration of the cardiac precursor cells during gastrulation (Chaudhry et al., 2014; Freire et al., 2014). Gastrulation forms the three embryonic germ layers endoderm, mesoderm and ectoderm in mouse around embryonic day (E) 6.5 (Freire et al., 2014). At around E7 - E7.5 the progenitor cells of the heart migrate through the primitive streak and form the cardiac crescent or first heart field (Gessert & Kühl, 2010). At more advanced stages these cells will form the left ventricle. The elongation and expansion of the early heart tube is caused by a second progenitor cell type found outside the early heart in mesoderm which is called second heart field (Rochais et al., 2009). During development, cells derived from second heart field will form the outflow tract, the right ventricle and the atria (Cai et al., 2003).

Progenitor cells from the first and second heart field can be distinguished by several gene expression patterns. The transcription factor *Isl1* is exclusively expressed in cells of the second heart field (Prall et al., 2007; Kelly, 2012) whereas the first heart field cells strongly express *Tbx5* (Gessert & Kühl, 2010; Rochais et al., 2009). Due to the more anterior and lateral localisation of the first heart field these cells are exposed to different bone morphogenetic proteins (BMPs), fibroblast growth factors (FGFs) and inhibitors of Wnt signalling which results in the initial

cardiac differentiation marked by the expression of *Nkx2.5* and *Tbx5* (Brade et al., 2013). Further cardiac differentiation is indicated by induced expression of contractile proteins like myosin light chain-2a (MLC2a) and sarcomeric myosin heavy chain (MHC) through the linear heart tube (Kubalak et al., 1994). *Isl1* expression in the second heart field cells is required for correct proliferation and migration into the primitive linear heart tube (formed by the first heart field). The second heart field is also characterised by prolonged proliferation and differentiation delay due to active Wnt/β-catenin signalling (Rochais et al., 2009). Specific expression of *Isl1* and *Nkx2.5* generates later both myocytic and vascular cells (Kattman et al., 2006; Moretti et al., 2006). Inside the primitive heart tube, second heart field cells are located at the poles of the heart (Chaudhry et al., 2014).

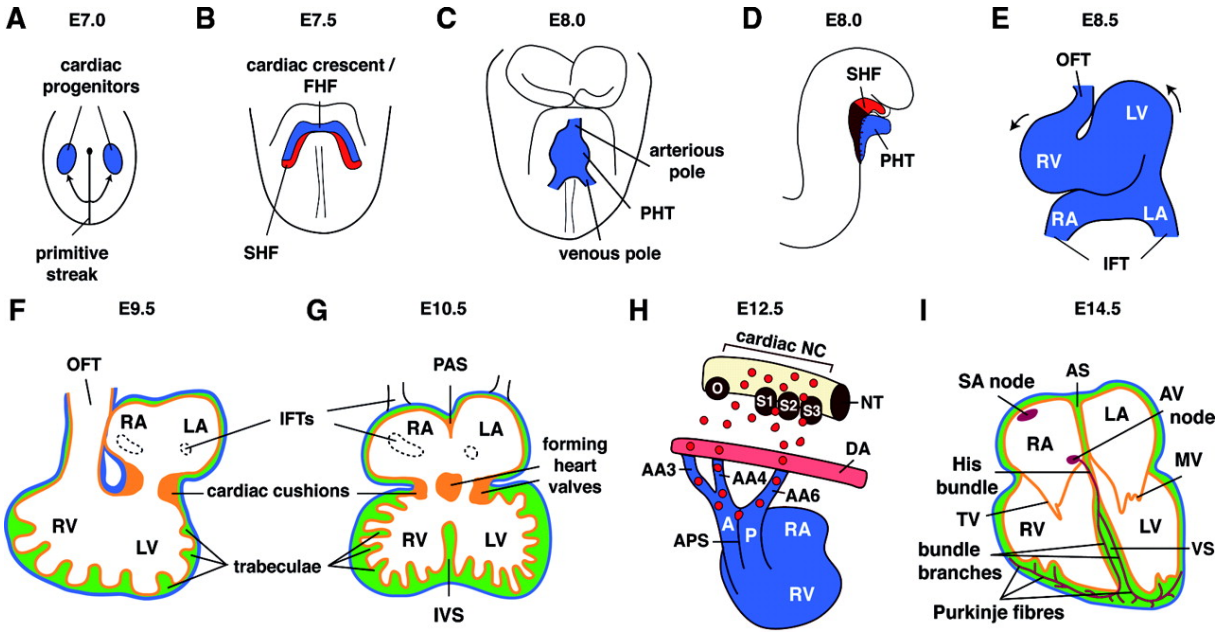

Figure 1.1: The embryonic development of the heart. The schematic overview of the embryonic heart development includes the first cardiac progenitors which migrate over the primitive streak to form the first heart field (A), the second heart field formation (B), the growth of the first linear heart tube (C, D) and followed by the looping of the linear heart tube (E). Afterwards, epicard (blue), myocard (green) and cardic jelly (organge) arise and the chamber formation starts (F, G). The cardiac neural crest originates at the dorsal neural tube and migrate toward the outflow tract (H). At last the cardiac pacemaking and conduction system is formed at E14.5 (I). A, aorta; AA, aortic arch arteries; AS, atrial septum; APS, aorticopulmanory septum; FHF, first heart field; IFT, inflow tract; IVS, interventricular septum; LA, left atrium; LV, left ventricle; MV, mitral valve; NC, neural crest; NT, neural tube; O, otic vesicle; OFT, outflow tract; P, pulmonary trunk; PAS, primary atrial septum; PHT, primary heart tube; RA, right atrium; RV, right ventricle; S, somite; SA, sinuatrial; SHF, second heart field; TV, tricuspid valve; VS, ventricular septum. Image taken from Gessert & Kühl, 2010.

Looping of the heart occurs after elongation of the primitive heart tube due to increased number of cells and proliferation (Moorman et al., 2003). During cardiac looping the different sections of the heart are placed in the right orientation to the developing vessels to promote optimal topographical connection (Harvey, 1998). The period of cardiac looping can be divided into

three phases: the dextral-looping, formation of the early s-looping and late s-looping. During the dextral looping the primary heart tube is converted into a c-shaped loop and the basic left-right asymmetry of the heart is established. In the second phase the c-loop is transformed to a s-shaped loop and the arterial-venous pole distance shortens. During late s-looping the outflow tract is moved leftwards and the early atrial and ventricular parts increase in size (Harvey, 1998; Männer, 2009; Taber, 2006).

Cardiac septation promotes the chamber formation by division of the lumen and the arterial trunks into pulmonary and systematic flow pathways (Männer, 2009). The atrial chamber is divided by a primary septum which then fuses with the atrioventricular cushions. The septation of the ventricle is undertaken from ventricular cardiomyocytes which form the ventricular septum (Anderson et al., 2003; Moorman et al., 2003; Moorman & Christoffels, 2003). Further, the endocardial cushions are formed through epithelial cells of the endocardium (localized between the atrial and the ventricle chambers) which migrate between endocardium and myocardium and proliferate there to the cushions (Gessert & Kühl, 2010). During later development the cardiac cushions form the valves and membranous septa of the heart (Risebro & Riley, 2006).

The correct septation of the outflow tract into the pulmonary trunk and the aorta is mainly performed by cardiac neural crest cells (Gessert & Kühl, 2010). These non-cardiac precursor cells are arised from the dorsal neural tube between the otic vesicle and the third somite and further migrate through the pharyngeal arches 3, 4 and 6 along the aortic arteries to the heart (Brade et al., 2013; Gessert & Kühl, 2010). After reaching the outflow cushions the septation of the outflow tract occurs between the neural crest cell area and the dorsal wall of the aortic sac (Chaudhry et al., 2014; van den Hoff et al., 1999). Most of the neural crest cells die by apoptosis after septation and are removed by cardiomyocytes of the outflow tract which then form the two muscular tubes of the outflow tract (Poelmann et al., 1998).

The establishment of the correct working conduction system in the newly formed four chambered heart is the last major step to complete the development of the heart. Therefore at first *Isl1*-positive progenitor cells differentiate to cardiac pacemaking cells in the early right atrium. These cells later form the sinoatrial node, the atrioventricular node (AV node) and the atrioventricular bundle in which the cardiac beating originates and then is transmitted through the whole heart (Chaudhry et al., 2014; Gessert & Kühl, 2010). Thereby different cardiac transcription factors regulate the specific expression of ion channels inside the pacemaking cells: *Tbx5, Tbx3, Nkx2.5* induce the expression of connexin 30.2 and 40 and the hyperpolarization-activated cation channels (HCN) inside the AV node. Increased conduction in the AV bundles is caused by expression of Hcn4, connexin 40 and 43 and sodium channel Nav1.5 (Boukens & Christoffels, 2012; Christoffels et al., 2010).

1.2 The excitation-contraction coupling in the heart

Cardiac excitation-contraction coupling is the interaction of electrical excitation of cardiomyocytes and the corresponding contraction of the heart (Bers, 2002). In the adult heart the electrical impulse is generated in the sinus node by pacemaker cells and then transmitted through the atria to the atrioventricular node (AV node). After transmission of the electrical pulse via the AV bundles, its branches and via the Purkinje fibers to the ventricles the working myocyardium is excited and contraction of the heart occurs (Boukens & Christoffels, 2012; Nerbonne & Kass, 2005). Inside the cardiomyocytes Ca^{2+} plays a major role for contraction: during every single heart beat cytosolic Ca^{2+} increases, binds to troponin C to induce contraction of the myofilaments and afterwards intracellular Ca^{2+} decreases to allow relaxation (summarized in fig. 1.2).

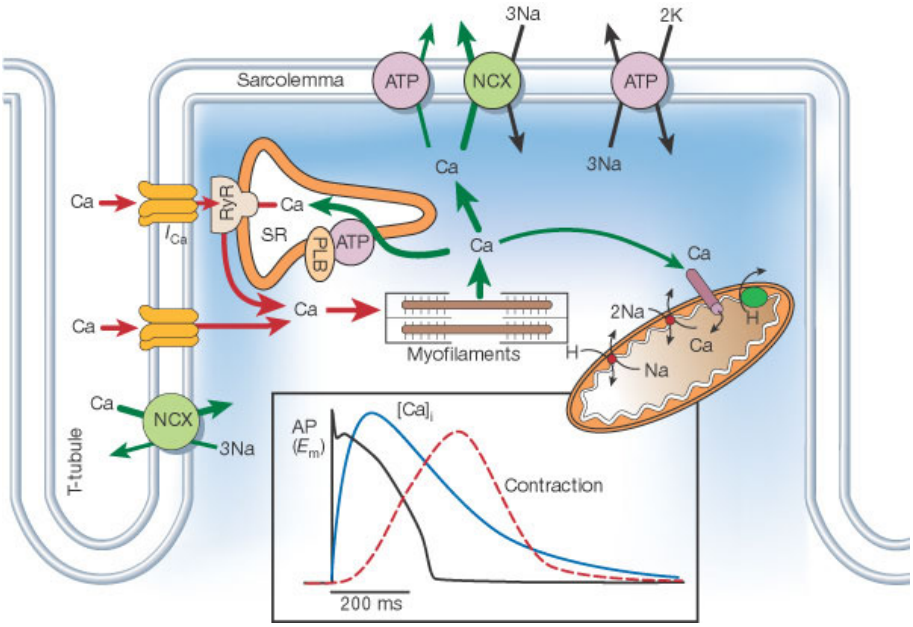

Figure 1.2: The cardiac excitation-contraction coupling. After depolarization of the cardiomyocyte plasma membrane voltage-gated Ca^{2+} channels open and the corresponding Ca^{2+} influx triggers Ca^{2+} release from the sarcoplasmic reticulum (SR). Therefore the intracellular Ca^{2+} increases and Ca^{2+} binds to troponin C which is released from myosin. Afterwards the myosin heads are able to bind to the actin filament and contraction arise. Relaxation occurs after Ca^{2+} decline whereby the SR Ca^{2+} ATPase (SERCA), sodium calcium exchanger (NCX), plasma membrane Ca^{2+} ATPase (PMCA) and mitochondria are involved. Image taken from Bers, 2002.

1.2.1 The role of calcium

Ca^{2+} is an important second messenger in various cellular processes like cell proliferation, apoptosis, metabolism or vesicle trafficking (Berridge et al., 2000, 2003; Clapham, 2007; Evenas et al., 1998). During cardiac excitation-contraction coupling Ca^{2+} undergoes a fast cycling

process. To increase cytosolic Ca^{2+} concentration a fast influx of extracellular Ca^{2+} and the release of Ca^{2+} from the sarcoplasmic reticulum (SR) must occur (Bers, 2002; Clapham, 2007). Comparison of the action potential time course and cytosolic Ca^{2+} cycling reveals that at first the cardiomyocyte membrane becomes depolarized (fig. 1.2). A large, rapid Na^+ current depolarizes the cell (from the steady state membrane potential -70 mV to +30 mV) very fast which consequently increases the intracellular Na^+ concentration from 4 mM to 16 mM for 5-10 ms (Aronsen et al., 2013; Keurs, 2011). Therefore the sodium calcium exchanger (NCX) is activated in its reverse mode and Ca^{2+} entry occurs (Bers & Perez-Reyes, 1999; Keurs, 2011). Further, the depolarization opens the voltage-gated Ca^{2+} channels and Ca^{2+} influx increases cytosolic Ca^{2+} concentration (Bers & Perez-Reyes, 1999; Mesirca et al., 2015; Nerbonne & Kass, 2005). In cardiac cells different types of Ca^{2+} channels were found: the T-type channel is activated very fast at lower voltage (around -50 mV). L-, N-, P- and Q-type Ca^{2+} channels are high voltage-activated channels (activation at membrane potential of -20 mV) and inactivate much slower. However, in the heart the L- and T-type Ca^{2+} channels are ubiquitously expressed and can be found already in early embryonic stages (Bers & Perez-Reyes, 1999; Mesirca et al., 2015; Nerbonne & Kass, 2005). Inactivation of voltage-gated Ca^{2+} channels occurs either by Ca^{2+}/calmodulin binding to the channels or voltage-dependent conformational changes (Tadross et al., 2010).

The fast initialization of the action potential due to inward Na^+ current is followed by a partial repolarization caused by a rapid outward K^+ current (Snyders, 1999). The cardiac cell repolarizes (to 0 mV) resulting in action potential plateau phase and therefore K^+ currents control duration and height of the action potential (Barry & Nerbonne, 1996). In the heart various K^+ channels are expressed and a wide range of different K^+ currents were recorded whereby a change in expression and current recordings is found during development as well as in the particular cell types of the heart (atria, ventricle, pacemaker cells). However, two basic types of voltage-gated K^+ currents can be distinguished: the 4-aminopyridine sensitive, rapidly activating and inactivating transient outward current and the slowly activating and inactivating delayed outward current (Barry & Nerbonne, 1996). Due to the different kinetic and voltage dependent properties specific K^+ currents contribute to either the early, rapid phase of repolarization or the later phases and ending of the action potential (Barry & Nerbonne, 1996; Keurs, 2011; Nerbonne & Kass, 2005). Beside theses depolarization activated K^+ currents also non-voltage-gated inward K^+ currents occur which only play a minor role during normal physiological conditions (Nerbonne & Kass, 2005).

The via voltage-gated Ca^{2+} channels entered Ca^{2+} ions bind to the ryanodine receptors (RyR) localized in the membrane of the SR which in turn triggers the release of Ca^{2+} stored inside the SR (ca. 40 µM Ca^{2+}). Consequently, free cytosolic Ca^{2+} increases from 0.1 to 1 µM and then binds to troponin C (Bers, 2002; Poláková et al., 2008). However, the intensity of Ca^{2+} induced SR Ca^{2+} release depends on the amount of voltage-gated Ca^{2+} channels and the duration of the

channel opening (Poláková et al., 2008). Further the steric arrangement of cardiac cell membrane with its Ca^{2+} channels and the SR and the RyR plays a critical role (Keurs, 2011; Renken et al., 2009). This well described process is also called Ca^{2+} induced Ca^{2+} release (CICR) whereby the only minor and locally restricted cytosolic Ca^{2+} increase due to inward Ca^{2+} currents is strongly magnified through the release of Ca^{2+} from the SR via the RyR (Bers & Perez-Reyes, 1999; Pfeiffer et al., 2014). This increase in Ca^{2+} in the cytosol is followed by cardiomyocyte contraction.

Troponin C contains two high affinity and one low affinity Ca^{2+} binding sites whereby at the high affinity sites Ca^{2+} is always bound (Holroydes et al., 1980; Kobayashi & Solaro, 2005). However, during cardiac beating the increased amount of Ca^{2+} binds to the low affinity site and induces a conformational change which allows the binding of the myosin heads to actin filaments (Gordon et al., 2000). After ATP hydrolysis a conformational change in the myosin heads is induced and contraction occurs. Relaxation of the cardiac muscle is obtained after the cytosolic Ca^{2+} concentration declines. SR Ca^{2+} ATPase (SERCA), sodium calcium exchanger (NCX), plasmamembrane Ca^{2+} ATPase (PMCA) and mitochondria participate in the extrusion of intracellular free Ca^{2+}. The reduction of intracellular Ca^{2+} then decreases the sensitivity for Ca^{2+} binding to troponin C which leads to dissociation of the Ca^{2+}-troponin C complex (Bers, 2002; Janssen, 2010; Keurs, 2011).

The excitation-contraction coupling allows the intact heart to convert electrical excitation of cardiomyocytes to contraction force. One major important property of the heart is the capability to adjust the contractile strength and therefore the force to external stress like exercise or pathologic changes. To increase the contraction output the heart can regulate the frequency and force of contraction. This positive force-frequency relationship is caused by raised Ca^{2+} transients which lead to increased intracellular Ca^{2+} level and higher Ca^{2+} transient amplitudes (Endoh, 2004; Gwathmey et al., 1990; Janssen, 2010). Upon induced Ca^{2+} binding to troponin C, the number of contraction competent proteins increases and therefore more force is generated (Janssen, 2010). Due to the higher frequency rate also the relaxation must occur faster. Therefore Ca^{2+} decline is faster at higher pacing rates (Keurs, 2011). Further, diastolic Ca^{2+} concentration is increased whereby the duration of Ca^{2+} decline is shorter. Also the Ca^{2+} sensitivity is decreased in the myofilament during higher beating frequency which also allows faster relaxation (Janssen, 2010; Varian & Janssen, 2007). The contraction is also regulated by the length of the cardiac fibers whereby the myofilaments become more sensitive to Ca^{2+} when sarcomere length raises due to an increase in actin/myosin/troponin cross bridges (Farman et al., 2010; Mamidi et al., 2014).

1.2.2 The sarcoplasmic reticulum

The sarcoplasmic reticulum (SR) is an internal membrane system in cardiomyocytes and striated muscle cells which differs in composition and function with the endoplasmic reticulum (ER) that is found in all cell types (Doroudgar & Glembotski, 2013; Michalak & Opas, 2009). Crucial function of the SR is the regulation and control of Ca^{2+} cycling and therefore the SR is involved in the excitation-contraction coupling of the heart (Michalak & Opas, 2009). The SR is the main intracellular Ca^{2+} store and is able to retain up to 90 % of the cytosolic, cycling Ca^{2+} (Bers, 2002; Rossi & Dirksen, 2006). The SR membrane contains specific Ca^{2+} handling proteins enabling the transfer of free Ca^{2+} from the cytosol to the inside of the SR, to store and to release Ca^{2+}. Inside the cardiomyocytes the SR surrounds the myofilaments whereby two parts of SR can be distinguished (Glembotski, 2012). The junctional SR is located near the t-tubules and the voltage-gated ion channels of the myocytes. The longitudinal SR consists of numerous tubules which connect with each other and join in the terminal cisternae or junctional SR (Bers & Shannon, 2013; Rossi et al., 2008). Both regions can be further distinguished by expression of specific proteins and its functions whereby the longitudinal SR contains SERCA and its regulatory protein phospholamban (PLB) for fast re-uptake of cytosolic Ca^{2+} (Michalak & Opas, 2009; Rossi et al., 2008). The Ca^{2+} release mechanism including ryanodine receptors (RyR) and inositol 1,4,5-trisphosphate (IP3) receptors (IP3Rs) are expressed in the junctional SR. Further, the most important Ca^{2+} buffer and storage protein - calsequestrin - is expressed in the terminal SR. Calsequestrin gets polymerized by increasing Ca^{2+} binding and is anchored to the SR membrane through junctins, triadin and RyR (Beard et al., 2009; Rossi & Dirksen, 2006). Beside these Ca^{2+} handling proteins also other proteins like sarcolumenin, histidine-rich protein and junctate are found in the membrane of the SR to support Ca^{2+} buffering and Ca^{2+} transport inside the SR (Rossi & Dirksen, 2006; Michalak & Opas, 2009).

Ca^{2+} release from the SR is critical for proper generation of cardiomyocyte contraction and is mainly performed by ryanodine receptors (RyR). Three different genes encode the isoforms RyR1-3 whereby RyR2 is mainly expressed in cardiac cells (Lanner et al., 2001; Takeshima et al., 1989; Zorzato et al., 1990). RyR are the largest ion channels up to date identified with a molecular mass around 2.2 MDa due to formation of a homotetrameric structure (Van Petegem, 2015). Often neighbouring RyR form regular arrays, a so called checkerboard pattern, in which single RyR influence each other mechanically due to allosteric movements or chemical via Ca^{2+} release (Van Petegem, 2012). The RyR2 Ca^{2+} release complex consists of four subunits which form the membrane spanning channel. The receptor is anchored in the SR membrane whereby 80% of the complex is inside the cytoplasm (Berridge et al., 2003). This mushroom-like complex contains many cavities and micro-structures in which various small molecules, solvents or protein modulators can bind or interact (Lanner et al., 2001). Besides Ca^{2+} also caffeine, ATP, calmodulin or S100A1 can induce RyR opening. Sorcin, ryanodine, Mg^{2+} or dantrolene decrease RyR activity (Van Petegem, 2015). In the SR lumen calsequestrin is co-localized via junctin

and triadin which binds directly to RyR2 (Beard et al., 2009). Calsequestrin regulates the Ca^{2+} sensitivity of the receptor complex. At low SR Ca^{2+} concentrations calsequestrin binds to junctin and triadin and therefore inhibits RyR activity to prevent complete depletion of SR. High SR Ca^{2+} concentration induces dissociation of calsequestrin from triadin resulting in RyR activity increase (Györke et al., 2009; Wei et al., 2009). However, RyR open probability is also highly regulated by free Ca^{2+} in the SR lumen whereby decrease of Ca^{2+} to 1 mM forces the termination of Ca^{2+} release to the cytoplasm (Györke et al., 2009; Terentyev et al., 2002). Further, RyR2 can be phosphorylated by cAMP-dependent protein kinase (PKA), cGMP-dependent protein kinase (PKG) or Ca^{2+}/calmodulin-dependent protein kinase II (CamKII) whereby the kinases are anchored through an A-kinase anchoring protein (AKAP) (Berridge et al., 2003). CamKII phosphorylates Ser-2808 and Ser-2814 in RyR2 and can induce RyR open probability. PKA phosphorylation at Ser2030 and Ser-2808 is often discussed with regard to Ca^{2+} leak of the RyR and heart failure (Van Petegem, 2012).

The SR Ca^{2+} leak summarizes spontaneous short term Ca^{2+} sparks which are localized near the SR membrane and often mediated by only a few RyR (Bers, 2014). This leakage of Ca^{2+} from SR to the cytoplasm appears during diastole and therefore is not induced through spontaneous excitation. Detection of these spontaneous Ca^{2+} events can be done by confocal microscopy and line scan analysis as well as application of tetracaine which completely abolishes the leakage (Bers, 2014; Shannon, 2002). However, locally restricted Ca^{2+} sparks can be amplified in cardiomyocytes due to Ca^{2+} induced Ca^{2+} release resulting in increase of unregulated spontaneous contraction (burst). Several studies in heart failure and atrial fibrillation suggest that due to increased SR Ca^{2+} leak the generation of action potentials and contraction of the heart is disturbed. Further, hyperphosphorylation of RyR2 by either CamKII or PKA was proposed to cause an induction of Ca^{2+} leakage (Bers, 2014; Fischer et al., 2013; Neef et al., 2010; Voigt et al., 2012).

The inositol 1,4,5-trisphosphate (IP3) receptor (IP3R) is widely expressed in many tissues including neurons, glia cells, cardiomyocytes, hepatocytes and pancreatic cells and is located in the membrane of ER and SR (Berridge, 2009). The receptor consists of 2700 amino acid residues and has a molecular mass of 300 kDa (Bosanac et al., 2004). It can be regulated by cytosolic Ca^{2+}, ATP, PKA and CamKII (Vervloessem et al., 2014). Activation of the membrane anchored phospholipase C (PLC) by various receptor stimuli (via G protein kinase receptors) results in IP3 generation that consequently diffuse to ER/SR and bind to its receptor (Foskett et al., 2007). Binding of IP3 to its receptor triggers a Ca^{2+} release to induce several signaling pathways (Berridge, 2009; Vervloessem et al., 2014). In the heart, the isoform IP3R2 is mainly expressed already at early embryonic development stages (Lipp et al., 2000; Rapila et al., 2008; Vervloessem et al., 2014). IP3R activation induces Ca^{2+} release and therefore can also increase the RyR open probability resulting in an increased Ca^{2+} transient (Ju et al., 2012; Lipp et al., 2000). However, IP3 only has a minor, more modulatory role in excitation-contraction coupling in adult cardiomyocytes (Bers, 2002). In contrast, during embryogenesis IP3R1/2 are required

for correct heart development and further induced IP3 concentration triggers spontaneous rate of Ca^{2+} transients (Rapila et al., 2008; Vervloessem et al., 2014).

1.2.3 Calcium extrusion mechanism

Relaxation of the heart and its cardiomyocytes only can occur if the high cytosolic Ca^{2+} concentration caused by systolic Ca^{2+} transients is removed. The Ca^{2+} extrusion process must be realised very fast because normal heart beat generation only can appear by correct Ca^{2+} cycling (Bers, 2002). There are existing several Ca^{2+} extrusion mechanism in the cardiomyocytes (fig. 1.3). The most important Ca^{2+} removal protein is the ATP dependent active transporter SR Ca^{2+} ATPase (SERCA) which eliminates up to 90% of systolic Ca^{2+} (90% in rat and mouse, 70% in human and rabbit). Further, the sodium calcium exchanger (NCX) removes higher amounts of free Ca^{2+} from the cytosol outside the cardiomyocytes (ca. 5-9%). Slow Ca^{2+} extrusion processes includes plasmamembrane Ca^{2+} ATPase (PMCA) and mitochondria whereby both only remove approx. 1% of systolic Ca^{2+} (Bassani et al., 1994; Bers, 2002; Clapham, 2007; Gaffin, 1999).

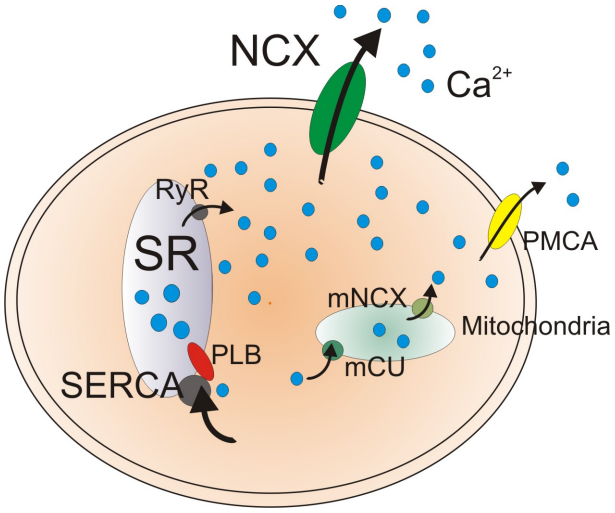

Figure 1.3: The cardiac Ca^{2+} extrusion mechanism. Increased systolic Ca^{2+} must be removed very fast to ensure constant Ca^{2+} cycling. Therefore the three Ca^{2+} extrusion proteins SERCA, NCX and PMCA and the mitochondria are responsible. The bulk of cytosolic Ca^{2+} is removed by SERCA back to the SR. Also NCX transfers higher amounts of Ca^{2+} outside the cardiomyocyte. PMCA and mitochondria only play a minor role for Ca^{2+} extrusion. PLB, phospholamban; mNCX, mitochondrial NCX; mCU, mitochondrial calcium uniporter.

The velocity of Ca^{2+} removal determines the beating frequency of cardiomyocytes. Fast Ca^{2+} extrusion by SERCA allows rapid refill of the SR with Ca^{2+} which consequently induce the open probability of RyR. Further, also L-type voltage gated Ca^{2+} channels are highly Ca^{2+} sensitive and high concentrations of cytosolic Ca^{2+} inhibit the inward Ca^{2+} current which is needed for proper generation of contraction in the cardiomyocytes. Therefore quick Ca^{2+} extrusions

regulates the recovery of the cell to trigger the next excitation-coupling cycle (Bers, 2002). In the following, the mentioned Ca^{2+} extrusion proteins and its functions (fig. 1.3) will be described in more detail.

As the major intracellular Ca^{2+} store, the SR must be refilled after every single contraction cycle. Due to the high Ca^{2+} gradient across the membrane of the SR (cytosolic Ca^{2+} 100 - 600 nM vs. 15 - 76 µM Ca^{2+} in SR) SERCA is needed for active Ca^{2+} transport from the cytosol into the SR against this high Ca^{2+} concentration gradient (Frank et al., 2003; Trafford et al., 1999). There are three homologous genes (SERCA1-3) which forms several alternative splicing variants whereby each isoform is expressed in specific tissues or at specific developmental stages. SERCA1 is only found in skeletal muscle, SERCA2a is the main isoform in cardiac tissue (also SERCA2c), SERCA2b expression is predominant in non-muscular and neuronal cells and SERCA3 is restricted to epithel and endothelial cells (Frank et al., 2003; Kranias & Hajjar, 2012; Periasamy et al., 2008). Already at very early embryonic development stages (from E9) SERCA2a is expressed in the early heart tube (Moorman et al., 1995). The activity of the Ca^{2+} transport by SERCA2 can be influenced by several factors including phospholamban (PLB) and CamKII (Frank & Kranias, 2000). Phospholamban is the major inhibitory regulator of SERCA2. This 52 amino acid containing protein (6 kDa) is localized in the SR membrane and its amino acid sequence is highly conserved across species (Simmerman & Jones, 1998). PLB expression is first detected around E9 during heart development and uniquely in cardiac tissue and to less extend in smooth muscle cells (Moorman et al., 1995; Simmerman & Jones, 1998). The regulation of SERCA2 by PLB results from binding of PLB to SERCA2 at low cytosolic Ca^{2+} concentrations (100 nM). In this inhibitory state the transmembrane domains of PLB and SERCA2 closely interact with each other and the affinity for Ca^{2+} is reduced (Periasamy et al., 2008). However, systolic Ca^{2+} increase allows Ca^{2+} binding to SERCA2 which forces a conformational change inside the SERCA2 molecule that triggers the dissociation of PLB. The PLB monomers associate to a pentamer inside the SR membrane (MacLennan & Kranias, 2003). The inhibitory effect of PLB also can be diminished by phosphorylation of specific phosphorylation sites: Ser-16 is phosphorylated by PKA, Thr-17 by CamKII and Ser-10 by PKC (Frank et al., 2003; Kranias & Hajjar, 2012). This indicates that PLB is a major regulator for cardiac beating. Upon $\beta-$adrenergic stimulation cAMP is generated which activates PKA and further phosphorylates PLB (Kranias & Hajjar, 2012). Moreover, PLB overexpressing cardiomyocytes revealed significant smaller Ca^{2+} transient amplitudes, reduced beating frequency and slower Ca^{2+} transport from cytosol into the SR (Brittsan, 2000; Kadambi et al., 1996). However, ablation of PLB induces cytosolic Ca^{2+} transport via SERCA2 due to increased Ca^{2+} affinity of SERCA2. Consequently, Ca^{2+} extrusion is faster and an increase in cardiomyocyte shortening was observed (Luo et al., 1994; Wolska et al., 1996). These data clearly indicate that the SERCA2/PLB protein interplay highly regulates contractility in the heart.

Besides SERCA2 also the sodium calcium exchanger (NCX) is able to reduce cytoslic Ca^{2+} whereby in contrast to SERCA the NCX carries Ca^{2+} to the extracellular side of the cell and to a less extent (Aronsen et al., 2013). The sodium calcium exchanger family (SLC8) contains three different genes NCX1-3 whereas NCX1 is widely expressed in many tissues and already found in the embryonic heart, NCX2 and NCX3 were only detected in brain and skeletal muscles (Quednau et al., 2004; Reed et al., 2002; Reppel et al., 2007c,a). This 108 kDa transmembrane protein is a uniporter system which extrudes 1 Ca^{2+} ion and simultaneously 3 Na^{+} ions are transfered into the cell resulting in a noticeable Na^{+} inward current (Blaustein & Lederer, 1999; Hilgemann, 2004; Lytton, 2007). NCX1 is highly regulated by the Ca^{2+} concentration gradient and extracellular Na^{+} concentrations and contains several Ca^{2+} binding sites at the cytoplasmic domain (Blaustein & Lederer, 1999). Therefore, NCX1 also can work in the reverse mode in which Ca^{2+} influx and Na^{+} efflux occur. However the working mode always depends on the concentration gradient of Ca^{2+} and Na^{+} across the cell membrane and the membrane potential (Ottolia et al., 2013). Overexpressing NCX1 mouse models further revealed the strong influence on cardiac Ca^{2+} extrusion as shown for caffeine induced Ca^{2+} transients that significantly decline faster compared to recordings on wt cardiomyocytes (Adachi-Akahane et al., 1997; Reuter et al., 2004; Yao et al., 1998). In contrast, in cardiac NCX1 knockout mouse models a prolonged Ca^{2+} decline and a reduced inward Ca^{2+} current was observed which however did not dramatically change heart rate (Pott et al., 2005; Henderson et al., 2004; Reuter, 2002).

The plasma-membrane Ca^{2+} ATPase (PMCA) is also located in the cell membrane and transfers cytosolic Ca^{2+} across the membrane by using ATP whereby the influence on systolic Ca^{2+} decline is only minor (<1%). Four PMCA genes encode several isoforms which differ at the C-terminus and show tissue and developmental specific expression. However, in the heart mainly PMCA1 and PMCA4 in different splice variants are detected (Oceandy et al., 2007; Strehler et al., 2008). PMCA contains 10 transmembrane domains and the cytoplasmic domains include a calmodulin binding site and consensus sites for PKA and PKC (Brini & Carafoli, 2011). The effect of PMCA on cardiac outcome is marginal which was further supported by Hammes et al. (1998). Cardiac overexpression of PMCA4 revealed no significant improve in systolic Ca^{2+} decline. Further heart rate and membrane potential was not changed (Hammes et al., 1998). However, PMCA is suggested to be involved in cellular signalling of nNOS (neuronal nitric oxide synthase), calcineurin and Ras (Oceandy et al., 2007).

In addition, mitochondria are also able to store Ca^{2+} in form of calcium phosphate to recover the cytosolic Ca^{2+} concentration. However, their primary function is the extensive generation of ATP to ensure the energy demand during beating (Gustafsson & Gottlieb, 2008). Ca^{2+} can enter mitochondria through various channels like the mitochondrial Ca^{2+} uniporter (mCU), rapid mode of Ca^{2+} uptake channel (RAM) or the mitochondrial RyR (mRyR). The mCU is the extensively studied and most important Ca^{2+} uptake channel and is driven by a large electrochemical gradient across the mitochondrial membrane (Dedkova & Blatter, 2013; Pan et al., 2013). Predominant

Ca^{2+} efflux channel is the mitochondrial NCX (mNCX) by transfering for 1 Ca^{2+} from the mitochondrial matrix to the cytosol 3 Na^{+} across the mitochondrial membrane (Duchen, 2000; Gustafsson & Gottlieb, 2008). Up to date the exact mechanism of Ca^{2+} entry/buffer/efflux in mitochondria is not well understood. Two different conflicting models describe mitochondrial Ca^{2+} signalling in cardiac cells: model I comprises a slow, long term Ca^{2+} uptake in which Ca^{2+} phosphate accumulates inside the mitochondria. In contrast, model II suggest a rapid beat-to-beat Ca^{2+} signalling which conforms to the cytosolic Ca^{2+} cycling during cardiac beating (Dedkova & Blatter, 2013; Robert et al., 2001).

1.2.4 The excitation-contraction coupling in the developing heart

During embryonic development the heart is the first organ which is formed. Already at early embryonic stages (between E8.5 - E10.5) the heart is able to beat continuously. The mechanism behind these spontaneous beats still is not clear. Several studies investigated that spontaneous membrane depolarizations triggers Ca^{2+} influx via voltage-gated Ca^{2+} channels which induce contraction. Further, it was shown that spontaneous Ca^{2+} sparks from the SR cause cardiomyocyte contraction. Also, the *funny current* via HCN channels was suggested to induce beating in early embryonic cardiomyocytes. In fact, all proposed mechanisms feature possible explanations and below the reported results will be discussed.

During heart development the expression of ion channels as well as components of the pacemaking machinery are changing until the final excitation-contraction system is fully established (Harrell et al., 2007). There is an upregulation of repolarizing K^{+} current channels like Kir2.1 or Kir3.1. Also different Na^{+} and Ca^{2+} channels are upregulted after birth, whereby NCX is downregulated in adult stages (Harrell et al., 2007; Liu et al., 2002). These data indicate that the spontaneous Ca^{2+} transients which are observed in cultivated embryonic cardiomyocytes are created unlike in the adult heart. Spontaneous Ca^{2+} transients and therefore also contractions were already recorded at E8.5 (Liang et al., 2010). Further, primitive and mature-like action potentials were observed and expression of different Ca^{2+} channels (Ca1.2, Ca3.2), the HCN channel and NCX1 were already detected suggesting a higher impact of ion channels on these very early heart beats. Blocking of either L-type Ca^{2+} channels, T-type Ca^{2+} channels or NCX induce the halt of action potentials and contraction (Liang et al., 2010). Also Liu et al. (2002) showed in E9.5 cardiomyocytes that blocking of L-type Ca^{2+} channels by nisoldipine completely abolished any Ca^{2+} transients. Surprisingly, inhibition of RyR and SERCA did not alter the spontaneous Ca^{2+} transients. Also blocking of NCX did not result in a loss of beating (Liu et al., 2002). Furthermore, application of verapamil, a very effective L-type Ca^{2+} channel blocker, to spontaneously beating embryonic bodies caused a stop of beating (Reppel et al., 2007b). In addition, Takeshima et al. (1998) generated a mouse model lacking RyR2 which leads to embryonic death at E10 due to malformations of the heart. However, analysing the RyR2 knock out myocytes at E9.5

revealed spontaneous beating and Ca^{2+} transients. Further, wild type E9.5 cardiomyocytes were treated with ryanodine to completely block RyR and recorded Ca^{2+} transients did not show any difference (Takeshima et al., 1998).

Besides Ca^{2+} channels and NCX also the hyperpolarization-activated cation channels (HCN) and its corresponding *funny current* were suggested to induce early embryonic beating. The HCN channels are activated by hyperpolarization of the cell membrane (ca. -50 to -60 mV) and transfer Na^{+} or K^{+} (Biel et al., 2009; DiFrancesco, 2010). In the adult heart, HCN1, 2 and 4 are expressed whereby HCN2 is the predominant form (Herrmann et al., 2011). In contrast to many other voltage-gated cation channels, HCN activity can be modulated by cAMP whereas at high cAMP concentration cAMP binds to the HCN channels and therefore the channels open faster and at more positive membrane potentials (Biel et al., 2009). The HCN current also is called pacemaker current because of its responsibility for spontaneous depolarization in sinoatrial node (pacemaker cells) which then triggers contraction of the heart (Baruscotti et al., 2010; Biel et al., 2002). Already in E9.5 cardiomyocytes expression of HCN4 as predominant form is revealed and a corresponding HCN current could be recorded in spontaneous beating myocytes (Stieber et al., 2003; Liang et al., 2010; Yasui et al., 2001). Surprisingly, in later stages of embryonic development (E18) the HCN current decreased caused by decreasing mRNA expression of HCN1,2 and 4 which is consistent with the loss of spontaneous beating in derived cardiomyocytes (Yasui et al., 2001). These data suggest a high influence of HCN current in spontaneous beating of cardiomyocytes. Further, HCN4 knockout cardiomyocytes die at E11.5 and no mature pacemaker action potentials could be recorded. However, HCN4 lacking cardiomyocytes still beat but slower compared to wild type (Stieber et al., 2003). Also spontaneous beating embryoid bodies treated with HCN blocker ZD7288 reduced their beating frequency but no complete lack of contraction was observed (Qu et al., 2008). Further, E10 cardiomyocytes treated with ZD7288 did not show a strong decrease in spontaneous beating frequency (Rapila et al., 2008; Wang et al., 2013). Taken these data together, during early embryonic excitation-contraction coupling and spontaneous cardiomyocyte activity the HCN current only plays a minor role whereby in later development and adult stages the HCN current is required for proper generation of cardiac action potential.

In contrast to the outlined above data, several studies suggest that spontaneous contraction of early embryonic cardiomyocytes is caused by intracellular Ca^{2+} events. Blocking of voltage-gated Ca^{2+} channels by nisoldipine or inhibition of NCX by Ni^{2+} in embryonic stem cell-derived cardiomyocytes (similar to E11) did not influence beating frequency. Instead, blocking of SERCA by thapsigargin lead to complete loss of beating (Viatchenko-Karpinski et al., 1999). Further, 2D confocal Ca^{2+} imaging revealed small localized Ca^{2+} sparks in E10 cardiomyocytes which were inhibited by blocking RyR and IP3R or SERCA. These spontaneous Ca^{2+} events activate NCX followed by depolarization of the cell membrane (Sasse et al., 2007). Also spontaneous Ca^{2+} sparks were observed around the nucleus (Janowski et al., 2006) or the SR in embryonic cardiomyocytes (Korhonen et al., 2010). Already E10 cardiomyocytes have established the

IP3R-RyR induction mechanism whereby IP3 binds to IP3R and triggers small, localized Ca^{2+} sparks which consequently induce a strong Ca^{2+} release via RyR (Rapila et al., 2008).

The regulation and initiation of the embryonic heart beat and corresponding spontaneous activity of embryonic cardiomyocytes remains controversial. Both mechanism, spontaneous activation of Ca^{2+} channels or spontaneous intracellular Ca^{2+} events, were investigated and opposite results were obtained. However, there are already some studies in which both mechanism coexist. Fu et al. (2006) used mouse embryonic stem cells during cardiac differentiation and analysed the influence of L-type Ca^{2+} channels. Blocking L-type Ca^{2+} channels resulted in complete lack of spontaneous beating in later differentiation. Further, inhibition of RyR, IP3R and SERCA also abolished Ca^{2+} transients which suggest that spontaneous beating already at these stages is dependent on sarcolemmal Ca^{2+} channels and SR Ca^{2+} release (Fu et al., 2006). Rapila et al. (2008) also observed a complete lack of beating after inhibition of SERCA, RyR, IP3R or L-type Ca^{2+} channel. Surprisingly, the Ca^{2+} content stored in the SR is also significant decreased after blocking L-type Ca^{2+} channels which suggest that for proper function of spontaneous SR Ca^{2+} release and beating of the cardiomyocytes voltage-gated Ca^{2+} influx is required. This decrease in SR Ca^{2+} concentration is caused by NCX which permanently extrude cytosolic Ca^{2+}. Blocking L-type Ca^{2+} channels and NCX simultaneously rescued the fast stop of beating which indicates that the spontaneous SR Ca^{2+} oscillations can continue independently for a certain period of time (Rapila et al., 2008; Korhonen et al., 2008). However, the cardiomyocytes did not beat after longer inhibition of L-type Ca^{2+} channels and NCX. Comparison of E10 and E12 rat cardiomyocytes revealed that blocking the RyR by ryanodine resulted in different changes of spontaneous Ca^{2+} cycling: E10 cardiomyocytes showed less inhibition in intensity of Ca^{2+} transients compared to E12 myocytes (Seki et al., 2003). Taken this result and the above detailed described experiments together it could be concluded that in very early embryonic cardiomyocytes (E8.5 - E10) sarcolemmal Ca^{2+} influx via voltage-gated Ca^{2+} channels is required for spontaneous Ca^{2+} transients and beating because the SR Ca^{2+} release machinery is not fully developed. In later embryonic stages (from E11/E12) the SR is completely developed and the interplay between Ca^{2+} influx and Ca^{2+} induced Ca^{2+} release from the SR is established which results in proper generation of mature action potentials, Ca^{2+} transients and beating.

1.3 The cell adhesion protein CAR and its function in heart development and beating

The cell adhesion protein coxsackievirus and adenovirus receptor (CAR) was first identified independently by Bergelson et al. (1997) and Tomko et al. (1997) as a receptor for several coxsackieviruses and adenoviruses. However, further studies revealed important physiological functions during embryonic development of the heart and in disease. Below the properties of CAR as cell adhesion protein and its function in heart development and excitation-contraction coupling will be discussed.

1.3.1 The protein structure of CAR and its subgroup of IgCAMs

The CAR gene is located on the murine chromosome 16 and is composed of 8 exons. Human CAR gene localisation was identified at the chromosome 21 (21q11.2) and also includes 8 exons (Bergelson et al., 1997; Bowles et al., 1999; Chen et al., 2003; Excoffon et al., 2010). Two splice variants of murine CAR were detected in which the cytoplasmic domain is altered (Chen et al., 2003). Further sequencing analysis revealed three additional splice variants of the human CAR mRNA differing in exon numbers (Thoelen et al., 2001a). Exon 1 encodes the signal peptide (19 amino acids), exon 2 and 3 the D1 domain, exon 4 and 5 the D2 domain, the transmembrane region is encoded by the first part of exon 6 and the rest of exon 6 and 7 or 8 constitute the cytoplasmic tail (Bowles et al., 1999; Chen et al., 2003; Thoelen et al., 2001a). Full length human CAR protein consists of 365 amino acids resulting in a molecular mass of 40 kDa, the murine CAR protein is composed of 352 amino acids and a mass of 39 kDa (Tomko et al., 1997). CAR homologous were also found in rats, pigs, dogs, chick and zebrafish and revealed a highly conserved amino acid sequence with up to 95% identity within the cytoplasmic domain between mouse and human CAR (Coyne & Bergelson, 2005; Fechner et al., 1999; Patzke et al., 2010; Petrella et al., 2002; Thoelen et al., 2001b). The extracellular domain can be divided into two immunoglobulin (Ig) domains which are connected via a short transmembrane domain with the cytoplasmic tail (compare fig. 1.4 A). The V-like Ig domain (also called D1) contains a disulfide bond between amino acid 35 and 130 (Tomko et al., 1997). Further it was shown that virus binding and CAR-CAR dimer formation (fig. 1.4 B) is mediated by only the D1 domain whereas the binding of the adenovirus fiber knob and CAR-CAR binding includes the same residues (Howitt et al., 2003; Law & Davidson, 2005; van Raaij et al., 2000). The binding affinity of the fiber knob to CAR is 1000-fold higher compared to homodimer formation probably to ensure correct attachment of the virus for proper cell entry (Kirby et al., 2000; van Raaij et al., 2000). For coxsackievirus B3 binding also the D1 domain is required, however compared to adenovirus binding different amino acid residues are involved (He et al., 2001). The second C2-like Ig domaine (D2) mainly is not necessary for correct virus binding or homodimer formation but

promotes the overall organisation of CAR (Carson, 2001; van Raaij et al., 2000). Nevertheless, in polarized airway epithel cells the complete extracellular domain (including D1 and D2) was required for efficient adenovirus binding and infection (Excoffon et al., 2005). Both Ig domains are connected through a short junction amino acid sequence (fig. 1.4 A).

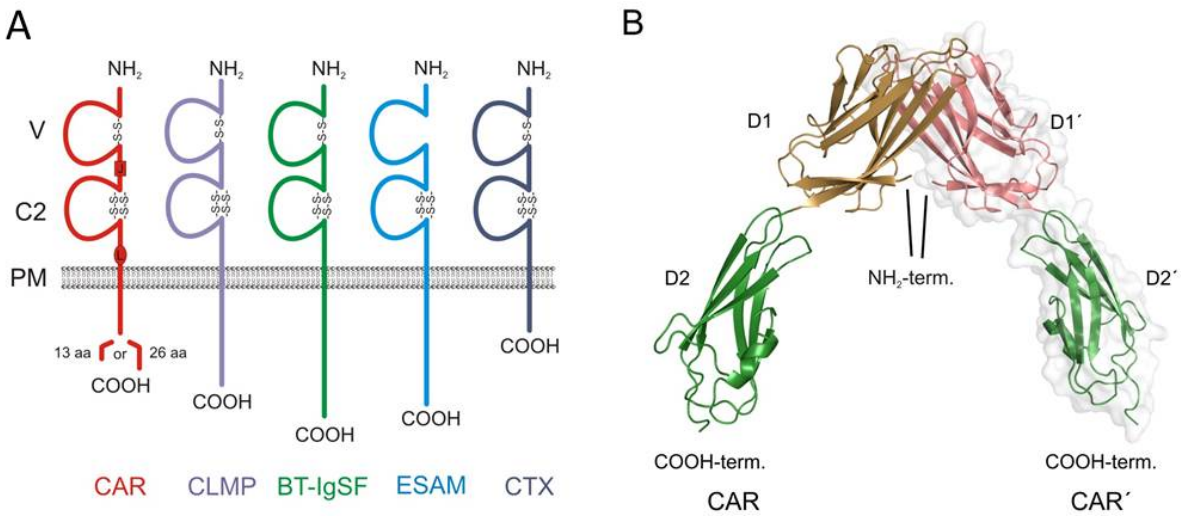

Figure 1.4: The CAR subgroup. Besides CAR further proteins are included into the CAR subgroup: CAR-like membrane protein (CLMP), brain- and testis-specific immunoglobulin superfamily (BT-IgSF), endothelial cell-selective adhesion molecule (ESAM) and marker for cortical thymocytes of Xenopus (CTX). All proteins consist of two extracellular Ig domains (loops, V and C2) linked by a short junction (J), a transmembrane region connected through a linker sequence (L, only found in CAR) and a short cytoplasmic tail (A). Homophilic interaction of two extracellular CAR domains is mediated by dimer formation of D1 (B). PM, plasma membrane. Figure taken from Matthäus et al. (2014).

Furthermore interaction between D1 and D2 domains of neighbouring CAR molecules were described (Patzke et al., 2010). Heterophilic binding of CAR with several extracellular matrix proteins like fibronectin, agrin or tenascin-R as well as other cell adhesion proteins like the junctional adhesion molecule (JAM-L and JAM-C) has been identified (Mirza et al., 2006; Patzke et al., 2010; Verdino et al., 2010; Witherden et al., 2010). The cytoplasmic tail of CAR includes a class 1 PDZ (PSD-95/Disc-large/ZO-1) binding motif which is involved in protein association. Deletion of the PDZ required amino acid residues resulted in altered cell adhesion and cell growth in airway epithelia cells suggesting CAR interaction with different intracellular signalling molecules (Excoffon et al., 2004). Several partners were identified that bind to the PDZ class I binding motif of human or murine CAR including the tight junction protein ZO-1 (Zona occludens 1), MUPP-1 (Multi-PDZ domain protein-1), MAGI-1b (Membrane associated guanylate kinase, WW and PDZ domain containing 1b), PICK-1 (Protein interacting with C kinase 1), the synaptic scaffolding protein PSD-95 (postsynaptic density protein 95) and LNX (Ligand-of-Numb protein-X) and LNX2 (Cohen et al., 2001; Coyne et al., 2004; Kolawole et al., 2012; Mirza et al., 2005; Raschperger et al., 2006; Sollerbrant et al., 2003). In growth cone particles CAR seems to interact with actin to influence organisation of the cytoskeleton in

cell growth and migration (Huang et al., 2007). Further, CAR is able to mediate localisation of E-cadherin and may serve to stabilize cell-cell adhesion in human epithelial cells (Morton et al., 2013). These results indicate CAR as a cell adhesion molecule that is involved in cell-cell interactions, cell growth and migration.

CAR forms its own subgroup inside the family of the immunoglobulins. Besides CAR also CAR-like membrane protein (CLMP), brain- and testis-specific immunoglobulin superfamily (BT-IgSF), endothelial cell-selective adhesion molecule (ESAM) and marker for cortical thymocytes of Xenopus (CTX) are included to the subgroup (fig. 1.4 A). All proteins share the same overall structure of a transmembrane protein I consisting of two Ig domains, a transmembrane region and a cytoplasmic tail (Matthäus et al., 2014). Further, all proteins are localised at cell-cell contacts and are found in various tissues (Raschperger et al., 2004).

1.3.2 Expression and localization of CAR in the heart

CAR is widely expressed in many tissues and organs like brain, retina, liver, heart and lung (Coyne & Bergelson, 2005; Patzke et al., 2010; Raschperger et al., 2006; Tomko et al., 1997, 2000). In more detail, CAR is predominantly expressed in epithel cells where it is found in tight junctions colocalised with ZO-1 and occludin (Cohen et al., 2001; Raschperger et al., 2006). Endothel cells lack expression of CAR (Raschperger et al., 2006). Interestingly, CAR expression is highly regulated during development. In embryonic stages, CAR can be detected mainly in brain tissue and the heart. Shortly after birth, CAR expression significantly decreases throughout the whole body (Coyne & Bergelson, 2005; Dorner et al., 2005; Honda et al., 2000; Hotta et al., 2003; Matthäus et al., 2014).

In the developing mouse heart, CAR RNA is first detected around E7 and immunostainings revealed strong expression of CAR in the myocardium (Asher et al., 2005; Dorner et al., 2005). Closer investigations showed strong expression of CAR in the cell membrane of embryonic and newborn cardiomyocytes near the contact sites to neighbouring cells (Kashimura et al., 2004; Poller et al., 2002). In the mature heart, CAR expression is significant reduced compared to embryonic hearts. However, in adult cardiac muscle only in the intercalated discs CAR is strongly expressed (Lim et al., 2008; Poller et al., 2002; Shaw et al., 2004). Further, it was shown that CAR colocalised with connexin 43 (Cx43), Cx45 and ZO-1 (Kashimura et al., 2004; Lim et al., 2008; Lisewski et al., 2008).

As receptor for several coxsackieviruses, CAR can cause virus-induced myocarditis whereby CAR initiates strong immune response after virus binding and furthermore, CAR expression increases during myocarditis (Ito et al., 2000; Yuen et al., 2011). It was shown that cardiac specific overexpression of CAR results in cardiac inflammation via the inflammatory mitogen-

activated protein kinase (MAPK) pathway (Yuen et al., 2011). Furthermore, after myocardial infarction CAR expression is also increased locally in the cardiomyocytes of the infarct zone (Fechner, 2003). Surprisingly, CAR gets also re-expressed in hearts of patients suffering from dilated cardiomyopathy (DCM) (Bowles et al., 2002; Kaur et al., 2012; Noutsias et al., 2001; Toivonen et al., 2010). The authors showed increased CAR staining in heart sections as well as increased CAR protein in the DCM hearts. However, no mechanism was suggested why CAR gets re-expressed in DCM. Therefore a cardiac specific CAR overexpression mouse model was generated in which shortly after birth the mice develop a severe cardiomyopathy (Caruso et al., 2010). Further, the authors found in CAR overexpressing hearts induced nuclear translocalisation of β-catenin suggesting a stimulation of β-catenin by CAR. Up to date, the exact molecular mechanism of CAR re-expression in heart failure is unknown but these data suggest a similar expression profile as already shown for many cardiac transcription factors or signaling molecules. Cardiac stress or disease can induce the embryonic gene program in which CAR is included (Freire et al., 2014; Rajabi et al., 2007).

1.3.3 CAR is essential for embryonic heart development

Several CAR knock out (KO) mouse models were generated to closer study the physiological role of CAR during development. All global CAR KO mouse models, independently which CAR exon (1 or 2) was deleted, share the same strong phenotype: CAR KO embryos die around E11.5 - E12.5 (Asher et al., 2005; Chen et al., 2006; Dorner et al., 2005). Comparison of the three models revealed that all CAR KO embryos at E11 - E11.5 suffer from strong hemorrhage around the heart. Therefore it was suggested that malformations of the heart trigger the embryonic death. Further investigations of CAR KO hearts indicated an engorgement of cardinal veins and increased thickness of the left ventricular wall (Chen et al., 2006). Asher et al. (2005) also reported an increase in the ventricle and atrium wall as well as extensive lesions in the ventricle wall suggesting blood outflow. Similar observations were determined by Dorner et al. (2005): CAR KO embryos showed enlarged pericards and a decreased ventricle lumen indicating an increase in the ventricle wall which is seen in the published figure of the CAR KO embryo paraffin section (fig. 5B, Dorner et al., 2005). Further the authors found enlarged endocardial cushions and only a single atrioventricular canal compared to normally two canals in wt embryos. The increase of ventricle wall was identified by Chen et al. (2006) as increase in cardiomyocyte numbers. CAR KO hearts showed an increase in expression of the proliferation marker Ki67. However, proliferation assays with BrdU incorporation did not indicate an increase in proliferation in CAR KO hearts (Dorner et al., 2005). The different observations on proliferation could be caused by the varying embryonic development time points when the proliferation assays were performed. Dorner et al. (2005) applied BrdU at E11.5 which is shortly before death of the CAR KO embryos and therefore probably no induced proliferation was observed anymore. Chen et al. (2006) analysed Ki67 expression in CAR KO hearts at E10.5 promoting induced proliferation.

Also Asher et al. (2005) analysed the increase in thickness of the ventricle walls by haematoxylin and eosin staining. In the displayed sections an increased cardiomyocyte cell number can be noticed as found in the study of Chen et al. (2006). However, they also showed an increase in apoptosis that was not observed by either Dorner et al. (2005) or Chen et al. (2006).

Beside the described malformations, lesions and increase in cardiomyocyte cell number the authors also reported highly disorganised myofibrils in cultivated CAR KO cardiomyocytes (Dorner et al., 2005), thinner myofibers in electron microscopic images of CAR KO embryos compared to CAR wt as well as altered and reduced intercellular junctions between neighbouring cardiomyocytes (Chen et al., 2006). Further, Chen et al. (2006) showed that cardiac-specific CAR KO at later development stages (from E11) resulted in normal heart development and CAR KO mice survived until adulthood suggesting that CAR expression is mainly needed during very early heart development when looping of the heart and chamber formation occurs.

1.3.4 The role of CAR for correct electrical conduction in the mature heart

The specific CAR expression at the intercalated discs in adult hearts suggest an involvement of CAR for correct heart function besides its function for virus entry. Therefore three different independent inducible CAR KO mouse models were generated to overcome the embryonic heart failure phenotype and to analyse CAR function in adult stages (Lim et al., 2008; Lisewski et al., 2008; Pazirandeh et al., 2011). Surprisingly, all published studies observed altered electrical properties and impaired electrical conduction of the CAR KO hearts. Lim et al. (2008) reported a hindered atrioventricular (AV) conduction in which transmission of electrical excitation is not transmitted correctly from the atrium to the ventricles. Further, in several electrocardial recordings of CAR KO mice a complete block of AV conduction was observed. Lisewski et al. (2008) also showed prolongation and impaired alteration in electrical conduction in the AV node resulting in a first degree AV conduction block. The same result was found by Pazirandeh et al. (2011) in their inducible CAR KO mouse model. These data suggest that correct conduction of the electrical excitation signal from the atrium to the ventricles inside the AV node requires CAR. Both Lim et al. (2008) and Lisewski et al. (2008) also found decreased expression of Cx45 in CAR KO hearts compared to the wild type. Further, CAR and Cx45 co-immunoprecipitation was shown whereby deletion of the PDZ binding domain at the cytoplasmic tail of the CAR protein led to a lack of co-precipitation with Cx45 (Lim et al., 2008). In contrast, increased dye coupling of cardiomyocytes was detected in CAR KO cardiomyocytes which was not expected after decreased Cx45 expression (Lisewski et al., 2008). However, the authors suggesting a crosstalk between tight and gap junctions because expression of Cx40 and Cx43 was not changed and therefore correct gap junction generation is still possible.

Comparison of CAR KO hearts and wt hearts in the described konditional CAR KO mouse model of Lim et al. (2008) revealed a similar finding as already published by Dorner et al. (2005): the ventricle lumen is decreased due to induced thickness of the ventricle walls. Haematoxylin and eosin stainings of CAR KO heart sections (fig. 7A, Lim et al., 2008) can not clarify if the number of cardiomyocytes is increased as observed from Chen et al. (2006). Again thinner myofibrils were observed in cardiac CAR KO muscle tissue as well as altered intercellular connections (Pazirandeh et al., 2011). Taken these data together, besides the virus-entry CAR has two different physiological functions inside the heart. First, during heart development and cardiac disease or heart failure it is necessary for correct formation of the ventricle myocardium and generation of proper intercellular contact sites at tight and gap junctions. Second, in the mature heart CAR is only found at the intercalated discs whereby it is required for electrical conduction in the AV node as component of tight and gap junctions. Combining these two functions, it is very interesting to study the function of CAR during initiation of the first heart beats which up to date is still not clearly understood. Further, the role of CAR in early heart beats was not analysed yet.

1.4 Aim of the study

The strong expression of CAR in brain and heart during early and late phases of embryonic development suggest a specific physiological function. CAR as a cell adhesion molecule could be important for correct placement of cells and communication between neighbouring cells. Surprisingly, global CAR knockout mouse models revealed a strong malformation of heart which induce embryonic death around E11.5 - E12.5. Further, conditional CAR KO mouse models also identified impaired excitation conduction in the heart. Therefore during this study the physiological role of CAR during embryonic heart development was investigated. Further the relevance of CAR for exact and correct excitation coupling system inside the embryonic heart was studied. Especially the communication between neighbouring cardiomyocytes was analysed with regard to beating frequency and Ca^{2+} cycling. Embryonic cardiomyocytes beat spontaneously due to constant Ca^{2+} cycling and signaling. This study also analysed the influence of CAR on the Ca^{2+} signaling and the Ca^{2+} related proteins.

To identify the physiological function of CAR in the heart two main approaches were used. First, a global CAR knock out mouse model published by Dorner et al. (2005) was used to analyse the role of CAR during heart development and excitation coupling in embryonic cardiomyocytes. The second approach includes the investigation of CAR signaling pathways in cardiomyocytes. Therefore E15 wild type cardiomyocytes which strongly express CAR at its cell membrane were treated with specific CAR binding reagents. Afterwards intracellular Ca^{2+} signaling was studied because unpublished results revealed an induced Ca^{2+} cycling after CAR activation in embryonic neuron cultures. However, the observed CAR induced increased Ca^{2+} cycling could not be explained and no detailed signaling pathway was found. Therefore during this study a closer investigation of CAR induced Ca^{2+} cycling was carried out.

2 Materials and Methods

2.1 Materials

2.1.1 Animals

Pregnant wild type C57BL/6N mice (E15) were obtained from Charles River for wild type cardiomyocytes and neuron cultures. The global CAR-deficient mouse line (CAR KO) was generated and published by Dorner et al. (2005). To obtain CAR KO embryos heterozygous CAR mice backcrossed into C57BL/6 were breeded and embryos were collected on embryonic day E10.5. The tails of the embryos were harvested for genotyping by genomic PCR. All animals were handeled according to governmental animal welfare guidelines.

2.1.2 HL-1 cell line

The HL-1 cell line was generated by Claycomb et al. (1998). This cardiac muscle cell line was established from an AT-1 subcutaneous atrial mouse tumor and maintains specific cardiac properties. $3x10^3$ cells were plated in 5 ml Claycomb Medium and splitted after 3-5 days. For calcium imaging experiments and immunocytostaining 10000 cells were resuspended in 50 µl Claycomb Medium and plated on 13 mm coverslips coated with fibronectin (20 µg/ml). Spontanous beating was observed after 2-5 days in culture.

Claycomb Medium :	500 ml	Claycomb Medium (Sigma-Aldrich)
	10%	FCS (Gibco)
	1%	Penicillin/Streptomycin (Gibco)
	0.1 mM	Norepinephrine (Sigma-Aldrich)
	2 mM	L-Glutamine (Gibco)

2.1.3 Antibodies

The following table contains all used antibodies for immunocytostaining (ICS), staining of cryostat sections (IHS) and western blots (WB).

Antibody	ICS	IHS	WB	Company
mCAR-Rb80	3 µg/ml	3 µg/ml	1-3 µg/ml	AG Rathjen
mouse-sacromeric-α actinin	1:800	1:800		Sigma-Aldrich
mouse-β actin	1:200	1:100	1:1000	Sigma-Aldrich
mouse-Troponin C	1:200	1:100	1:1000	DSHB
mouse-Calsequestrin			1:1000	Transduction Laboratories
mouse-Calretinin			1:1000	Transduction Laboratories
mouse-Calreticulin			1:1000	Transduction Laboratories
rabbit-Connexin40	1:200	1:200	1:1000	Almone Labs
mouse-Connexin43	1:200	1:200	1:1000	Transduction Laboratories
rabbit-Connexin45	1:200	1:200	1:1000	Almone Labs
rabbit-AKT			1:1000	Cell Signaling
rabbit-phospho-AKT			1:1000	Cell Signaling
rabbit-PLB	1:1000	1:1000	1:1000	Cell Signaling
rabbit-SERCA2a	1:1000	1:1000	1:1000	Cell Signaling
mouse-NCX	1:200	1:200	1:1000	Cell Signaling
rabbit-GSK3β			1:1000	Cell Signaling
rabbit-phospho-GSK3β			1:1000	Cell Signaling
mouse-GAPDH			1:1000	Calbiochem
rabbit-Cy3	1:400	1:400		Dianova
mouse-Alexa488	1:400	1:400		Molecular Probes
DAPI	1:1000	1:1000		Sigma-Aldrich
rabbit-HRP			1:20000	Dianova
mouse-HRP			1:20000	Dianova

2.1.4 Chemicals

The following table includes all used chemicals to prepare buffers, reagents or solutions.

Name	Company
2-mercaptoethanol	Sigma-Aldrich
37% formaldehyde	Merck
acetic acid	Merck
acryl amid	BioRad
Agarose NEO Ultra-Quality	Carl Roth
Ammonium persulfate	GE Healthcare
Aprotinin	Carl Roth
Boric acid	Sigma-Aldrich
BSA	Biomol
Caffeine	Sigma-Aldrich
Calcium chloride dihydrate	Merck
Calyculin A	New England Biolabs
CHAPS	Merck
Dextran-Rhodamine B	Sigma-Aldrich
Dihydrogen sodium phosphate	Merck
DMSO	Merck
dNTPs mixture	Clonetech
EDTA	Merck
EGTA	Merck
Ethanol	Merck
Ethidium bromide	AppliChem
Fura-2AM	Molecular Probes
Glucose	Merck
Glycine	Merck
Hydrochloric acid 32% solution	Merck
Isopropanol	Merck
Leupeptin hemisulfat salt	Sigma-Aldrich
Lithium chloride	Merck
Lucifer Yellow	Invitrogen
Magnesium chloride hexahydrate	Merck
Methanol	Merck
Molecular mass standards for SDS-PAGE	BioRad
Mowiol	Calbiochem
Nickel chloride	Merck
Okadaic acid	Enzo Life Science
o-Phenylenediamine (OPD)	Sigma-Aldrich
PBS	Biochrom
Pepstatin A	Sigma-Aldrich
para-Formaldehyde (PFA)	Merck
Pluronic acid	AAAT Bioquest
PMSF	Enzo Life Science

Name	Company
Potassium chloride	Merck
Proteinase K	Roche
SDS solution 10%	BioRad
Sodium chloride	Merck
Sodium hydroxide	Merck
Sodium tetraborate	Merck
Sucrose	Merck
Sulphuric acid	Merck
TEMED	GE Healthcare
Tris	Merck
Triton X-100	Merck
Trypsin/EDTA 10%	Gibco
Trypsin	Invitrogen
Tween-20	Sigma-Aldrich

2.1.5 Devices

The following table lists the used devices.

Name	Manufacturer
AndorClara CCD camera	Zeiss
CellTram Oil applicator	Eppendorf
Mini 25 micromaipulator	Luigs & Neumann
SM-5 III Controller	Luigs & Neumann
Examiner A1	Zeiss
40x Achroplan 0.8 w Ph objective	Zeiss
Vibration isolation table	Newport
Vapor Pressure Osmometer 5520	Vapro
ChemiDoc XRS	BioRad
GelDoc XR+	BioRad
Microplate Reader 3550	BioRad
TC-10 automated cell counter	BioRad
Biophotometer	Eppendorf
UVvette	Eppendorf
Centrifuge 5424R	Eppendorf
Sorvall RC M150GX	Thermo Scientific
CB150 incubator	Binder
LSM 700 confocal microscope	Zeiss
Stemi-DRC stereomicroscope	Zeiss
Megafuge 1.0 R	Heraeus
Sorvall RC 6+ (Rotor SS34)	Thermo Scientific
Cryotome CM 1950	Leica

2.2 Methods

2.2.1 Cardiomyocyte cell culture preparation

For E15 wilde type cardiomyocyte cell cultures pregnant C57BL/6N mice were obtained from Charles River and were anesthetized with isoflorane by inhalation. After cervical dislocation the embryos were removed from the uterus and the embryonic hearts were prepared in PBS. Dissected heart tissue was incubated in trypsin/EDTA/PBS (1 mg Trypsin/ml) for 30 min at 37 °C. Cells were resuspended in 500 µl DMEM (Gibco)/10% FCS/0.1% penicillin/streptomycin, and 50 µl cell suspension was plated on a coverslip pre-coated with 20 µg/ml fibronectin and maintained at 37 °C in a humidified atmosphere of 95% air and 5% CO_2.

CAR KO cardiomyocyte cell cultures were obtained by preparation of embryonic hearts at E10.5. Dissected hearts were incubated in trypsin/EDTA/PBS for 10 min at 37 °C and resuspended in 80 µl DMEM/10% FCS/0.1% penicillin/streptomycin and plated on two coverslips (12 mm diameter) coated with fibronectin (20 µg/ml). Cultures were maintained at 37 °C in a humidified atmosphere of 95% air and 5% CO_2.

2.2.2 Whole heart cultures

Whole heart cultures were prepared from E15 and E10.5 embryos. Carefully, the prepared intact hearts were transferred to 6-well plates which contain a filter membrane (0.4 µm, Cell Culture Intect) and DMEM/10% FCS/0.1% penicillin/streptomycin. The medium was changed every second day.

Camera recordings of beating hearts were performed in the 6-well culture plates whereby the DMEM was removed by pre-warmed ACSF (130 mM NaCl, 4 mM KCl, 1.25 mM NaH_2PO_4, 25 mM $NaHCO_3$, 10 mM Glucose, 2 mM $CaCl_2$, 1 mM $MgCl_2$). The hearts were maintained on the filter during recording. To record the beating of the whole hearts the AndorClara CCD camera (Zeiss) and TILL Photonics LA software (version 2.3.0.18, 2013) was used.

2.2.3 Cortex primary cell culture preparation

E15 wild type or E10.5 CAR KO pregnant mice were anesthetized with isoflorane, cervical dislocated and the embryos were removed from the uterus. After the brain was dissected, the cortices were taken out and exempt from hippocampus. The cortices were incubated in S1

solution in 37 °C water bath for 15 min. Afterwards the trypsinized tissue was washed with Neurobasal (NB) medium, resuspended in NB+/10% FCS and 5x10^5 cells were plated in 1 ml NB+/10% FCS on poly-D-lysine (0.1 mg/ml) pre-coated coverslips and maintained at 37 °C in a humidified atmosphere of 95% air and 5% CO_2. Every second day 50% of the medium was changed by NB+ medium.

S1 solution :	2.5 ml	10x Trypsin (Sigma-Aldrich)
	22 ml	HBSS (Gibco)
	1%	Penicillin/Streptomycin (Gibco)
	0.25 ml	DNAse I (2.5 µg/ml HBSS)

Poly-D-lysine: 5 mg (Sigma-Aldrich) were dissolved in 50 ml borat buffer (1.24 g boric acid and 1.9 g borax in 400 ml dH_2O, steril filtration, pH 8.4)

NB+ medium :	170	ml	Neurobasal medium (Gibco)
	20	ml	FCS (Gibco)
	2	ml	Penicillin/Streptomycin (Gibco)
	4	ml	B27 (Gibco)
	250	µl	Glutamax (Gibco)
	100	µl	β-mercapotoethanol (Gibco)
	4	ml	BME amino acids (Sigma-Aldrich)

2.2.4 Ad2 fiber knob preparation

Competent E. coli BL21(DE3) were transfected with pET15b-Ad2KC428N for expression of Ad2 fiber knob C428N. Bacteria were grown in Terrific Broth (Merck) media with 0.004% glycerine and Ad2 fiber knob C428N expression was induced by 40 µM IPTG (Merck). To obtain Ad2 fiber knob protein the bacteria were harvested and lysed. The protein fraction was washed and separated with a DE-52-column following by a Ni-NTA column. The Ad2 fiber knob fractions were eluted by 200 mM imidazol, united and protein concentration was measured. For application during calcium imaging recordings the isolated Ad2 fiber knob was dialysed to ACSF.

2.2.5 mD1D2-Fc generation

COS-7 cells (80% confluent) were transfected with a plasmid encoding pIG-plus-mD1D2-Fc. Lipofectamine 2000 (1 mg/ml, Invitrogen) was used as transfection reagent and was removed after 6 h of incubation at 37 °C. The transfected cells were grown for 5 days in DMEM/0.05% penicillin/streptomycin at 37 °C in a humidified atmosphere of 95% air and 5% CO_2. The supernatant was collected and purified via a Protein-A-sepharose column. mD1D2-Fc was eluted by 150 mM NaCl/0.58% acetic acid. The protein fractions were collected, the protein concentration was measured followed by a dialysis to ACSF.

2.2.6 Calcium Imaging

Calcium is involved in many cellular signaling pathways as second messenger and therefore measurement of intracellular Ca^{2+} is very important to better understand these processes. Calcium imaging is used to analyse changes in intracellular Ca^{2+} concentrations in cultivated cells, organ slices or intact tissue samples (Hayashi & Miyata, 1994; Takahashi et al., 1999). Therefore Ca^{2+} sensitive fluorescence dyes are commonly used to monitor changes in cytosolic Ca^{2+} concentration due to their fast response, simple cell loading and high resolution (Moore et al., 1990; Takahashi et al., 1999). Fura-2 and indo-1 are the most popular Ca^{2+} sensitive dyes among a high variety of available dyes (Hayashi & Miyata, 1994; Grynkiewicz et al., 1985; Takahashi et al., 1999). Compared to other Ca^{2+} indicators Fura-2 has a higher quantum yield and a higher extinction coefficient resulting in a very high brightness per molecule (Connor & Silver, 2007). Further, Fura-2 shows a better selectivity against magnesium and heavy metals, is more resistant to photobleaching and has only low background fluorescence. Calibration can be done more easily because Ca^{2+} is bound to Fura-2 in a 1:1 ratio. However, the most important advantage of Fura-2 is the change of fluorescence intensities depending on Ca^{2+} concentration: the peak excitation wavelength shifts from 363 nm to 335 nm when Ca^{2+} increases (Hayashi & Miyata, 1994; Grynkiewicz et al., 1985; Moore et al., 1990; Takahashi et al., 1999). Therefore during calcium imaging recordings the fluorescence intensity of two excitation wavelengths - 340 nm and 380 nm - is measured. The emission wavelength for Ca^{2+} bound and Ca^{2+} free Fura-2 is always 500 nm. This shift in peak excitation wavelength is required for ratio fluorescence imaging.

Fluorescence emission of a biological sample is dependent on the geometric dimensions, the excitation intensity, the quantum yield of the sample, the extinction coefficient of the probe, the cell loading and fluorescence dye concentration and background noise of the instrumentation set up (Connor & Silver, 2007). All these factors influence the recorded fluorescence intensity and therefore also can affect the measurements of intracellular Ca^{2+} concentration. To overcome these

limitations dual-wavelength fluorescence dyes are used whereby the fluorescence intensity changes due to binding of Ca^{2+}. For Fura-2, the ratio (R) of the recorded fluorescence intensities at 340 nm and 380 nm excitations is used to monitor the intracellular Ca^{2+} changes independent on cell loading, fluorescence intensity or experimental limitations (Connor & Silver, 2007; Takahashi et al., 1999). The ratio (R) is calculated by dividing the recorded fluorescence intensity of 340 nm excitation (F_{340nm}) by the recorded fluorescence intensity of 380 nm excitation (F_{380nm}, compare fig. 2.1 B, C).

Fura-2 and other Ca^{2+} sensitive dyes need carboxy groups to bind Ca^{2+} which results in a negative charge of the molecule. However, charged molecules can not diffuse through the cell membrane into the cytosol. Therefore a membrane permeable form of Fura-2 (and other Ca^{2+} indicators) was generated whereby the carboxy groups were replaced by neutral charged acetoxymethyl (AM) esters. The lipophilic Fura-2AM can easily pass the cell membrane and after entering the cytosol the acetoxymethyl ester is hydrolyzed by intracellular esterases and the carboxy groups are present to bind free Ca^{2+} (Connor & Silver, 2007; Hayashi & Miyata, 1994; Grynkiewicz et al., 1985).

Fura-2AM has the disadvantage that often no complete deesterification occurs which leads to an accumulation of Fura-2AM inside the cell. Further, the fluorescence intensity of Fura-2AM is relative strong but not Ca^{2+} sensitive and therefore false-positive cells could be recorded. Due to the high lipophilicity Fura-2AM also can distribute and accumulate into intracellular compartments like the nucleus, sarcoplasmic reticulum or mitochondria where the dye properties are changed. However, compartmentalization can be avoided by reduced dye concentration, lower temperature during cell loading and shorter loading times. Further, photobleaching can effect the Ca^{2+} measurement, as well as protein binding of Fura-2AM. Moreover, high concentration of the Ca^{2+} indicators inside the cell can buffer the cytosolic Ca^{2+} and no changes in free Ca^{2+} concentration is observed anymore (Connor & Silver, 2007; Hayashi & Miyata, 1994; Moore et al., 1990; Takahashi et al., 1999).

Cultivated embryonic cardiomyocytes beat spontaneously whereby the beating is related to intracellular Ca^{2+} transients (Janowski et al., 2006; Liu et al., 2002; Rapila et al., 2008; Sasse et al., 2007; Seki et al., 2003). Therefore calcium imaging using Fura-2AM was performed to analyse spontaneously beating in cultivated cardiomyocytes. After 4 days in culture (DIV4) the plated cardiomyocytes were treated with 1 µM Fura-2AM (Invitrogen, dissolved in 20% pluronic F-127/DMSO) for 1 h at 37 °C in DMEM. Afterwards the loaded cells were washed with DMEM and moved to ACSF (130 mM NaCl, 4 mM KCl, 1.25 mM NaH_2PO_4, 25 mM $NaHCO_3$, 10 mM Glucose, 2 mM $CaCl_2$, 1 mM $MgCl_2$).

During calcium imaging experiments the fluorescence intensities were recorded alternating between excitation at 340 nm and 380 nm (fig. 2.1 A, B). Emission wavelength was for both excitation

wavelengths 510 nm. Afterwards the ratio of both fluorescence intensities was calculated and the change of cytosolic Ca^{2+} could be monitored (fig. 2.1 C). The fluorescence intensities of 340 nm and 380 nm are determined by the concentration of Fura-2AM (c), the diameter of the object (d), extinction coefficient (K) and the intracellular Ca^{2+} concentration (fig.2.1 C). Consequently the ratio of the recorded fluorescence intensities represents the intracellular Ca^{2+} changes during the beating whereby during one beat the cytosolic Ca^{2+} increases and then shortly afterwards decreases. Comparison of beating (events/min) counted by eye and recorded by calcium imaging showed a significant smaller beating frequency for calcium imaging (fig.2.1 D). Decreased beating in Fura-2AM loaded cardiomyocytes resulted from DMSO and pluronic acid treatment.

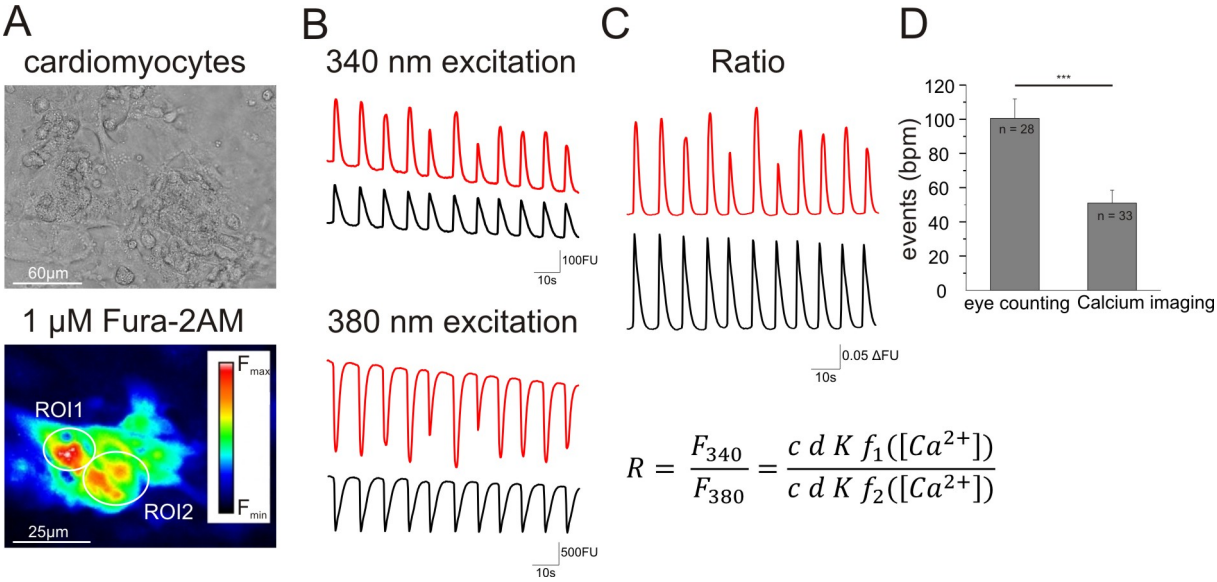

Figure 2.1: Calcium imaging in cardiomyocytes by Fura-2AM. At DIV4 cultivated E10.5 or E15 cardiomyocytes were treated with 1 µM Fura-2AM for 1 h (A) and fluorescence intensity was recorded alternating between excitation at 340 nm and 380 nm at the marked region of interest (ROI 1 and 2, B). Beating of cardiomyocytes is analysed by calculation of the ratio (R) of the fluorescence intensities ($F_{340nm,380nm}$, concentration of Fura-2AM (c), the diameter of the object (d), extinction coefficient (K)(C)). Recorded beating events/min by calcium imaging are significant decreased compared to eye counting (D).

Exposure time of excitation and cycle time depended on Fura-2AM loaded cells and aim of the experiment. For kinetic analysis of Ca^{2+} transients (frequency, amplitude, decay time constant) the exposure time of 340 nm and 380 nm excitation wavelength was reduced to 10 ms, the cycle time was 42 ms and the total experiment duration was 1 min. For investigation the effect of specific pharmacological blockers on beating in cardiomyocytes the exposure times were increased to 20 ms, the cycle time was also raised to 150 ms to prevent photobleaching. The total duration time of an experiment depended on the particular applied blocker but normally varied between 5 and 30 min.

The ratiometric imaging of Fura-2AM requires a fast switch of the excitation and emission wavelengths, short duration of exposure time and a fast image acquisition. Therefore a Xenon lamp and a monochromator is used to gain short excitation duration (TILL Photonics Polychrome V) and to switch very fast from 340 nm to 380 nm excitation wavelength (1.4 ms). All recordings were obtained with Zeiss Axio Examiner A1 (fig.2.2) and Zeiss objectives (40x). The use of the charge-couple device (CCD) camera (AndorClara) allows a very high sensitivity and good resolution for fast image acquisition. Fluorescence recording and analysis of intracellular Ca^{2+} transients was performed with TILL Photonics LA software (version 2.3.0.18, 2013). For further investigations of determined Ca^{2+} ratios Origin7 (Additive), IgorPro (WaveMetrics) and Fiji (Image J, version 1.49m, 2015) was used.

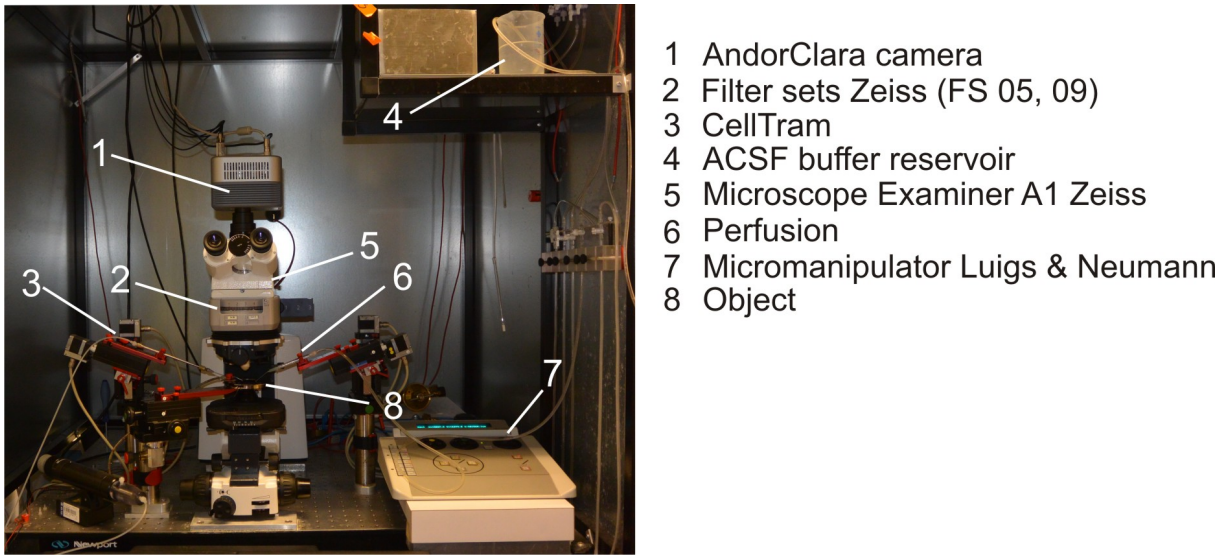

Figure 2.2: Calcium imaging set up. Fura-2AM loaded cardiomyocytes were transferred to ACSF and placed in the object carrier. During recording the cells are superfused with ACSF. Specific blocker and reagents were applied by a glas pipette using CellTram for withdrawal and a micromanipulator for correct positioning.

Intracellular calcium concentration determination

Cytosolic Ca^{2+} can be measured by using a calcium calibration protocol (Doeller & Wittenberg, 1990). After specific recordings to record steady state beating cultivated E10.5 cardiomyocytes were treated first with calcium free solution to obtain R_{min} and afterwards calcium high solution (to record R_{max}) was applied during recording of fluorescence intensity (fig.2.3 A). Calcium free solution contained of 15 mM EGTA (Merck) and 10 µM ionomycin (Invitrogen) diluted in ACSF. 25 mM $CaCl_2$ and 10 µM ionomycin in ACSF is used as calcium high solution. Intracellular Ca^{2+} concentration was calculated accordingly to Doeller and Wittenberg (1990) and the formulas are illustrated in fig.2.3 B. As K_d of Fura2-Ca^{2+} 225 nM was used (Doeller and Wittenberg, 1990). E15 cardiomyocytes were prepared to establish this protocol (fig. 2.3 C). During diastole

cytosolic Ca^{2+} is decreased and for E15 myocytes 150 nM Ca^{2+} were determined. Strong increase of cytosolic Ca^{2+} to 225 nM was measured in the systolic phase of the beating (fig. 2.3 C).

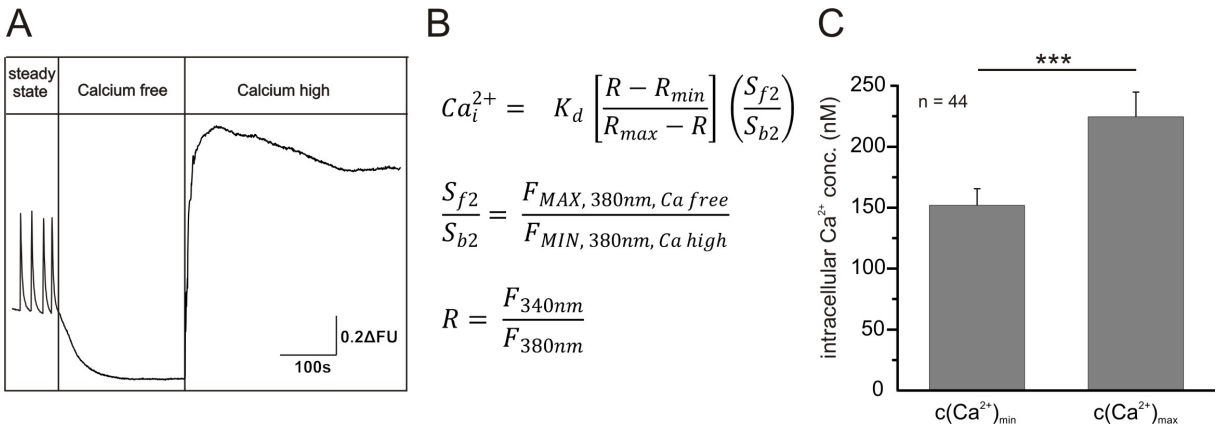

Figure 2.3: Intracellular Ca^{2+} concentration determination The calcium calibration protocol includes the recording of the flourescence intensity during normal beating (steady state), calcium free environment and calcium high environment (A). The cytosolic Ca^{2+} concentration was calculated accordingly to Doeller and Wittenberg (1990) (B). E15 cardiomyocytes contain 150 nM Ca^{2+} during diastolic phase of beating which increases during systole to 225 nM (C).

Ca^{2+} extrusion analysis

During cardiac beating cytosolic Ca^{2+} increases and decreases very fast. Therefore the Ca^{2+} extrusion proteins NCX, SERCA2a, PMCA and mitochondria and its function were analysed in more detail. Application of caffeine triggers a complete release of Ca^{2+} from the sacroplasmic reticulum which induces a strong, long-lasting Ca^{2+} transient. Depending on the relevant Ca^{2+} extrusion protein the suitable inhibitors were applied or their enzyme function was downregulated by extracellular buffer changes. After short incubation (compare the following table of inhibitors) 10 mM caffeine diluted in ACSF was applied manually and the Ca^{2+} transient was recorded.

Application of specific blocker

The beating frequency of cardiomyocytes can be pharmacological modified. For detailed investigations of proteins and enzymes implicated in beating specific inhibitors were applied. The inhibitors were diluted in DMSO or ACSF and carefully applied to the myocytes. Concentration and incubation time are depended on inhibitor and the blocked enzyme. The following table summarises the applied inhibitors:

Inhibitor	Target	Conc.	Incubation	Company
Thapsigargin	SERCA2a	10 µM	20 min	Sigma-Aldrich
CPA	SERCA2a	10 µM	30 min	Sigma-Aldrich
Ru360	mCU	20 µM	30 min	Sigma-Aldrich
CGP-37157	mNCX	20 µM	5 min	Sigma-Aldrich
H-89	PKA	10 µM	10 min	Sigma-Aldrich
ZD7288	HCN channel	25 µM	30 min	Tocris Bioscience
DIDS	chloride channel	20 µM	20 min	Calbiochem
2-APB	IP3 receptor	50 µM	5 min	Tocris Bioscience
Ryanodine	RyR receptor	50 µM	5 min	Biozol
Tetracaine	RyR receptor	10 µM	10 s	Sigma-Aldrich
KN-93	CamKII	1 µM	10 min	Adipogen
Verapamil	L-type Ca^{2+} channel	1 µM	1 min	Sigma-Aldrich
Nimodipine	L-type Ca^{2+} channel	1 µM	1 min	Sigma-Aldrich
ω-Conotoxin MVIIC	Ca^{2+} channels	1 µM	1 min	Alomone Labs
ω-Conotoxin GVIA	N-type Ca^{2+} channel	1 µM	1 min	Alomone Labs
ω-Agatoxin	P-type Ca^{2+} channel	1 µM	1 min	Alomone Labs
Wortmannin	PI3K	1 µM	30 min	Sigma-Aldrich
LY924002	PI3K	50 µM	30 min	Cell Signalling
Bepridil	NCX	10 µM	3 min	Tocris Bioscience
KB-R7943	NCX	100 nM	3 min	Caymen Chemicals
NPPB	gap junctions	100 µM	10 min	Sigma-Aldrich
CBX	gap junctions	200 µM	10 min	Sigma-Aldrich

2.2.7 Dye spreading

Dye spreading was used to analyse the function and activity of gap junctions. Cultivated cardiomyocytes were transferred to ACSF and 1% lucifer yellow/intracellular solution (90 mM KCl, 3 mM NaCl, 5 mM EGTA, 5 mM HEPES, 5 mM Glucose· H_2O, 0.5 mM $CaCl_2 \cdot 2H_2O$, 4 mM $MgCl_2 \cdot 6\ H_2O$) was carefully injected in a single cardiomoycyte by a glas pipette via the CellTram. Afterwards the dye spreading to the neighbouring cardiomyocytes was recorded by Zeiss Axio Examiner A1 and Zeiss objective 40x. Lucifer yellow excitation wavelength was 428 nm, emission 542 nm wherefore the Zeiss filter set 05 was used. This filter allows excitation wavelength between 395-440 nm, and emission from 470-780 nm due to the beam splitter at 460 nm. To measure the area of dye spreading the recorded image files from the injected cardiomyocyte and the dye spreading after 5 min were analysed by the Fiji/Image J Fiji/ Image J (Version v1.49m, 2015) software. The total area of dye spreading was corrected by the size of the injected cardiomyocyte cell area.

Neurobiotin staining was also performed by injecting 2% neurobiotin (Vector)/1% lucifer yellow/intracellular solution in a single cardiomyocyte. Lucifer yellow was used to monitor correct injection and dye spreading in the cardiomyocytes. The dye spreading to neighbouring cardiomy-

ocytes was observed by Zeiss Axio Examiner A1. After injecting three different cardiomyocytes on one cell culture dish and incubation of 5 min the cardiomyocytes were fixated in 4% PFA/PBS solution, washed with PBS and permeabilised by 0.1% triton X-100/PBS/1% goat serum for 20 min. After blocking for 10 min with 0.1% BSA/PBS neurobiotin was detected by application of streptavidin-Cy5 antibody for 1 h. The specific binding of streptavidin to the biotin molecule allows the correct detection of the spreaded neurobiotin. After staining the nuclei with DAPI for 10 min, the cardiomyocytes were washed with PBS and embedded in Mowiol. Detection of neurobiotin was performed by using confocal microscopy and analysis with Fiji/Image J software.

Further, the following gap junction blockers were applied to cultivated cardiomyocytes and incubated for 10 min: 200 µM carbenoxolone (CBX, Sigma-Aldrich) and 100 µM 5-nitro-2-(3-phenylpropylamino)benzoic acid (NPPB, Sigma-Aldrich). Afterwards dye spreading with lucifer yellow was performed.

Dextran-rhodamine B (Sigma-Aldrich) injection in cultivated cardiomyocytes (DIV4) was performed as described above for lucifer yellow and neurobiotin. Injected dextran is not able to migrate to neighbouring cardiomyocytes due to its high molecular weight (10.000 kDa). Therefore dextran-rhodamine B is used to determine the injected cell and its cell dimension. As excitation wavelength 542 nm was used, emission wavelength is 625 nm. Further, the specific emission filter D605/55M (Zeiss, 63166) was used for correct signal detection.

2.2.8 Glycogen Assay

Glycogen concentration of E11 embryo hearts was determined by using Glycogen Colorimetric/Fluorometric Assay Kit (Biovision). Freshly dissected E11 embryo hearts were rapidly frozen in liquid nitrogen and afterwards homogenised in 50 µl dest. water. The assay was performed according to the instruction guidelines of the manufactor.

2.2.9 MitoTracker staining

Size measurement of mitochondria in cultivated cardiomyocytes (DIV4) was performed by using MitoTracker Red CMX Ros (Invitrogen). 200 nM MitoTracker Red diluted in prewarmed (37 °C) DMEM was applied to the cultivated cardiomyocytes and incubated for 30 min at 37 °C. After the staining, the cells were washed with PBS, fixated with DMEM/ 10% FCS/ 3.7% formaldehyde for 15 min and embedded in mowiol. The stained mitochondria were analysed by confocal microscopy, ZEN software (Zeiss) and LSM Manager software (Zeiss).

2.2.10 cAMP assay

The cAMP assay kit (Cell Signaling) was performed to measure the intracellular cAMP concentration in E10.5 heart tissue. Therefore E10.5 embryos were prepared as described above and the dissected heart tissue was lysed in Cell Lysis Buffer (Cell Signaling) and the assay was performed according to the instruction guidelines. An internal cAMP standard curve was generated to accurately determine cAMP concentration in the samples (Fig. 2.4). A linear fit of the plotted absorbance against log(cAMP) was generated and used to calculated the sample cAMP concentration.

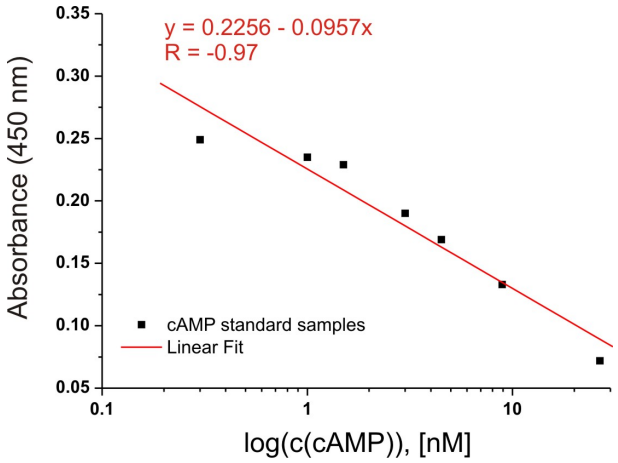

Figure 2.4: cAMP standard curve. The absorbance (450 nm) of 8 in concentration decreasing cAMP samples was measured and plotted against log(c(cAMP)). A linear fit was applied to calculate the specific cAMP concentration in the samples.

2.2.11 Immunocytostaining

For cell surface staining cultivated cardiomyocytes were washed twice with PBS and incubated for 1 h with the primary antibody diluted in PBS/5% goat serum/ 0.1% BSA. After carefully washing twice with PBS, the cells were fixated by treatment of 3.7% formaldehyde/PBS for 10 min. Afterwards the second antibody was applied for 1 h in absence of light, and nuclei were stained with DAPI for 10 min. The stained cardiomyocytes were washed, embedded in Mowiol (Merck) and dried over night.

Staining of intracellular proteins was performed as described above whereby the cells were fixated and treated for 10 min with permeabilization buffer before the first antibody was applied.

2.2.12 Immunohistochemistry of cryostat sections

E11 embryos, E15 or adult hearts were fixed in 4% PFA/PBS for 1.5-4 h, followed by incubation in 15% sucrose/PBS for 2 h and over night incubation in 30% sucrose/PBS. For cryostat sections the fixated embryos or hearts were embedded in Tissue Tek (Sakura) and frozen on dry ice. 16 µm thick sections were cut using a cryotome (Leica CM 1950) and plated on gelatine coated glas slides. After drying at room temperature the cryosections were permeabilized with 0.1% Triton X-100/PBS/1% heat-inactivated goat serum and the first antibody was incubated over night at 4 °C. The sections were washed (0.1% Triton X-100/PBS) and the secondary antibody was applied for 2 h at room temperature following by DAPI (1 µg/ml) staining. Afterwards, the cryosections were embedded in Mowiol and dried over night.

2.2.13 Confocal microscopy

The immunostained cryostat sections or cultivated cells were analysed with the LSM 700 confocal microscope (Zeiss). Therefore different objectives (Zeiss, 10x - 100x) and program settings (ZEN Zeiss software) were used depending on cell type, protein and region of interest. LSM Manager software (Zeiss) and Fiji/ Image J (Version v1.49m, 2015) were used for detailed analysis of localisation and arrangement of proteins, fluorescence intensity and co-localisation.

2.2.14 Haematoxylin and Eosin staining

Haematoxylin and Eosin staining was performed of E11 embryo plastic sections. Therefore E11 embryos were dissected and incubated in 4% PFA over night at 4 °C. Afterwards the fixated embryos were placed in 50%, 70%, 80%, 90% and 99% EtOH whereby each EtOH step was applied over night at 4 °C. The tissue embedding in plastic was performed with Technovit 7100 (Heraeus Kulzer GmbH) according to the instruction guidelines. Afterwards, 5 µm sections were prepared by using the rotary microtome HM 360 (Microm). To analyse the size and numbers of cardiomyocytes in E11 embryo hearts the collected sections were stained for 5 min in Gills haematoxylin (Sigma-Aldrich), washed with running tap water and to destaining the surrounding plastic the stained sections were shortly dipped into acid EtOH. After washing with tap water and dest. water the sections were placed for 2 min in Scotts tap water (20 g $MgSO_4$, 2g $NaHCO_3$, add 1 l tap water). Next, the sections were washed twice in dest. water and then incubated for 2 min in eosin (Sigma-Aldrich, 0.5 g/100ml EtOH) staining solution followed by replacement to 96% EtOH and 100% EtOH for 2 mins. Last, the embryo plastic sections are removed to xylene (Merck) for 2 min and then mounted with Roti-Histokit (Roth). To obtain images of single cardiomyocytes of the embryonic hearts light transmission microscopy (Zeiss Axiovert 135)

of the stained sections was performed and the the size of the cardiomyocytes was calculated by using Fiji/ Image J (Version v1.49m, 2015).

2.2.15 mCAR Genoytyping

For mCAR genotyping of adult animals or embryos, the tails were incubated for 3 h at 55 °C in tail lysis buffer added with 20 mg/ml proteinase K. After inactivation at 85 °C for 45 min, the mCAR PCR can be performed using the following primers: Neo2L (5'-GGCATCAGAGCAGCCGATTG-3', targeted allele), Dor25 (5'-CACTTCTAATAACTTGCCCACCAAGACC-3', targeted and wild-type allele) and GS3 (5'-ATCCCGCACAAGAGCACGAAG-3', wild-type allele). The mCAR-PCR MasterMix contains the following reagents:

MasterMix :	10.88	µl	dH_2O
	2	µl	10x LA PCR Buffer II
	2	µl	25 mM $MgCl_2$
	3.2	µl	dNTP Mixture (2.5 mM each)
	0.24	µl	Neo2L (50 µM)
	0.24	µl	Dor25 (50 µM)
	0.24	µl	GS3 (50 µM)
	0.2	µl	TaKaRa La Taq (Clontech)
	1	µl	tail lysis

mCAR-PCR :	94 °C	3 min	
	94 °C	30 s	35x
	63 °C	30 s	35x
	72 °C	2 min	35x
	72 °C	10 min	

PCR products were analysed by gel electrophoresis on 1.5% agarose gels containing ethidium bromide for 40 min at 100 mV. In CAR wild-type PCR product a 1kb band is found, for heterozygote PCR products bands of 1 kb and 1.6 kb were found. CAR KO was detected by bands at 1.6 kb bands.

2.2.16 Protein isolation

Dissected hearts of E11 embryos were collected accordingly to their genotype and homogenized together in 0.34 M sucrose added with proteinase inhibitors PMSF, aprotinin, leupeptin and pepstatin. After 10 min centrifugation at 800 x g the nucleus fraction was removed and the supernatant was ultracentrifuged for 20 min at 100.000 x g. The cytosolic fraction was obtained and the pellet (membrane fraction) was solubilized in 1% CHAPS/PBS and proteinase inhibitors for 1 h. After ultracentrifugation for 20 min at 100.000 x g the pellet was discarded and the membrane proteins were solved in the supernatant.

2.2.17 SDS-PAGE and Western Blot

Isolated cytosolic or membrane fraction of E11 embryo hearts were loaded on 8-12% acryl-amid gel and afterwards blotted on nitrocellulose transfer membranes (Schleider + Schitt). After blocking in 1xABS/TBS for 2 h at room temperature the membranes were incubated with the primary antibody diluted in 1xABS/TBS over night at 4 °C. The secondary antibody was applied for 2 h to the nitrocellulose membranes after washing three times with TBS-T. Detection was performed using ECL solution (ThermoScientific).

10x Running buffer:	30.3	g	Tris
	144	g	Glycine
	2	l	dH_2O

Transfer buffer:	100	ml	10x Running buffer
	200	ml	Methanol
	700	ml	dH_2O

10x TBS:	175.32	g	NaCl
	121.14	g	Tris
	2	l	dH_2O (pH 7.4)

TBS-T:	100	ml	10x TBS
	900	ml	dH_2O
	5	ml	Tween-20

3xABS:	6	%	BSA
	1.5	%	Tween-20
	0.03	%	Thiomersal
			in PBS, store at $-20\,^{\circ}C$

2.2.18 Gene expression analysis

Isolation of mRNA was performed from freshly dissected E11 hearts accordingly to the instructers protocol (Qiagen). Afterwards cDNA was generated with SuperScript II Reverse Transkriptase (Invitrogen). To analyse expression levels of different genes real-time PCR was performed using SYBR Select Master Mix (Applied biosystems) accordingly to the instructers protocol. The relative fold change of CAR KO gene expression compared to wt hearts was calculated by using the comparative real-time PCR method (Bustin & Nolan, 2004; Pfaffl et al., 2004; Pfaffl, 2004). Actin was used as reference gene. The comparative real-time PCR uses the treshold values (C_t) of target genes and reference gene and after normalization to the initial cDNA amount and PCR efficiency (equation 1 and 2), CAR wt and CAR KO gene expression was compared:

$$\Delta C_t^{wt} = C_t^{wt}Target - C_t^{wt}Actin \quad (1)$$

$$\Delta C_t^{KO} = C_t^{KO}Target - C_t^{KO}Actin \quad (2)$$

The comparison of the target gene expression of CAR KO to wt is calculated by subtraction of (2) by (1):

$$\Delta\Delta C_t = \Delta C_t^{KO}Target - \Delta C_t^{wt}Target \quad (3)$$

The relative fold change (F) can be calculated by equation 4 and illustrates if the target gene is over expressed or down regulated in CAR KO hearts:

$$F = 2^{-\Delta\Delta C_t} \quad (4)$$

The following table summarizes the used primers (10 pM):

Primer	Sequence (5'-3')	Product size (bp)
ActinFor	CGTGGGCCGCCCTAGGCACCA'	238
ActinRev	CTTAGGGTTCAGGGGGGC	
PlbFor	AGCTGGGACCAAAGGAACTT	223
PlbRev	TAGCCGAGCGAGTGAGGTAT	
CxadrFor	ACTCTCAGTCCCGAAGACCA	179
CxadrRev	TGCGTCGCCAGACTTGACAT	
NCX1For	AGCTCTCCTGGAGTTGTGGA	184
NCX1Rev	TGGAAGCTGGTCTGTCTCCT	
Hcn1For	CCATGCTGACAAAGCTCAAA	167
Hcn1Rev	GATCTCCCCGAAATAGGAGC	
Hcn2For	GCCATGCTGACAAAGCTCAAA	154
Hcn2Rev	TAGGAGCCATCCGACAGCTT	
Hcn4For	TCATCTCCTCCATCCCTGTC	202
Hcn4Rev	CTGGCCAGGTCATAGGTCAT	
Serca2aFor	CTGTGGAGACCCTTGGTTGT	245
Serca2aRev	CAGAGCACAGATGGTGGCTA	
RyR2For	TGCCGAGGTCTTCTCAAAGT	228
RyR2Rev	TGCTTTAGTCGTGAGGGCTT	
IP3R2For	ATGGCGAGGGTCTGTAACAC	166
IP3R2Rev	GCAGCTGGATAAAGACTGGC	
Cx40For	CTCTAAACGTGGAAGGCTCG	136
Cx40 Rev	TGAACAGGACAGTGAGCCAG	
Cx43For	GAACACGGCAAGGTGAAGAT	187
Cx43Rev	GACGTGAGAGGAAGCAGTCC	
Cx45For	AAAGAGCAGAGCCAACCAAA	113
Cx45Rev	CCCACCTCAAACACAGTCCT	

2.2.19 Statistical analysis

The results are represented as mean standard error of the mean (SE). For statistical analysis of data the program SigmaStat 3.5 (Systat Software, 2006) was used. At first, normality tests using the Kolmogorov-Smirnov test were carried out. If the analyzed data sets were normal distributed t-test or paired t-test were used to measure the significance between the groups of data. Not normal distributed data were analyzed with Mann-Whitney-Rank-Sum Test. The

following P-values were used to indicate a significant difference between two groups: * P <0.05, ** P <0.01, *** P <0.001

3 Results

3.1 The coxsackievirus and adenovirus receptor

3.1.1 CAR expression during heart development

First, the expression of CAR during development was investigated whereby cryostat sections of the heart of different developmental stages between E10.5 embryo and adulthood were analysed. The strongest expression of CAR can be found during embryonic developmental stages. Fig.3.1 shows CAR expression in different embryonic and adult developmental stages by immunostaining of cryostat sections. Already in E10.5 embryo cryosections CAR can be detected. During embryonic development CAR expression increases until birth and it can be found in the entire myocardium. As a cell adhesion protein CAR is localized at the cell membrane of the cardiomyocytes. Shortly after birth the CAR expression strongly decreases as illustrated in fig.3.1 for heart cryostat sections of P10 mice. At P10 CAR is only found at the intercalated discs. The same expression profile was detected for adult stages (fig.3.1 adult heart cryostat sections).

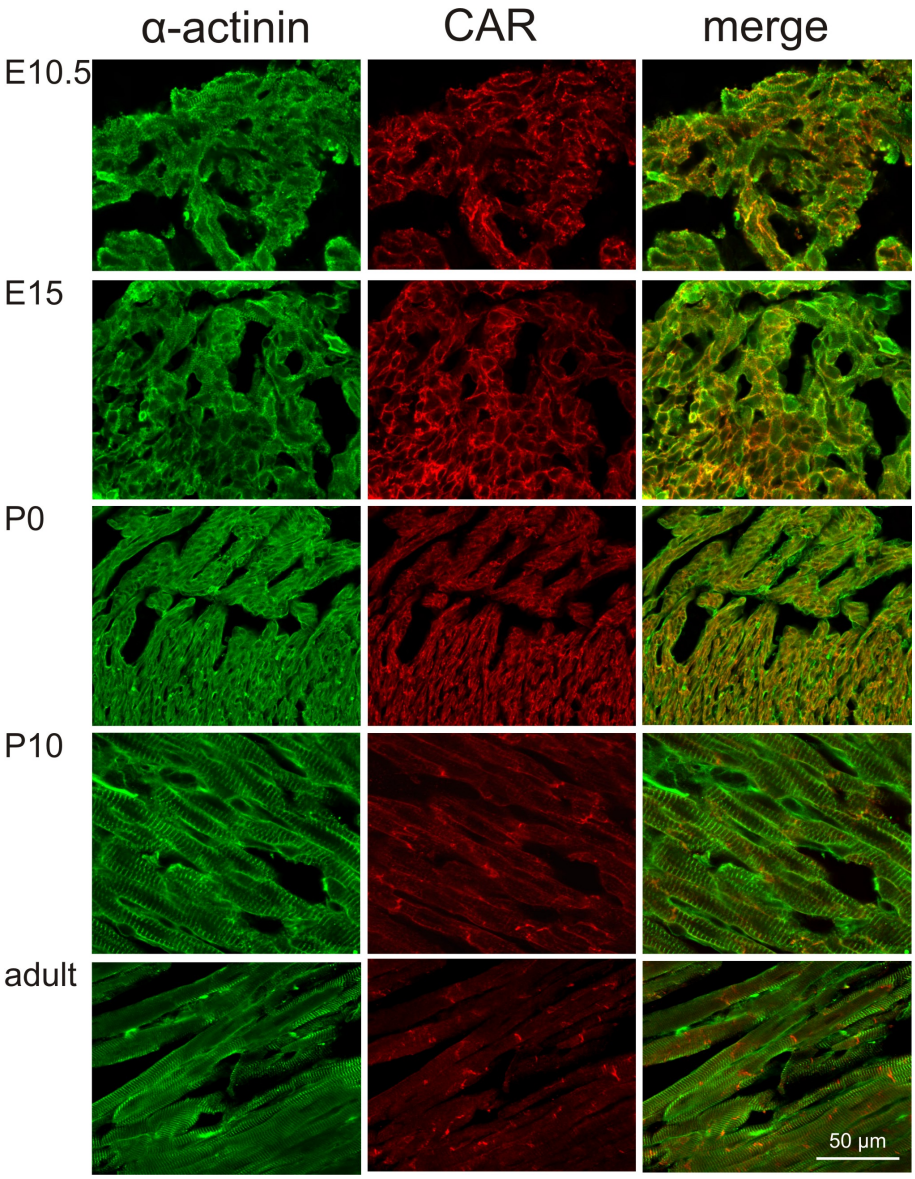

Figure 3.1: CAR expression during heart development. Cryostat sections of E10.5 embryos or hearts of E15 embryo, P0, P10 and adult mice were immunostained against α-actinin and CAR and analysed by confocal microscopy. For each developmental stage cryostat sections of three animals were investigated.

3.1.2 HL-1 cell line

The use of a cardiac cell line like the HL-1 cell line has the advantage of high cardiomyocyte cell numbers and the possibility to repeat experiments in high quantity. During the analysis of CAR signalling pathways the HL-1 cell line was used and therefore at first, expression and correct localisation of CAR in the cell membrane was investigated. The cardiac HL-1 cell line was generated by Claycomb et al. (1998) from an AT-1 subcutaneous tumor of an adult C57BL/6J

mouse. This cardiac myocyte cell line can be repeatedly passaged and the cardiomyocytes still remain a cardiac specific phenotype like spontaneous beating and expression of cardiac markers (Claycomb et al., 1998; White et al., 2004). Several studies already showed CAR expression in HL-1 cells but to verify these results CAR immunostaining and CAR gene expression was performed (Fechner et al., 2007; Pinkert et al., 2011). The HL-1 cells were immunostained against CAR (fig.3.2 A). Beside CAR also N-cadherin expression was tested by immunostaining and a co-localization of CAR and cadherin was found which indicates the correct localization of CAR in the cell membrane. Further, CAR gene expression as well as specific cardiac gene expression were tested by real-time PCR (fig.3.2 B). Compared to E15 wildtype hearts HL-1 cell express very weak CAR. However, real-time PCR and immunostaining illustrated sufficient CAR expression in cultivated HL-1. Specific cardiac genes like actin, sarcoplasmic reticulum calcium ATPase (SERCA2a) and phospholamban (Pln) were also detected (fig.3.2 B).

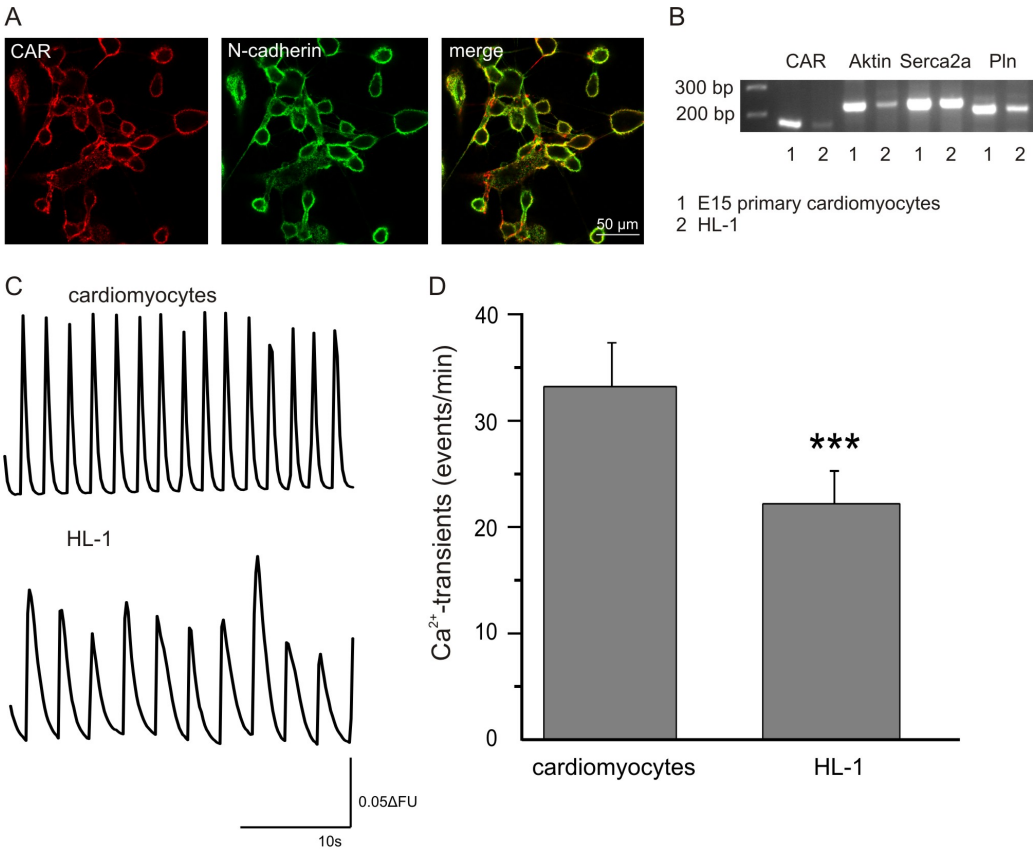

Figure 3.2: HL-1 cell line. Cultivated HL-1 cells were co-stained against CAR and N-cadherin to verify the correct localisation of CAR in the cell membrane (A). Specific cardiac genes and CAR expression was analysed by real-time PCR (B). Calcium imaging was used to analyse the spontaneous beating of cultivated HL-1 cells (DIV4). Compared to E15 cardiomoyctes (n=42) HL-1 cells (n=33) beat significant slower (C, D) *** $P<0.001$

For analysis of beating and Ca^{2+} transients calcium imaging was used. Compared to E15 cardiomyocytes HL-1 cells beat significant slower (22 bpm, fig.3.2C, D). Recorded Ca^{2+} transients revealed similar spontaneous beating as showed for E15 cardiomyocytes and therefore the HL-1 cell line was also used as artificial cardiac cell culture system to study the signaling pathway of CAR.

3.2 The constitutive CAR knockout mouse model

3.2.1 CAR KO embryos die due to malformation of the heart

The study of the physiological role of CAR during embryonic development was investigated by using a conventional global CAR knockout mouse model published by Dorner et al. (2005). CAR KO embryos die between embryonic development E11.5 and E12. Fig.3.3 illustrates a E11 CAR wt and KO embryo. The CAR KO embryos did not show any difference in size and overall body development compared to the wt littermates. However, in CAR KO embryos internal bleeding around the heart was found. Furthermore, some blood or lymphatic vessels indicated enhanced leakage of blood throughout the embryo body suggesting destroyed vessels walls.

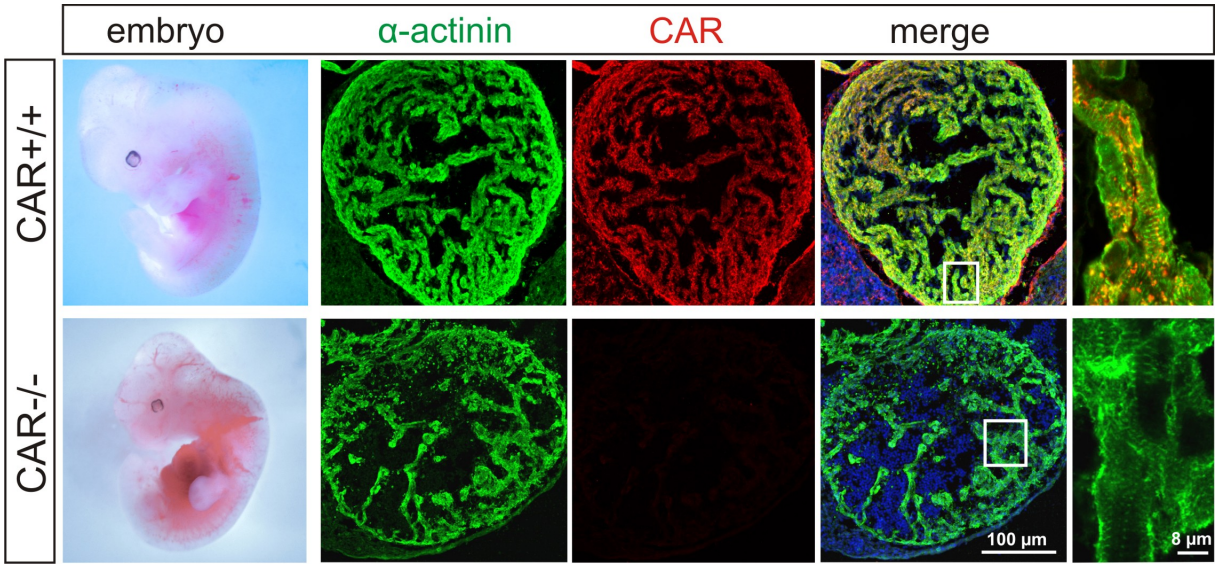

Figure 3.3: The global CAR knockout mouse model revealed intense internal bleeding and CAR KO embryos die around E11.5. A global CAR knockout mouse was generated by Dorner et al. (2005) and revealed that CAR KO embryos die around E11.5 and E12.5. High amount of blood was found throughout the CAR KO embryo. α-actinin staining of E11 embryo cryostat sections indicated malformation of the heart. Green - α-actinin, red - CAR, blue - DAPI

E11 embryo cryostat sections were co-stained against α-actinin and CAR. CAR wt embryos showed a strong CAR expression in the whole myocardium. However, CAR KO hearts revealed a misformation and loss of cardiac tissue. Nevertheless, α-actinin bundles still were highly organized and did not show any difference to wt hearts as shown in the higher magnification (fig.3.3).

To understand the function of CAR in the developing heart further wt and CAR deficient cardiomyocytes were analysed at the cellular level. Cardiomyocytes cell culture was used to analyse the beating and physiological function of the heart and in addition to investigate the

reason why CAR KO embryos die.

3.2.2 CAR KO cardiomyocytes and hearts beat significant faster

Cultivated E10.5 cardiomyocytes were studied at DIV4 by calcium imaging to analyse beating frequency and Ca^{2+} cycling. Furthermore, beating of cardiomyocytes were also analysed by eye counting. Fig. 3.4 A-C summarizes the results: compared to wt CAR KO cardiomyocytes beat significant faster. Eye counting of the beating events revealed for CAR KO (CAR-/-) 96 ± 7 bpm and only 59 ± 5 bpm for wt cardiomyocytes (fig. 3.4 B). In calcium imaging recordings 48 ± 4 Ca^{2+} transients per min were detected for CAR KO cardiomyocytes. In contrast, CAR wt (CAR+/+) and hz (CAR+/-) cardiomyocytes showed only 26 ± 3 (wt) and 27 ± 3 (hz) Ca^{2+} events per min (fig.3.4 C).

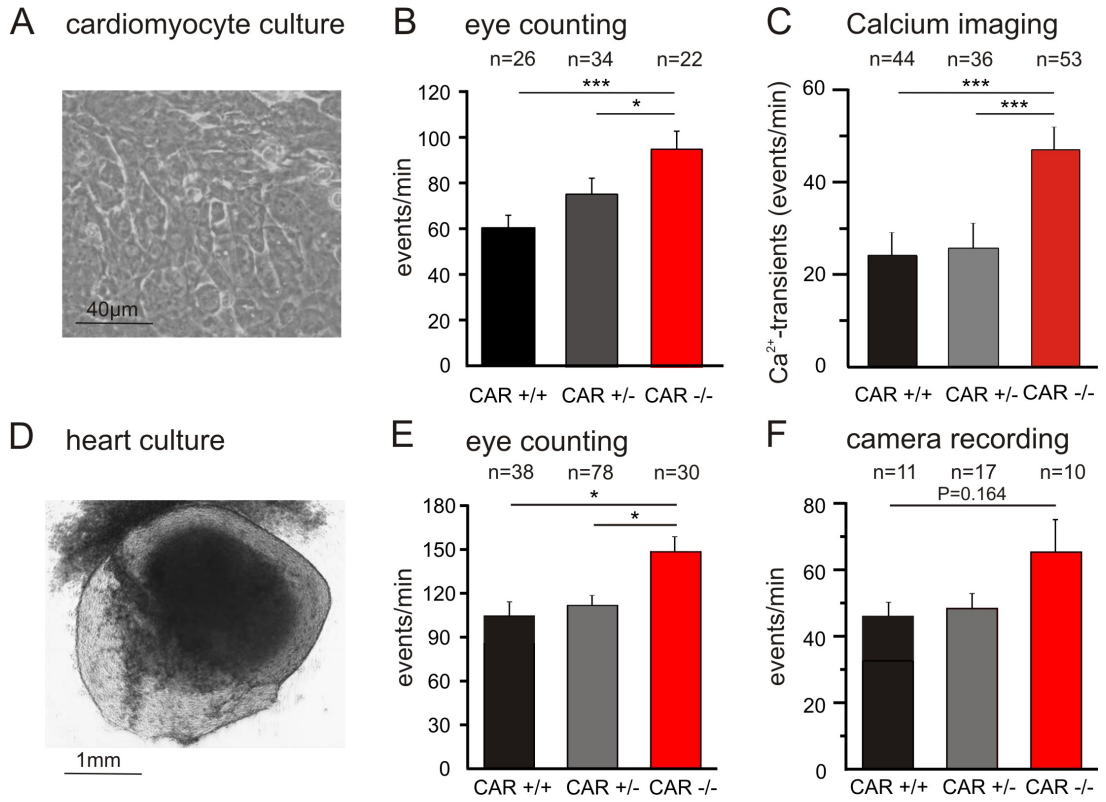

Figure 3.4: CAR KO cardiomyocytes beat significant faster. E10.5 cardiomyocytes were cultivated and at DIV4 (A) the beating was analysed by eye counting (B) and calcium imaging (C). Both methods revealed a significant faster beating for CAR KO cardiomyocytes (B, C). E11 hearts were dissected and cultivated and at DIV2 (D) the beating was studied by eye counting (E) and camera recording (F). CAR KO hearts beat significant faster when anaylsed by eye (E). Camera recordings did not reveal a difference in beating frequency (F). * P<0.05, *** P<0.001

To verify this beating effect, also whole hearts of E11 embryos were investigated. Therefore whole heart cultures were prepared and beating was counted per eye and by camera recording (fig.3.4 D-F). CAR KO hearts beated significant faster when beating frequency was investigated by eye (fig.3.4 E). The observed beating frequency of CAR KO hearts was 148 ± 13 bpm compared to CAR wt hearts 104 ± 10 bpm. Analysis of beating by camera did not show a statistical significant change in the frequency between CAR KO and wt hearts. Whole heart cultures were highly sensitive to movement and temperature changes which could cause the different result compared to the eye counting experiment. However, the same tendency that CAR KO hearts beat faster than wt hearts was observed.

The beating frequency of E10.5 cardiomyocyte cell cultures appeared less compared to the very fast beating of whole hearts (59 bpm vs. 104 bpm for CAR wt) independent of the genotype. During cardiomyocyte cell culture preparation the heart is dissected and dissociated which leads to a slower beating.

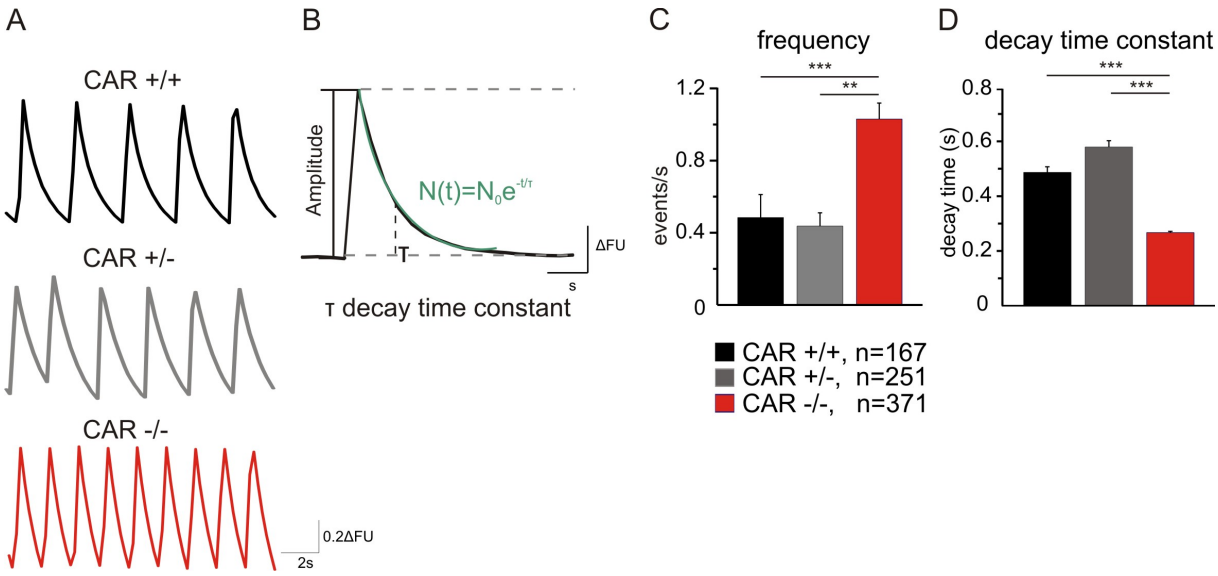

Figure 3.5: CAR KO cardiomyocytes revealed a significant smaller decay time constant of Ca^{2+} decline. Ca^{2+} transients were recorded by calcium imaging for CAR wt, hz and KO cardiomyocytes (A). To analyse Ca^{2+} decline IgorPro software was used and an exponential decay fit was plotted through the Ca^{2+} transients and the decay time constant was calculated (B). Frequency of CAR KO Ca^{2+} transients was significant higher (C) and the decay time constant was significant smaller compared to CAR wt cardiomyocytes (D). ** P<0.01, *** P<0.001

Ca^{2+} transients were recorded during calcium imaging experiments and further analysed by IgorPro software to study the Ca^{2+} decline (fig. 3.5 A-D). CAR wt cardiomyocytes showed spontaneous beating with uniform Ca^{2+} decline. Closer investigation of CAR KO Ca^{2+} transients revealed a faster decline of the systolic Ca^{2+} value to diastolic Ca^{2+} level (fig. 3.5 A). For accurate comparison of the Ca^{2+} decline a first order exponential decay fit was used to calculate the decay time constant (fig. 3.5 B). The frequency of Ca^{2+} transients recorded in CAR KO cardiomyocytes

was significant higher (C) and a significant smaller decay time constant was calculated compared to wt cardiomyocytes (fig. 3.5 D).

This result indicated that Ca^{2+} decline is significant faster in CAR KO cardiomyocytes which stimulated the faster beating. Faster decline of Ca^{2+} during the beating cycling may suggest that Ca^{2+} extrusion is changed in CAR KO cardiomyocytes.

3.2.3 Analysis of Ca^{2+} extrusion in CAR KO cardiomyocytes

The recorded Ca^{2+} transients of CAR KO cardiomyocytes revealed a significant faster Ca^{2+} decline which indicates that Ca^{2+} extrusion is most likely changed. Systolic Ca^{2+} extrusion is performed by SERCA2, NCX, PMCA and mitochondria (Bers, 2002). Primarily SERCA2 and NCX extrude the main amount of cytosolic Ca^{2+} during the beating cycles (Bassani et al., 1994; Bers & Despa, 2006). To further verify this effect 10 mM caffeine was applied to CAR wt and KO cardiomyocytes which induced a complete SR Ca^{2+} release and a long-lasting Ca^{2+} transient (fig.3.6 A). The calculated decay time constant for CAR KO cardiomyocytes was significant smaller compared to wt cardiomyocytes (B). These both experiments suggest that Ca^{2+} decline and therefore extrusion of systolic Ca^{2+} is faster in CAR KO cardiomocytes.

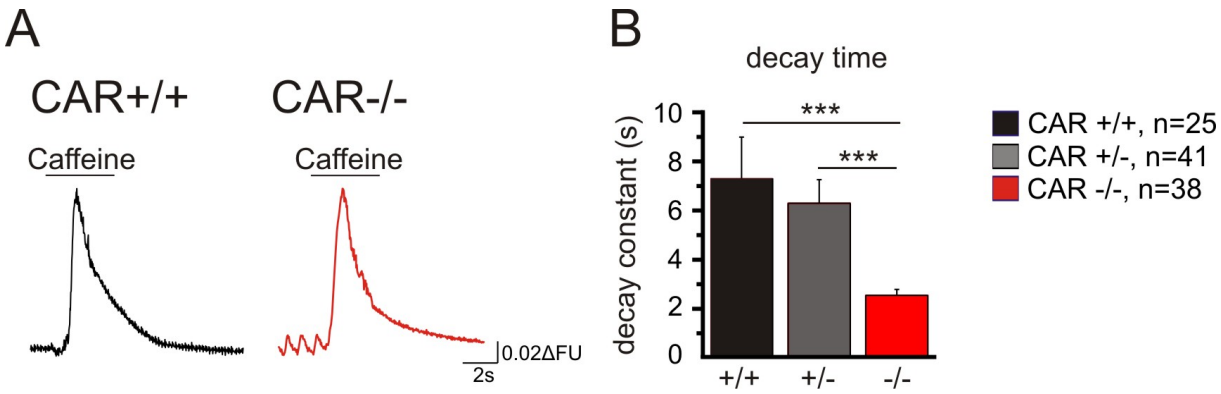

Figure 3.6: Caffeine induced Ca^{2+} transients also revealed a significant faster Ca^{2+} decline in CAR KO cardiomyocytes. Application of 10 mM caffeine triggered a long-lasting Ca^{2+} transient (A). Determination of decay time constants by using IgorPro software revealed a significant smaller decay time constant for CAR KO cardiomyocytes which indicates a faster Ca^{2+} decline (B). *** P<0.001

To investigate and evaluate the Ca^{2+} extrusion in CAR KO cardiomyocytes the rate constants for all 4 Ca^{2+} extrusion proteins were calculated by analysing the decay time constants. The rate constant (k) is defined as amount of how many Ca^{2+} per second are removed from the cytosol and can be calculated as reciprocal of the decay time constant (τ).

Quantification of Ca^{2+} extrusion rate constants

The rate constants for SERCA2, NCX, PMCA and mitochondria were calculated accordingly to Voigt et al. (2012). As described systolic Ca^{2+} decline is the combined extrusion of Ca^{2+} by SERCA2, NCX, PMCA and mitochondria. Therefore the following equation can be defined:

$$k_{syst} = k_{SERCA2} + k_{NCX} + k_{PMCA} + k_{mitochondria} \quad (1)$$

Application of caffeine triggers a complete release of Ca^{2+} from SR and uptake of cytosolic Ca^{2+} by SERCA2 is much slower compared to the fast release of Ca^{2+}. Therefore, during analysis of the Ca^{2+} decline of caffeine triggered Ca^{2+} transients SERCA2 is disregarded. The rate constant of caffeine induced Ca^{2+} transients consequently is composed of the NCX, PMCA and mitochondria extrusion:

$$k_{caff} = k_{NCX} + k_{PMCA} + k_{mitochondria} \quad (2)$$

The rate constant of SERCA2 can be calculated by replacement of equation (2) in equation (1):

$$k_{SERCA2} = k_{syst} - k_{caff} \quad (3)$$

To determine the NCX rate constant Na^{+}- and Ca^{2+}- free ACSF was applied which inhibits NCX activity completely. The cardiomyocytes were treated with 10 mM caffeine and the Ca^{2+} decline was analysed. Due to the lack of SERCA2 and NCX activity the Ca^{2+} extrusion is only performed by PMCA and mitochondria and the following equation can be defined:

$$k_{0Na+0Ca} = k_{PMCA} + k_{mitochondria} \quad (4)$$

Consequently the NCX rate constant can be calculated by substitution of equation (4) in (2):

$$k_{NCX} = k_{caff} - k_{0Na+0Ca} \quad (5)$$

The influence of PMCA on Ca^{2+} extrusion was determined by blocking NCX activity and mitochondria Ca^{2+} uptake with 20 µM Ru360. The caffeine induced cytosolic Ca^{2+} increase is only reduced by PMCA. Therefore the rate constant of PMCA can be determined by equation (6):

$$k_{0Na+0Ca,Ru360} = k_{PMCA} \quad (6)$$

Combination of equation (4) and (6) maintained the rate constant of mitochondria during Ca^{2+} extrusion:

$$k_{mitochondria} = k_{0Na+0Ca} - k_{0Na+0Ca,Ru360} \quad (7)$$

Equations 1 - 7 were used to investigate the rate constants of all 4 Ca^{2+} extrusion proteins in CAR wt and KO cardiomyocytes (fig.3.7). Rate constants for systolic Ca^{2+} decline as well as caffeine induced Ca^{2+} decline were significant higher in CAR KO cardiomyocytes compared to wt. Interestingly, also the SERCA2 rate constant is significant higher in CAR KO cardiomyocytes which revealed a higher activity of SERCA2 during extrusion of Ca^{2+}. The rate constant of NCX was also increased very strong for CAR KO cardiomyocytes. For PMCA and mitochondria the rate constants did not differ between wt and CAR KO cardiomyocytes.

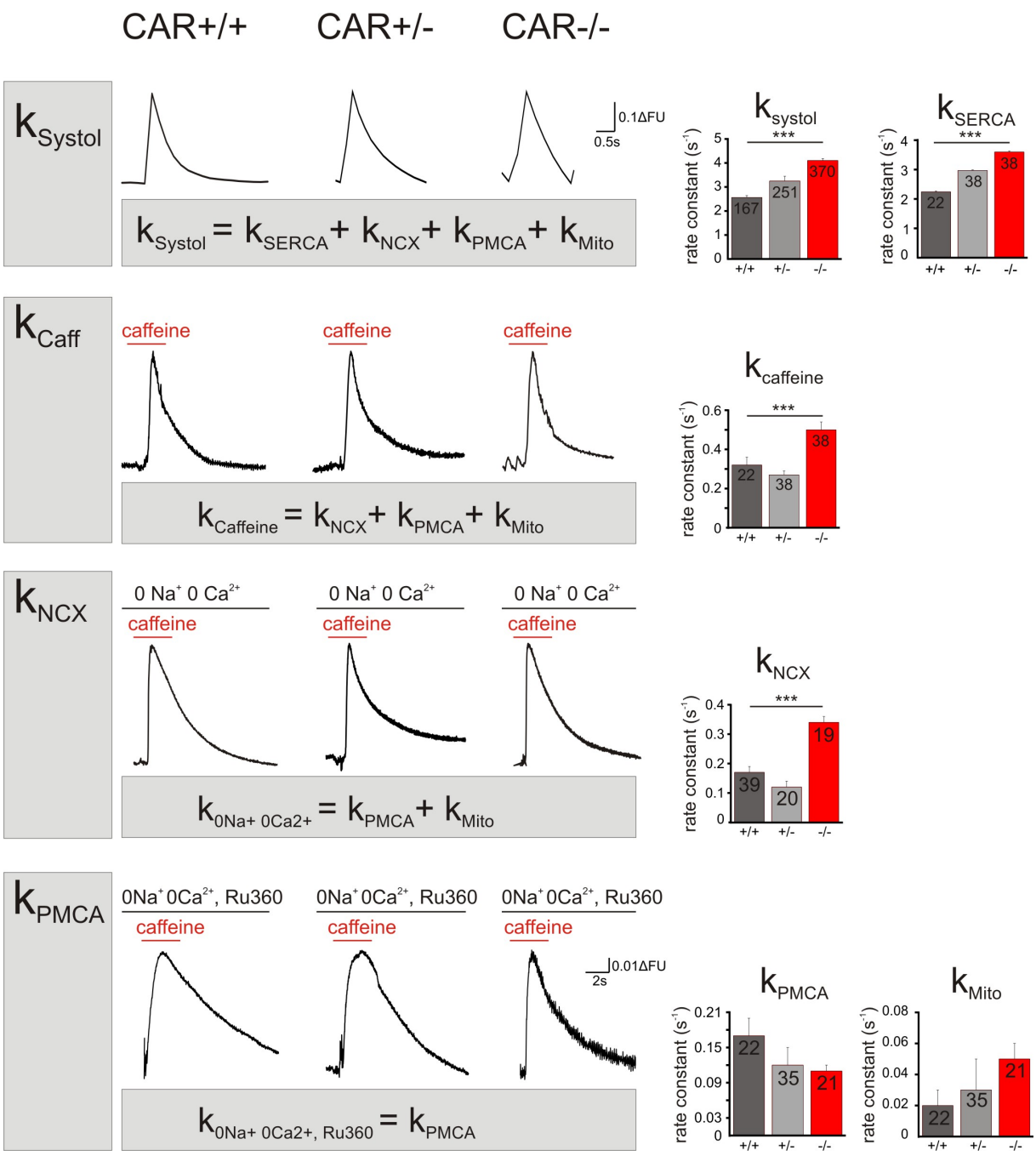

Figure 3.7: Quantification of Ca^{2+} extrusion in CAR wt and KO cardiomyocytes. Analysis of the rate constants of SERCA2, NCX, PMCA and mitochondria accordingly to Voigt et al. (2012). For further explanations see text and equations 1-7. Numbers in diagram columns indicate analysed Ca^{2+} transients. *** P<0.001

Fig.3.8 summarises the results for the quantification of the Ca^{2+} extrusion rate constants. For both, systolic Ca^{2+} decline and caffeine induced Ca^{2+} decline the rate constants in CAR KO were significant higher whereby compared to wt CAR KO cardiomycoytes revealed two times higher rate constants. During spontaneously beating the main amount of cytosolic Ca^{2+} is

extruded by SERCA2 for wt and KO cardiomyocytes. NCX, PMCA and mitochondria only play a minor role (fig.3.8 A). However, in CAR KO the rate constant for SERCA2 is significant higher. Further, NCX rate constant was increased in CAR KO cardiomyocytes. The portion of PMCA and mitochondria was only very small in both genotypes. If caffeine induced Ca^{2+} transients were analysed the major Ca^{2+} extrusion protein is NCX. Due to the lack of SERCA2 activity after caffeine application the Ca^{2+} decline is slower compared to spontaneous Ca^{2+} events (3.8 B). However, in CAR KO cardiomyocytes the rate constant was still significant higher compared to wt due to the higher activity of NCX. PMCA and mitochondria also did not play a greater role for Ca^{2+} decline.

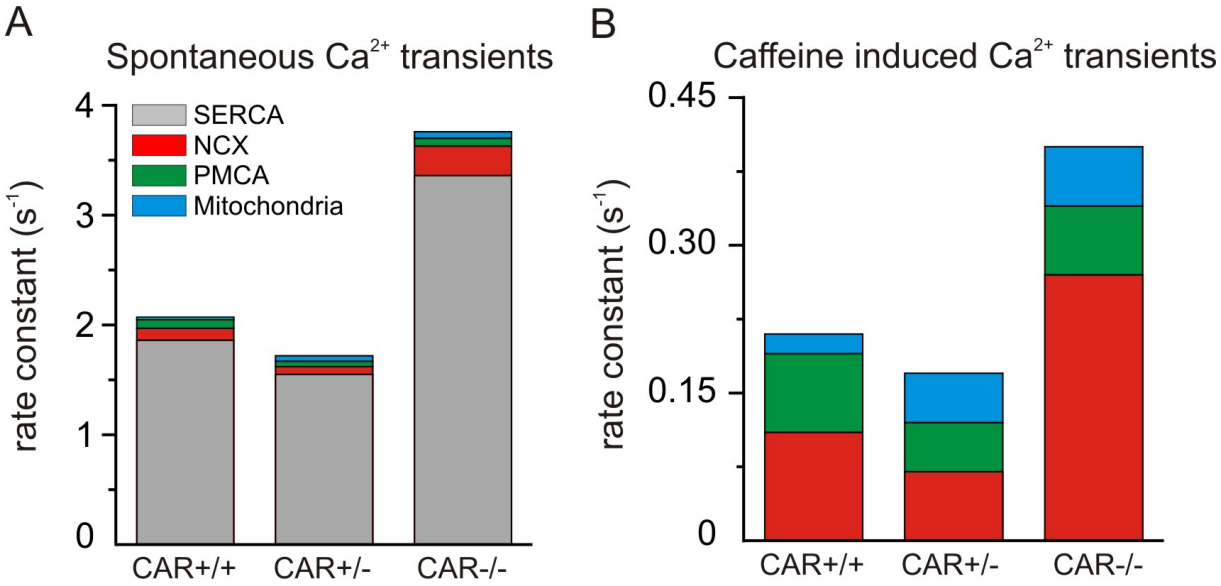

Figure 3.8: Summary of the rate constant analysis in CAR wt and KO cardiomyocytes. Ca^{2+} extrusion was investigated by determination of rate constants of SERCA2, NCX, PMCA and mitochondria. SERCA2 and NCX rate constant were significant higher in CAR KO cardiomyocytes. PMCA and mitochondria only played a minor role during Ca^{2+} decline.

Next the ratio of the respective Ca^{2+} extrusion proteins to the total cytosolic Ca^{2+} removal was calculated for spontaneous beating and caffeine induced Ca^{2+} transients (fig.3.9 A, B). Surprisingly the relative amount of Ca^{2+} which is reduced by SERCA2 did not differ between CAR wt and KO cardiomyocytes (fig.3.9 A). In cardiomyocytes of both genotypes about 90% of the cytosolic Ca^{2+} is removed by SERCA2. However, the amount of Ca^{2+} extruded by NCX was increased from 5% to 7% in CAR KO cardiomyocytes. This result indicates only a slight increase in NCX activity. However, in caffeine induced Ca^{2+} transients the proportion of NCX during intracellular Ca^{2+} removal is significant increased from ca. 50% in CAR wt cardiomyocytes to 66% in KO cardiomyocytes (fig.3.9 B). This strong induction of NCX activity in CAR KO cardiomyocytes could induce beating frequency by faster Ca^{2+} removal after systolic increase.

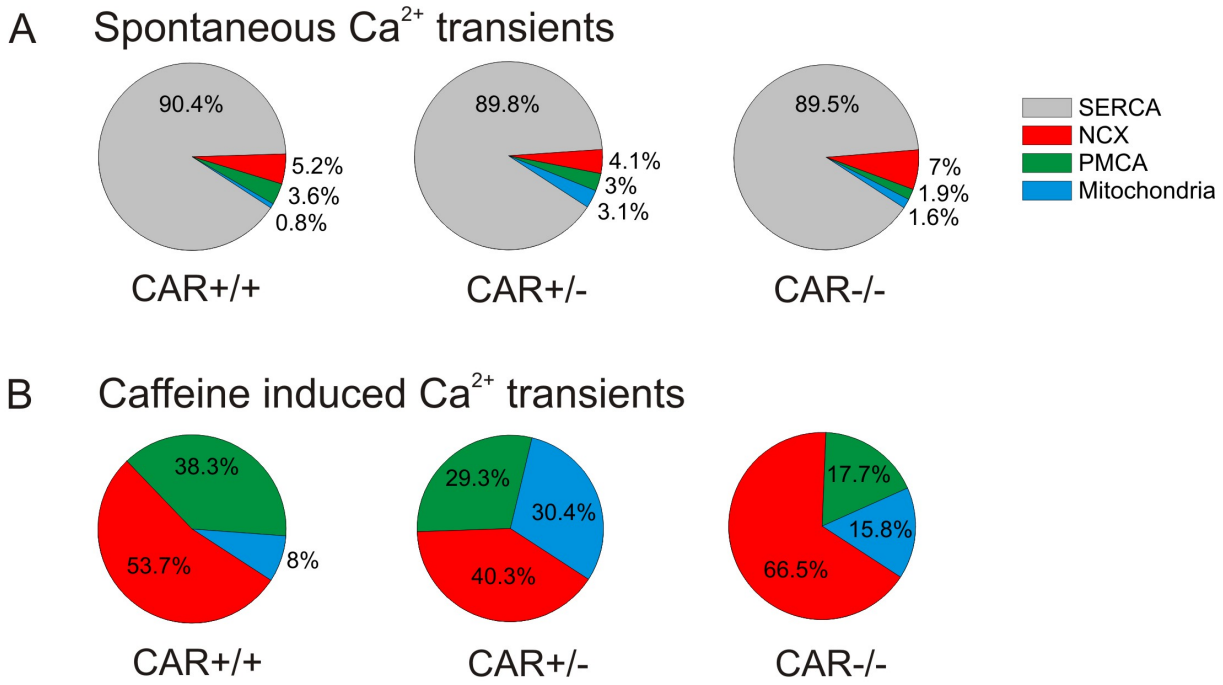

Figure 3.9: The proportion of Ca^{2+} removed by NCX is significant higher in CAR KO cardiomyocytes. The ratio of SERCA2, NCX, PMCA and mitochondria to the total removal of Ca^{2+} was calculated for spontaneous Ca^{2+} sparks and caffeine induced Ca^{2+} events. The amount of SERCA2 did not differ in wt and CAR KO cardiomyocytes (A). The amount of Ca^{2+} which is extruded by NCX is significant enhanced in CAR KO cardiomyocytes (B).

The analysis of Ca^{2+} extrusion in CAR wt and KO cardiomyocytes revealed a higher activity for SERCA2 and NCX in KO cardiomyocytes. Therefore the influence of SERCA2 and NCX on beating in cardiomyocytes is further investigated by calcium imaging, gene expression and western blot.

3.2.4 NCX activity is enhanced in CAR KO cardiomyocytes

The function of NCX in E10.5 cardiomyocytes was investigated by recording caffeine induced Ca^{2+} transients because SERCA2 Ca^{2+} transport into SR is slower than Ca^{2+} release via RyR and therefore under these experimental conditions NCX is the major Ca^{2+} extrusion protein. Application of caffeine triggers a long-lasting Ca^{2+} transient which is faster removed in CAR KO cardiomycytes (fig.3.10 A, black example trace). If NCX is blocked by extracellular 5 mM Ni^{2+} the Ca^{2+} decline dramatically increased in CAR KO cardiomyocytes (fig.3.10 A, B, green example trace). Further no difference is found anymore between the calculated decay time constants of wt and KO cardiomyocytes. To verify this result NCX activity was completely decreased by replacement of ACSF with Na^{+}- and Ca^{2+}- free ACSF. Analysis of caffeine induced Ca^{2+} transients also revealed a strong induction of the decay time constants for both genotypes

(fig.3.10 C, D, violet example trace). Also after blocking NCX there was no difference anymore between CAR wt and KO Ca^{2+} decline which indicates further that NCX activity is enhanced in CAR KO cardiomyocytes.

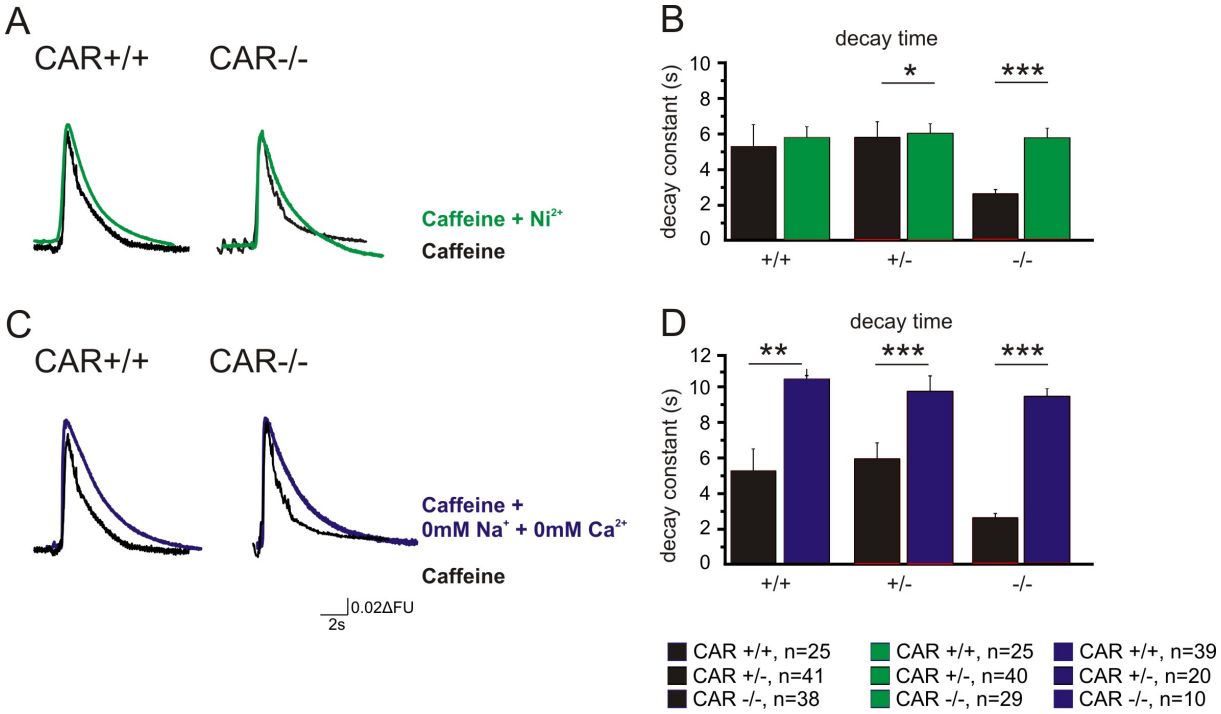

Figure 3.10: Enhanced NCX activity in CAR KO cardiomyocytes. E10.5 cultivated cardiomyocytes were loaded with Fura-2AM and caffeine (10 mM) induced Ca^{2+} transients were recorded at DIV4 (A, C). After blocking NCX by 5 mM Ni^{2+} (A, B) or Na^{+}- and Ca^{2+}- free ACSF (C, D) the Ca^{2+} decay time constant was calculated by Origin7.5 software. In both conditions, the Ca^{2+} decline increased dramatically when NCX is blocked (B, D). No significant change in decay time constants was detected anymore between CAR wt and KO cardiomyocytes. * P<0.05, ** P<0.01, *** P<0.001

To further verify the change of NCX activity in CAR KO cardiomyocytes the extracellular Na^{+} concentration was changed. As an antiporter system NCX can be regulated by intracellular Ca^{2+} concentration and extracellular Na^{+} concentration. An increase of extracellular Na^{+} increases the transport rate of Na^{+} into the cell and Ca^{2+} extrusion whereby the beating frequency rises. Increase from 130 mM to 180 mM extracellular Na^{+} resulted in a significant increase in beating frequency in CAR wt and KO cardiomyocytes (fig.3.11 A-C). Both genotypes strongly induced their frequency of spontaneous Ca^{2+} transients. However, CAR KO cardiomcytes still beat significant faster than wt cardiomcytes (fig.3.11 B). Surprisingly, the strongest induction of spontaneous beating was observed for CAR wt cardiomyocytes (fig.3.11 C), compared to CAR KO wt cardiomcytes increase their beating frequency up to 216% (CAR KO: 148%). Nevertheless, the increase was not significant, only CAR KO and hz cardiomyocytes revealed a significant induction compared to 130 mM extracellular Na^{+} concentration. Furthermore, the observed difference in induction of beating between CAR wt and KO was not significant (fig.3.11 C). After decrease of extracellular Na^{+} to 50 mM the beating frequency is reduced in wt cardiomyocytes

about 60% (fig.3.11 A, D, E). CAR KO cardiomyocytes also decreased the beating frequency but compared to wt the reduction was only around 40% and CAR KO cardiomyocytes still beat significant faster (fig.3.11 D, E). This results indicates that CAR KO cardiomyocytes were less sensitive to reduced extracellular Na^+ concentration possibly due to increased NCX protein level or raise in activity of the Na^+ and Ca^{2+} uniporter system.

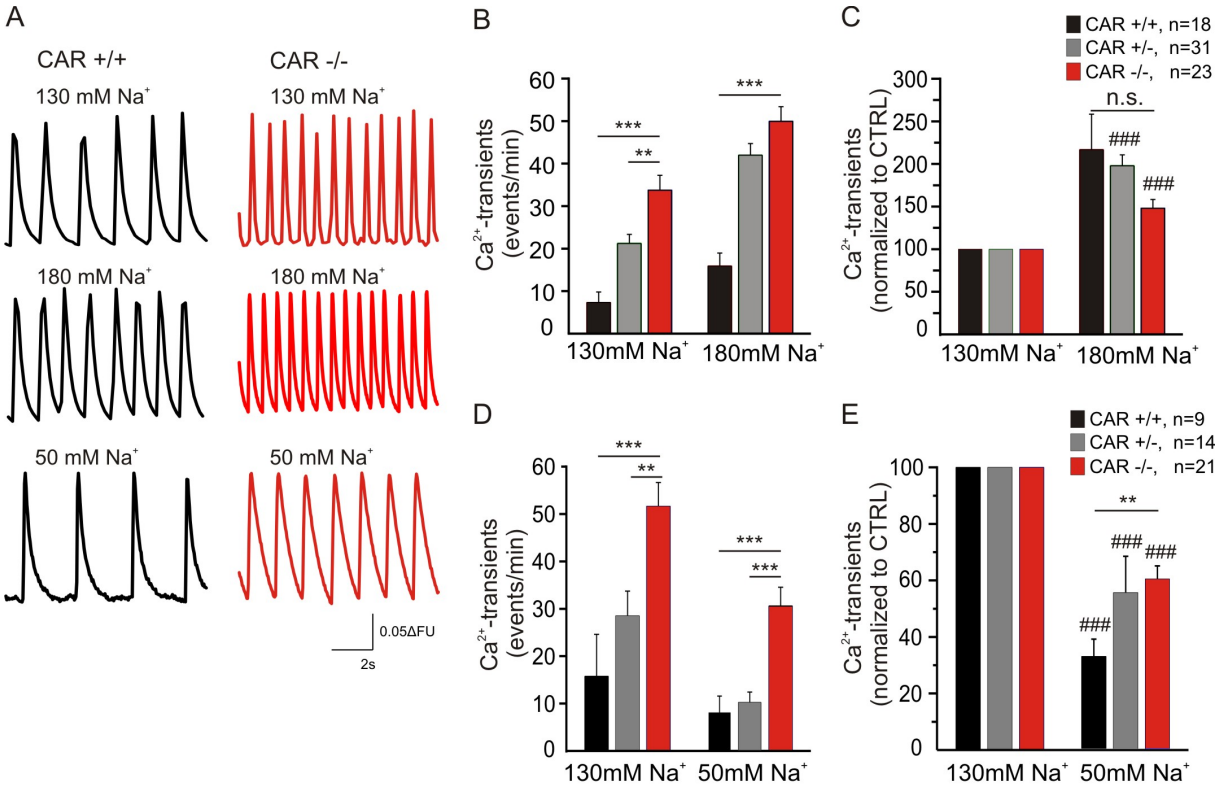

Figure 3.11: Alterations of NCX activity by changing extracellular Na^+ concentration. During calcium imaging the normal ACSF Na^+ concentration of 130 mM was raised to 180 mM to increase NCX activity (A, B, C). The reduction from 130 mM to 50 mM extracellular Na^+ reduced the NCX activity in wt and CAR KO cardiomyocytes (A). Compared to wt, CAR KO cardiomyocytes still revealed a significant higher beating frequency (D, E). * P<0.05, ** P<0.01, *** P<0.001; ### P<0.001 compared to 130 mM extracellular Na^+ concentration (CTRL, 100%).

Expression of NCX was analysed by real-time PCR, Western Blot and immunostaining of E11 embryo cryostat sections (fig.3.12). Gene expression analysis by real-time PCR did not reveal a significant difference for CAR wt and KO hearts (A). On protein level, NCX is also detected equally in wt and KO hearts as shown in the western blot (B). Further, E11 embryo cryostat sections were stained against NCX and CAR. Compared to the wt hearts, CAR KO sections did not differ in the staining of NCX (C). For both genotypes, the sections illustrate an uniform NCX staining in the heart tubules.

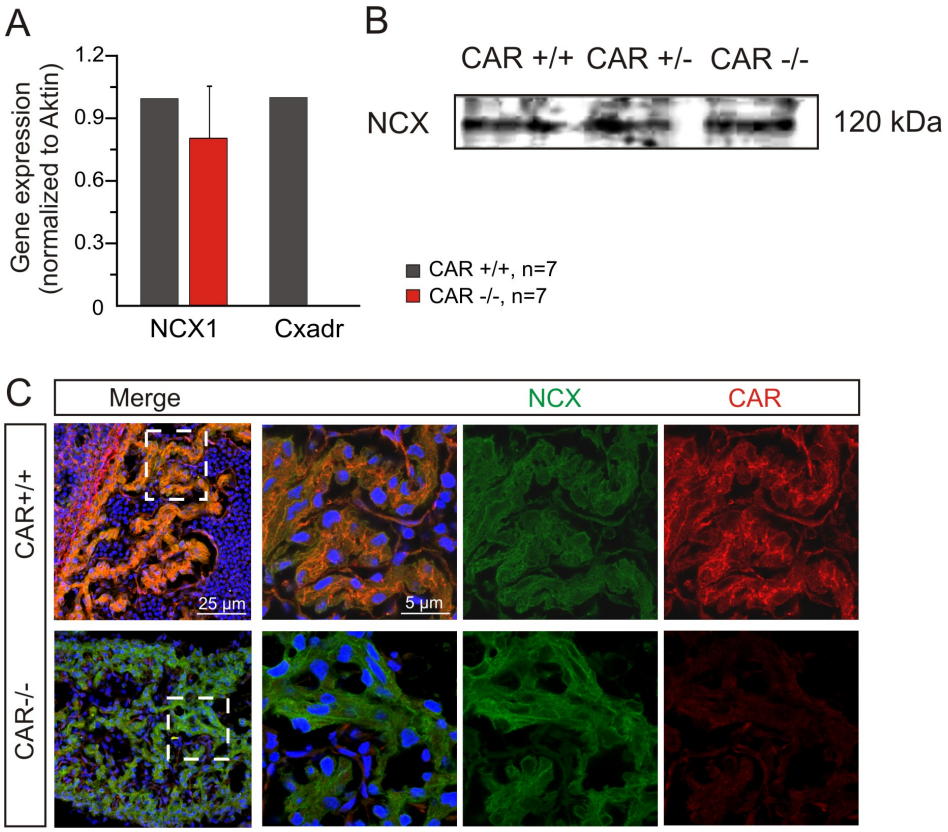

Figure 3.12: The NCX gene expression is not changed in CAR KO hearts. E10.5 hearts were dissected and RNA was isolated and NCX gene expression was analysed by real-time PCR. No significant change in NCX expression level was observed in CAR KO heart (A). Western blot analysis of NCX also did not reveal any difference between wt and CAR KO hearts (B). Staining of E11 embryo cryostat sections with the antibody against NCX (green) showed no change in fluorescence intensity or distribution within the heart (C). CAR - red, DAPI - blue.

During CAR KO beating NCX is strongly involved in Ca^{2+} extrusion. It was shown that NCX rate constant is significant higher compared to wt cardiomyocytes. After caffeine application mainly NCX reduced the cytosolic Ca^{2+}. Further the experiments revealed in CAR KO cardiomyocytes a significant higher stability to reduced extracellular Na^{+} with regard to beating frequency. To conclude, the higher NCX activity is a major cause of the faster beating in CAR KO cardiomyocytes. However, also the SERCA2 rate constant was increased. Therefore the following experiments will analyse the influence of SERCA2 on beating in CAR KO cardiomyocytes.

3.2.5 The role of SERCA2 during beating and Ca^{2+} extrusion

The rate constant of SERCA2 was significant higher in CAR KO cardiomyocytes compared to wt as described above. During systolic Ca^{2+} extrusion mainly SERCA2 removes cytosolic Ca^{2+}

and therefore SERCA2 also could increase the beating frequency in CAR KO cardiomyocytes. To analyse the influence of SERCA2 on beating frequency and Ca^{2+} cycling SERCA2 was at first blocked by 10 µM thapsigargin for 20 min and beating was recorded by calcium imaging. As expected in wt cardiomyocytes the beating frequency was dramatically reduced (fig.3.13 A-C). Inhibition of SERCA2 lead to decrease in Ca^{2+} extrusion and prevents the re-uptake of cytosolic Ca^{2+} to SR which is needed to induce the next beat. Surprisingly, CAR KO cardiomyocytes did not change the beating after blocking SERCA2 at 10 µM thapsigargin. Compared to wt CAR KO cardiomyocytes beat significant faster during the whole experiment (fig.3.13 B, C). Beating of wt cardiomyocytes was significant reduced and in contrast in CAR KO cardiomyocytes no alterations were detected (fig.3.13 C).

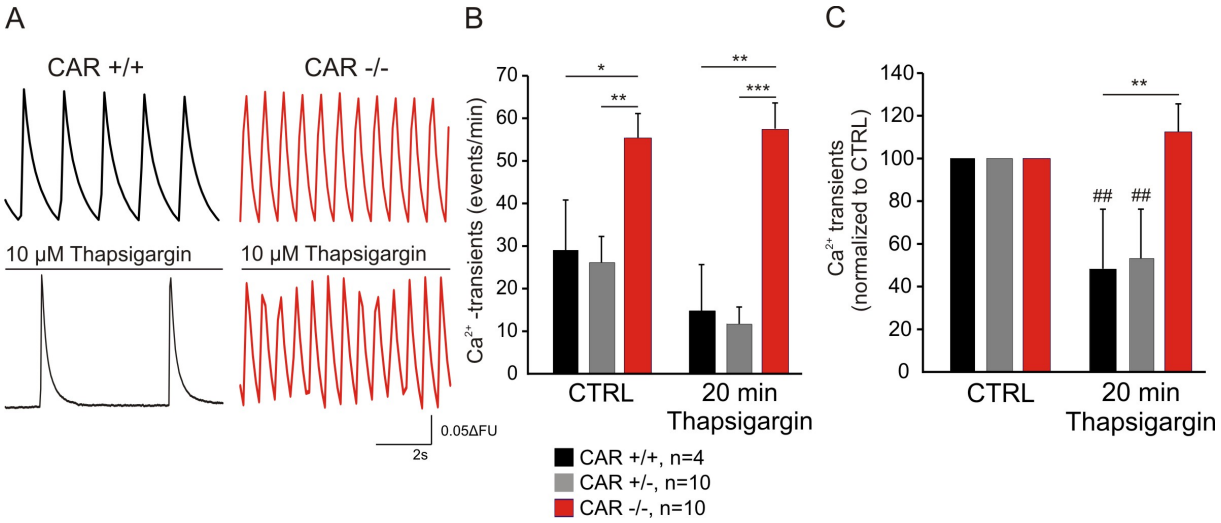

Figure 3.13: Inhibition of SERCA2 by thapsigargin did not change beating in CAR KO cardiomyocytes. Beating frequency was recorded by calcium imaging. In wt cardiomyocytes incubation with 10 µM thapsigargin decreased the beating significant (A, C ## P<0.01, compared to CTRL). Beating frequency of CAR KO cardiomyocytes did not change after thapsigargin treatment (A-C). * P<0.05, ** P<0.01, *** P<0.001

To verify this result a second SERCA2 inhibitor (CPA) was applied and the beating was analysed by calcium imaging. After application of 10 µM CPA the recorded wt Ca^{2+} transients revealed decreasing Ca^{2+} transients amplitudes (fig.3.14 A). After 30 min of CPA incubation wt cardiomyocytes did not beat anymore (fig.3.14 A, C). In contrast, in CAR KO cardiomyocytes spontaneous Ca^{2+} transients could be detected after CPA treatment. Also after 30 min of CPA incubation, CAR KO cardiomyocytes still beat uniform (fig.3.14 A, C). However, comparison of the calculated decay time constants of CAR KO Ca^{2+} transients before and after CPA application revealed a significant higher decay time for CPA treated transients (fig.3.14 D). The increase in Ca^{2+} decline is caused by CPA which blocks SERCA2 and therefore only NCX, mitochondria and PMCA remove systolic Ca^{2+}. These slower Ca^{2+} transports result in a slower extrusion of systolic Ca^{2+} compared to involvement of fully active SERCA2 Ca^{2+} extrusion.

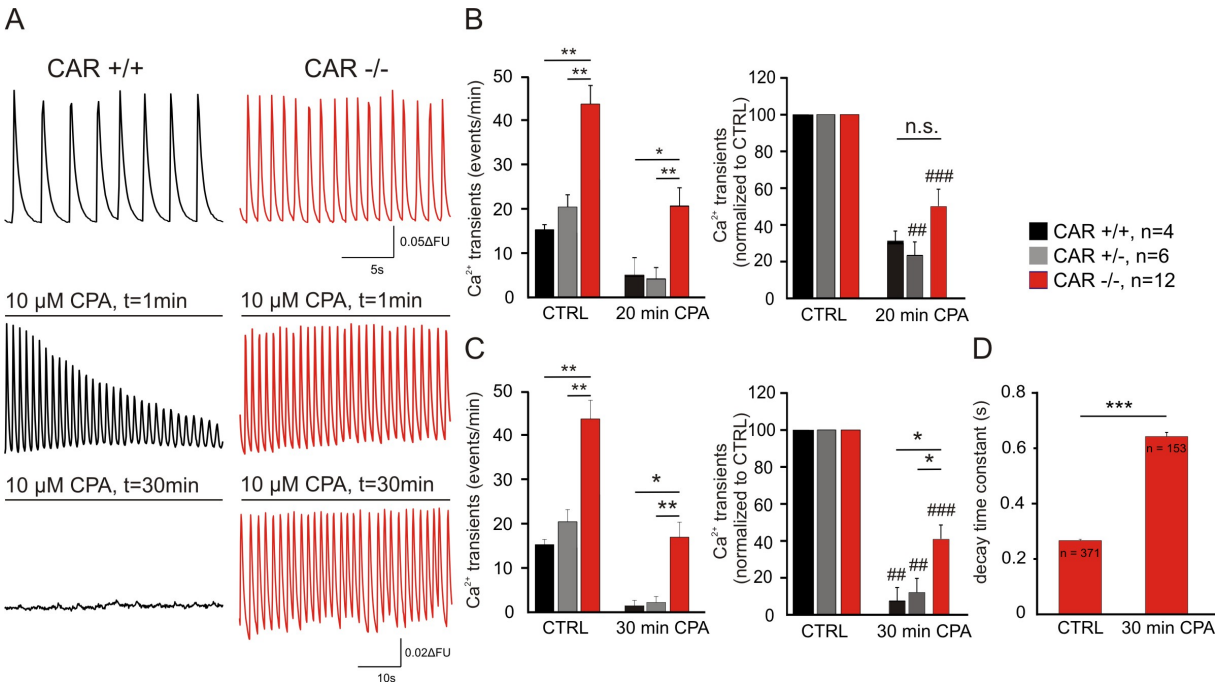

Figure 3.14: Blocking of SERAC2 by CPA. Application of SERCA2 inhibitor CPA decreased the amplitudes of wt Ca^{2+} transients already after 1 min (A). Beating frequency was strongly reduced in wt cardiomyoctes after 20 min (B). 30 min of CPA incubation caused complete stop of beating in wt (C). CPA treatment also reduced beating frequency in CAR KO cardiomyocytes (B, C). Compared to wt CAR KO beating is still significant faster (C). Decay time analysis by IgorPro revealed increase in Ca^{2+} decline after CPA treatment (D). * P<0.05, ** P<0.01, *** P<0.001; ## P<0.01, ### P<0.001 compared to CTRL (100%)

Blocking of SERCA2 by thapsigargin showed after 20 min incubation a severe reduction of beating frequency in wt cardiomyocytes. In contrast, a complete lack of beating after CPA application was not detected before 30 min of CPA treatment, but CPA already reduced the amplitudes of the recorded Ca^{2+} transients after 1 min. This difference of inhibition impact on SERCA2 and corresponding beating was also noticeable in CAR KO cardiomyocytes. Blocking SERCA2 by thapsigargin did not change the CAR KO beating. However, CPA treated CAR KO cardiomyocytes decreased the beating frequency after 20 min of incubation about 50% (fig.3.14 B). 30 min of CPA application still revealed a significant difference between wt and CAR KO beating. Also the example traces of Ca^{2+} transients showed for CAR KO constant beating compared to no beating in wt cardiomyocytes.

The reduced sensitivity of CAR KO cardiomyocytes to SERCA2 blockers could be caused by increased expression of SERCA2 or reduced PLB. Binding of PLB to SERCA2 deactivates the Ca^{2+} removement from cytosol inside the sarcoplasmic reticulum. After phosphorylation of PLB and SERCA2 by PKA the PLB monomer separates from SERCA2 and reassembles to PLB di-, tri- or pentamers (Frank & Kranias, 2000; Simmerman & Jones, 1998). Therefore decreased PLB expression could also effect beating frequency.

At first, E11 embryo cryostat sections were stained against SERCA2 and CAR (fig.3.15 A, B). CAR wt and KO hearts showed no difference in SERCA2 staining. CAR staining was completely abolished in CAR KO hearts.

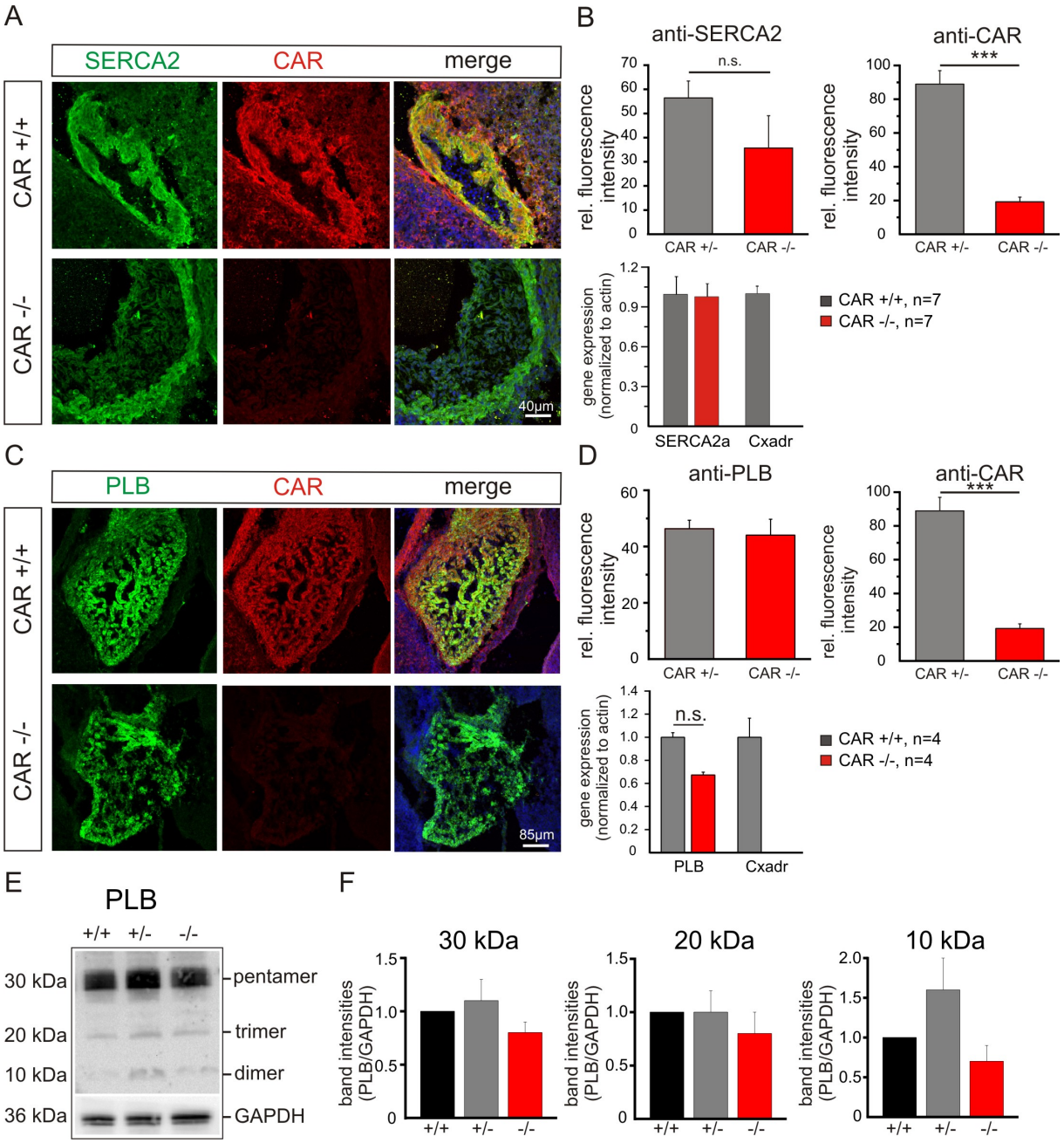

Figure 3.15: SERCA2 and PLB expression is not changed in CAR KO cardiomyocytes. E11 embryo cryostat sections were stained against SERCA2 and CAR (A, B) or against PLB and CAR (C, D). Fluorescence intensity was measured by Zeiss Zen software (B, D). There was no significant change in SERCA2 fluorescence intensity in wt and CAR KO heart sections (B). PLB staining also did not reveal any change (D). Gene expression analysis of SERCA2a and PLB was not different in CAR wt and KO hearts. PLB protein level was further investigated by western blot (E, F). Wt and CAR KO hearts showed the same ratio of PLB di-, tri and pentamers (F). *** P<0.001

To evaluate the SERCA protein level the fluorescence intensity was calculated by using Zeiss Zen software (fig.3.15 B). CAR KO cryostat sections revealed less SERCA staining. There was no significant change found. The reduced staining could be caused by smaller tissue sections or different parts of the investigated tissue. PLB staining also was similar for both genotypes (fig.3.15 C, D). Measurement of PLB fluorescence intensity in CAR KO heart sections was not altered compared to wt hearts. Further, gene expression analysis was performed by using real-time PCR. The cardiac gene SERCA2a was investigated in wt and KO hearts and no distinction was obtained. The same result was found for PLB expression analysis (fig.3.15 B, D). PLB was also investigated on protein level by western blot. The PLB monomer has a size of 6 kDa, but the applied antibody against PLB only detects di-, tri- and pentamer forms. Western blot band analysis of the PLB forms was done by Quantity One software and CAR wt and KO did not show any difference in their band intensities (fig.3.15 E, F).

In summary, SERCA2 and PLB gene expression as well as protein level did not differ in CAR KO hearts. Therefore the reduced sensitivity for SERCA2 blockers thapsigargin and CPA in regard to cardiomyocyte beating was not caused by an over expression of SERCA2 or down regulation of PLB.

3.2.6 The role of mitochondria during beating

Mitochondria are able to store Ca^{2+} for long- and short-term and therefore mitochondria also can influence Ca^{2+} extrusion and beating cycling in cardiomyocytes (Dedkova & Blatter, 2013; Gustafsson & Gottlieb, 2008). However, it was never studied the role of mitochondria during early embryonic beating. To analyse the role of mitochondria in Ca^{2+} extrusion mechanism the Ca^{2+} uptake via mitochondrial Ca^{2+} uniporter (mCU) was blocked by Ru360 and the release of mitochondrial Ca^{2+} via mitochondrial NCX (mNCX) was inhibited by CGP-37157. Afterwards the beating frequency and the corresponding Ca^{2+} transients were recorded by calcium imaging.

Application of 20 µM Ru360 increased the beating frequency in CAR wt cardiomyocytes compared to no change of beating in KO cardiomyocytes (fig.3.16 A-C). The wt beating was increased about 50% after 30 min incubation with Ru360. The increase in beating is caused due to the lack of the slow and long-term storage of cytosolic Ca^{2+} inside the mitochondria. Therefore more cytosolic Ca^{2+} is removed by SERCA2 to sarcoplasmic reticulum which afterwards can be released faster and more frequently. CAR KO cardiomyocytes did not increase the beating after blocking the mitochondrial Ca^{2+} uptake possibly because the KO beating frequency is already at its maximal rate. The inhibition of mNCX by 20 µM CGP-37157 completely abolished the Ca^{2+} release from mitochondria to cytosol. Both, CAR wt and KO cardiomyocytes stopped beating already after 5 min incubation with CGP-37157 (fig.3.16 A, D, E). The results suggest that mitochondria are very important for cytosolic Ca^{2+} extrusion already during early heart

beats. However, the increased beating of CAR KO cardiomyocytes was not caused by altered Ca^{2+} handling in mitochondria.

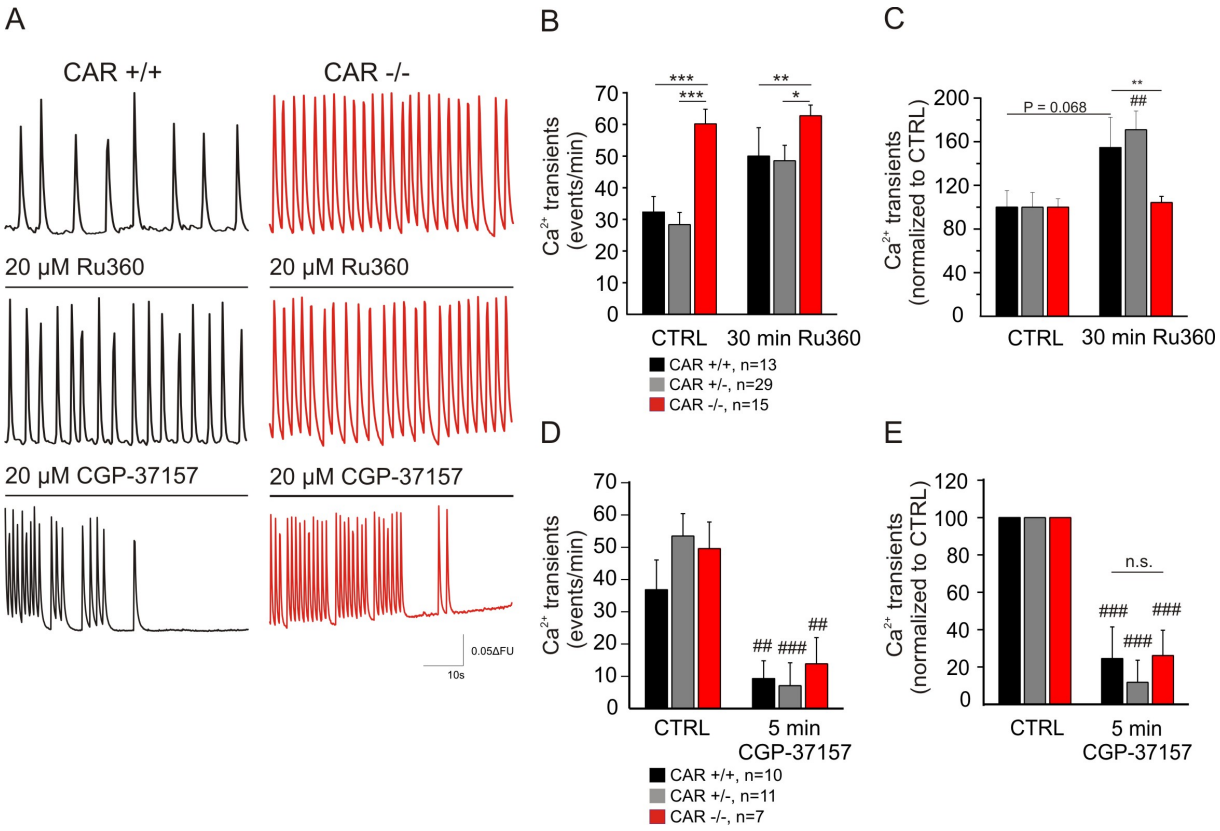

Figure 3.16: Mitochondria are involved in beating and Ca^{2+} extrusion mechanism in cardiomyocytes. CAR wt and KO cardiomyocytes were treated with 20 µM Ru360 and Ca^{2+} transients and beating was recorded by calcium imaging (A-C). Wt cardiomyocytes increased the beating frequency after 30 min of Ru360 incubation (B, C). CAR KO beating was not altered (B, C). Mitochondrial Ca^{2+} release via mNCX was blocked by application of 20 µM CGP-37157 and CAR wt and KO cardiomyocytes stopped beating after 5 min (A, D, E). * P<0.05, ** P<0.01, *** P<0.001; ## P<0.01, ### P<0.001 compared to CTRL (100%)

Dorner et al. (2005) published a size increase of mitochondria in heart sections of E11 embryos. Therefore, the mitochondria size of cultivated E10.5 cardiomyocytes was also measured by a specific mitochondrial fluorescence dye. 200 µM MitoTracker Red (Invitrogen) was applied for 30 min to CAR wt and KO cardiomyocytes and afterwards the mitochondria size was analysed in Zeiss Zen and LSM software. In contrast to Dorner et al. (2005) no raise in mitochondria size was detected for CAR KO cardiomyocytes (fig.3.17 A, B). For both genotypes, the calculated mitochondria area did not differ significant.

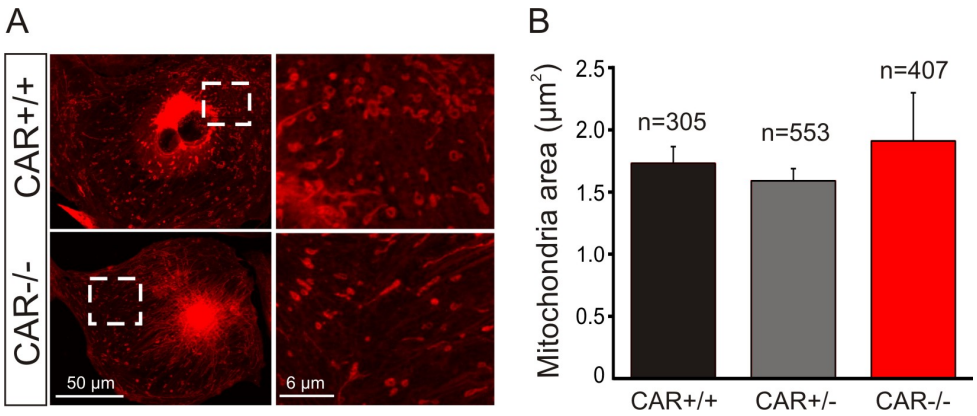

Figure 3.17: Analysis of mitochondria size in CAR wt and KO cardiomyocytes. E10.5 cultivated CAR wt and KO cardiomyocytes were treated with 200 µM MitoTracker Red for 30 min. Afterwards the mitochondria were analysed by confocal microscopy (A) and the area was measured with Zeiss LSM software (B).

3.2.7 cAMP concentration in CAR KO hearts

As second messenger cAMP plays an important role in many cellular processes like growth, metabolism or movement (Zaccolo & Pozzan, 2002). By β-adrenergic stimulation in the heart, cAMP is generated via a G-protein mediated process which then phosphorylates protein kinase A (PKA). Activation of PKA leads to phosphorylation of L-type Ca^{2+} channels, SERCA2 and PLB which induces Ca^{2+} cycling and therefore beating frequency of the heart as well as an increase in strength and duration of contraction (Wallukat, 2002; Zaccolo & Pozzan, 2002). Raised basal cAMP concentration therefore could induce beating frequency in CAR KO cardiomyocytes. Consequently cAMP concentration of E11 CAR wt and KO hearts was measured. Nevertheless, no difference in basal cAMP level was determined (fig.3.18).

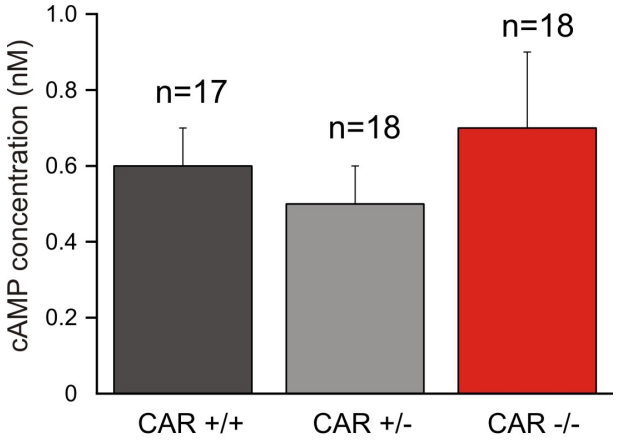

Figure 3.18: Basal cAMP concentration was not changed in CAR KO hearts. E11 embryo hearts were dissected and measurement of cAMP was performed. No significant change in CAR KO hearts was determined.

3.2.8 HCN channel expression and the influence of the corresponding I_f on beating was not changed in CAR KO cardiomyocytes

Several studies suggested that early embryonic heart beats were mainly induced by HCN pacemaker channel current (funny current, I_f) and L-type Ca^{2+} channel currents whereby the influence of HCN channels on the beating frequency was studied in detail (Liang et al., 2010; Stieber et al., 2003; Yasui et al., 2001). The hyperpolarization-activated cation current is activated by hyperpolarization of the membrane, carries K^+ and Na^+ and can be induced by cAMP binding (Biel et al., 2002; Liang et al., 2010; Yasui et al., 2001). Analysis of the role of HCN channels during beating in E10.5 cardiomyocytes was performed by calcium imaging and real-time PCR (fig.3.19 A-D).

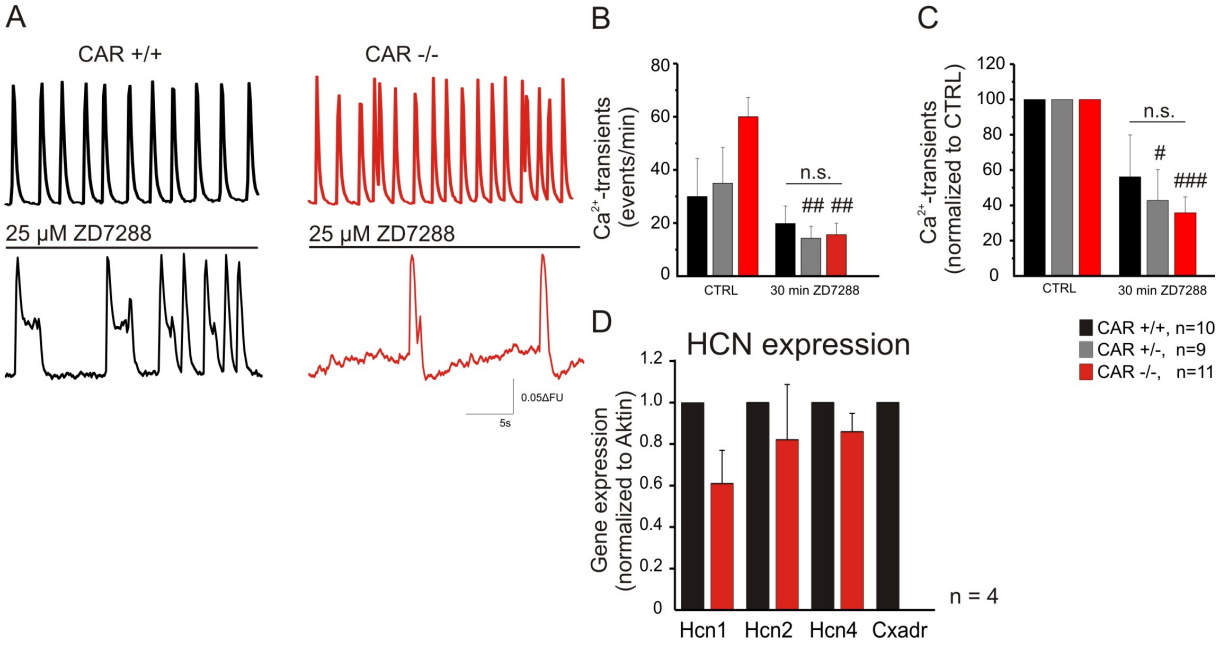

Figure 3.19: HCN channel expression and corresponding I_f was not changed in CAR KO cardiomyocytes. E10.5 cardiomyocytes were analysed by calcium imaging after incubation with 25 µM Zd7288 for 30 min (A). Zd7288 blocks specifically HCN channels and lead to decreasing beating frequency (B, C). No differences were found in CAR KO cardiomyocytes compared to wt. Hcn1, Hcn2 and Hcn4 gene expression was determined by real-time PCR but did not reveal any variation in CAR KO gene expression (D). # P<0.05, ## P<0.01, ### P<0.001 compared to CTRL (100%)

Ca^{2+} transients of CAR wt and KO cardiomoycytes were recorded after treatment with HCN channel blocker Zd7288. After 30 min of incubation the beating frequency was strongly reduced for both genoytpes (fig.3.19 B, C). The recorded Ca^{2+} transients did not show a normal decay trend (fig.3.19 A). Often long-term Ca^{2+} transients or un-coordinated burst of Ca^{2+} raise was detected. Further gene expression of the cardiac HCN genes Hcn1, Hcn2 and Hcn4 was studied by real-time PCR. However, no significant change in expression was found in CAR KO hearts compared to wt. These results suggest that HCN and its corresponding current do not cause the

increased beating frequency in CAR KO cardiomyocytes.

3.2.9 Cytosolic Ca^{2+} concentration in CAR knockout cardiomyocytes was not changed

In beating and conctraction of the heart Ca^{2+} is a major regulator which is involved in all processes. Cytosolic Ca^{2+} concentration itself can influence strength, duration and frequency of contraction and therefore intracellular Ca^{2+} concentration was measured (Doeller & Wittenberg, 1990). During steady state (diastole) 120 nM free Ca^{2+} was measured for CAR wt cardiomyocytes. Also CAR KO cardiomyocytes showed similar values of 130 nM. Systolic Ca^{2+} amount was found between 350-450 nM for both genotypes (fig.3.20). However, for CAR KO cardiomyocytes no significant change in intracellular Ca^{2+} concentration during the beating cycle was detected.

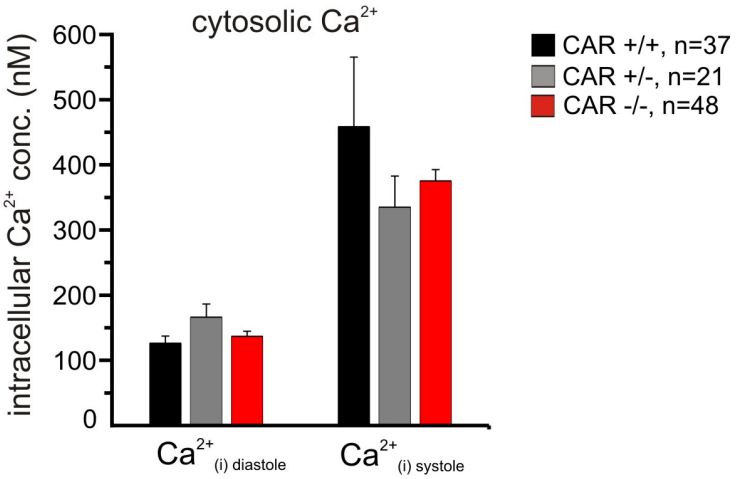

Figure 3.20: Cytosolic Ca^{2+} concentration in CAR KO cardiomyocytes did not differ from wt cardiomyocytes. Intracellular Ca^{2+} concentration of E10.5 cardiomyocytes was measured (Doeller & Wittenberg, 1990) and did not reveal any difference between wt and KO cardiomyocytes.

3.2.10 The influence of the sarcoplasmic reticulum on CAR KO beating

As internal Ca^{2+} store the sarcoplasmic reticulum (SR) plays an important role in Ca^{2+} regulation and cycle in cardiac cells. Uptake of Ca^{2+} from cytosol to sarcoplasmic reticulum is performed by SERCA2 whereby this Ca^{2+} pump itself is regulated by PLB. Ca^{2+} release from SR to cytosol is mainly realised by ryanodine receptors (RyR) and IP_3 receptors (IP3R) (Bers, 2002). In the following experiments the SR Ca^{2+} content and the SR Ca^{2+} leak was calculated and gene expression of RyR2 and IP_3R2 was determined. The influence of SERCA and PLB was further investigated as Ca^{2+} extrusion mechanism (compare chapter 3.2.5).

SR Ca^{2+} content

To measure SR Ca^{2+} content 10 mM caffeine was applied to E10.5 cardiomyocytes. Caffeine triggers a complete release of Ca^{2+} which is stored in the SR. By using calcium imaging a long lasting Ca^{2+} transient was recorded shortly after caffeine application. The amplitude size revealed the amount of Ca^{2+} which was released. Comparison of wt and CAR KO caffeine induced Ca^{2+} transients did not show any difference (fig.3.21). This results suggest that the amount of stored Ca^{2+} inside the SR is not changed in CAR KO cardiomyocytes.

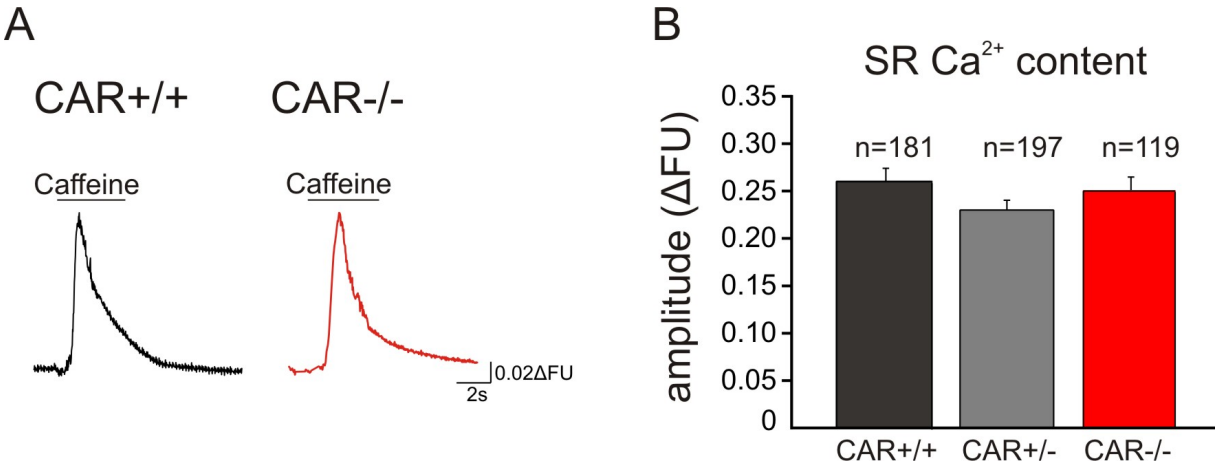

Figure 3.21: SR Ca^{2+} content did not differ in CAR KO cardiomyocytes compared to wt cardiomyocytes. Application of 10 mM caffeine triggers a complete release of Ca^{2+} which is stored in SR and can be detected by a long lasting Ca^{2+} transient. Comparison of the amplitude size did not revealed any significant change between CAR wt and KO cardiomyocytes.

Quantification of the SR Ca^{2+} leak

The SR Ca^{2+} leak can be defined as spontaneous SR Ca^{2+} release events via ryanodine receptors which are not corresponding to the normal excitation coupling process (Bers, 2014). Often these spontaneous Ca^{2+} events occur during fibrillation of the heart and therefore these events also could induce spontaneous beating of cardiomyocytes (Neef et al., 2010; Voigt et al., 2012). Measurement of the SR Ca^{2+} leak was performed in cultivated cardiomyocytes (Shannon, 2002; Voigt et al., 2012). Calcium imaging was used to record the change in cytosolic Ca^{2+} concentration (fig.3.22 A). Application of 1 mM tetracaine to Na^{+}- and Ca^{2+}- free ACSF completely blocked the ryanodine receptors and therefore the SR Ca^{2+} leak which consequently decreased the cytosolic Ca^{2+} concentration (fig.3.22 A). Wt and CAR KO cardiomyocytes did not show any significant difference in the intracellular Ca^{2+} drop (fig.3.22 B). Afterwards caffeine was applied to the cells which induced a complete SR release of Ca^{2+}. There was no difference of the Ca^{2+} transient amplitude between wt and CAR KO cardiomyocytes (fig.3.22 C).

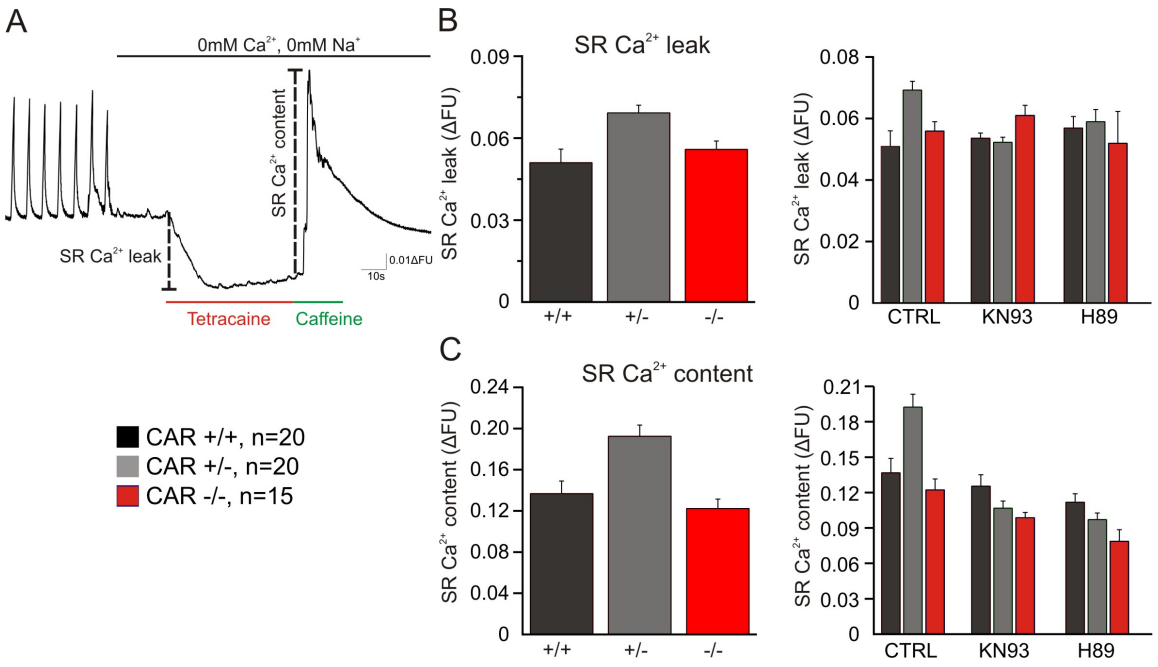

Figure 3.22: Quantification of the SR Ca^{2+} leak did not reveal a change in CAR KO cardiomyocytes. Determination of the SR Ca^{2+} leak by application of 1 mM tetracaine did not indicate a significant change between CAR wt and KO cardiomyocytes (A, B). Caffeine treatment induced a complete release of Ca^{2+} stored in the SR (A, C). Inhibition of CamKII or PKA by 1 µM KN-93 or 10 µM H89 did not vary the amount of measured SR Ca^{2+} leak (B, C).

The SR Ca^{2+} leak can be induced by hyperphosphorylation of ryanodine receptors via CamKII and PKA (Voigt et al., 2012). To determine the effect of phosphorylation of ryanodine receptors on the amount of SR Ca^{2+} leak both CamKII and PKA were inhibited by 1 µM KN-93 (CamKII inhibitor) or 10 µM H89 (PKA inhibitor) and afterwards tetracaine was applied to detect the Ca^{2+} leak (fig.3.22 B,C). However, no significant change was observed for CAR KO cardiomyocytes compared to wt cardiomyocytes. Blocking of CamKII or PKA did not show any effect on the SR Ca^{2+} leak level in CAR wt and KO cardiomyocytes as well as on the stored SR Ca^{2+} amount. This results could indicate that phosphorylation of ryanodine receptors only plays a minor role in early embryonic heart beating.

RyR and IP3R expression analysis

Expression of cardiac ryanodine receptor (RyR2) and cardiac IP3 receptor (IP3R2) was analysed by real-time PCR. An increase of both SR Ca^{2+} release channels could induce the beating frequency of cardiomyocytes and hearts. However, compared to wt hearts CAR KO hearts did not show a significant increase in gene expression for both genes (fig.3.23).

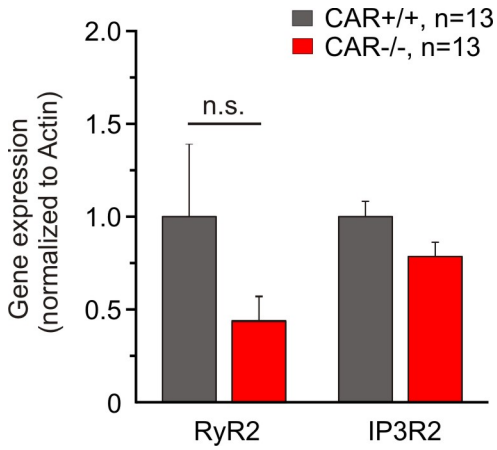

Figure 3.23: Expression of RyR2 and IP3R2 was not altered in CAR KO hearts. Gene expression of cardiac RyR2 and IP3R2 was measured by real-time PCR and did not revealed any difference between CAR wt and KO hearts.

Calcium binding proteins

Cytosolic Ca^{2+} concentration can be regulated by specific Ca^{2+} binding proteins which store Ca^{2+} for short- or longterm. Further also inside the sarcoplasmic reticulum the Ca^{2+} binding protein calsequestrin can store high amounts of Ca^{2+} (Beard et al., 2004). If this Ca^{2+} buffer system is changed the raise in free Ca^{2+} could induce beating of cardiomyocytes. Therefore western blot was used to analyse the protein amount of the Ca^{2+} binding proteins calsequestin, calretculin and calretinin.

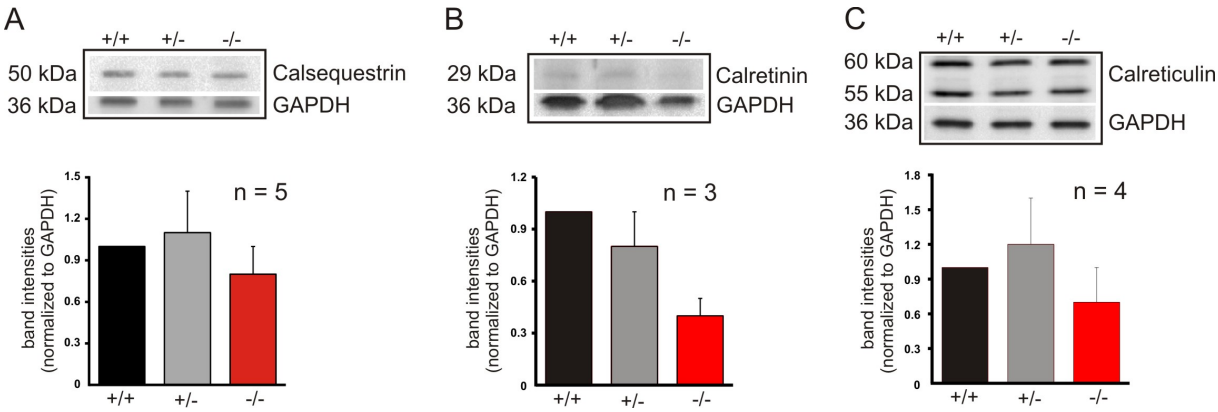

Figure 3.24: Expression of calcium binding proteins were not changed in CAR KO hearts. E11 CAR wt and KO hearts were dissected and membrane and cytosolic protein fraction were isolated. Cytosolic fractions were plotted and antibody against calsequestrin, calretinin and calreticulin were applied. Specific antibody binding was detected by ECL solution.

Calsequestrin and calreticulin did not show any change in CAR KO hearts compared to wt (fig.3.24 A, C). Also the quantitative analysis of the band intensities did not reveal any difference.

However, calretinin only could be detected slightly in western blot. Quantification of band intensities showed a decrease for CAR KO hearts which is not significant (fig.3.24 B). These variations could be caused by the fainting band intensities.

3.2.11 Troponin C and β-actin were not altered in CAR KO hearts

The increased beating frequency in CAR KO hearts and cardiomyocytes could alter the expression and distribution of troponin C or β-actin which are besides myosin the contraction proteins in the heart muscle. Therefore E11 embryo cryostat sections and cultivated E10.5 cardiomyocytes were stained against troponin C and β-actin. The β-actin stained heart sections showed for CAR wt and KO no difference (fig.3.25 A). The fluorescence intensity and distribution were similar. Troponin C staining of E11 hearts revealed the typically highly organised structure of muscle tissue as illustrated in CAR wt and KO hearts (fig.3.25 B). Also further magnification of the troponin C stained sections showed in CAR KO hearts the correct organisation of troponin bundles. Staining of cultivated E10.5 cardiomyocytes against β-actin also did not differ between wt and KO cardiomyocytes (fig.3.25 C).

As already shown for E11 heart sections, cultivated cardiomyocytes also present the highly organised structure of troponin-c bundles. Closer magnifications showed for CAR KO cardiomcytes no alterations compared to wt cardiomcytes (fig.3.25 D). Furthermore, the actual protein content of β-actin and troponin-C was determined by western blot. No significant change was observed for CAR KO hearts (fig.3.25 E). These results suggest that the contraction mechanism and its correlating proteins β-actin and troponin-C were not changed in CAR KO cardiomycytes due to the higher beating.

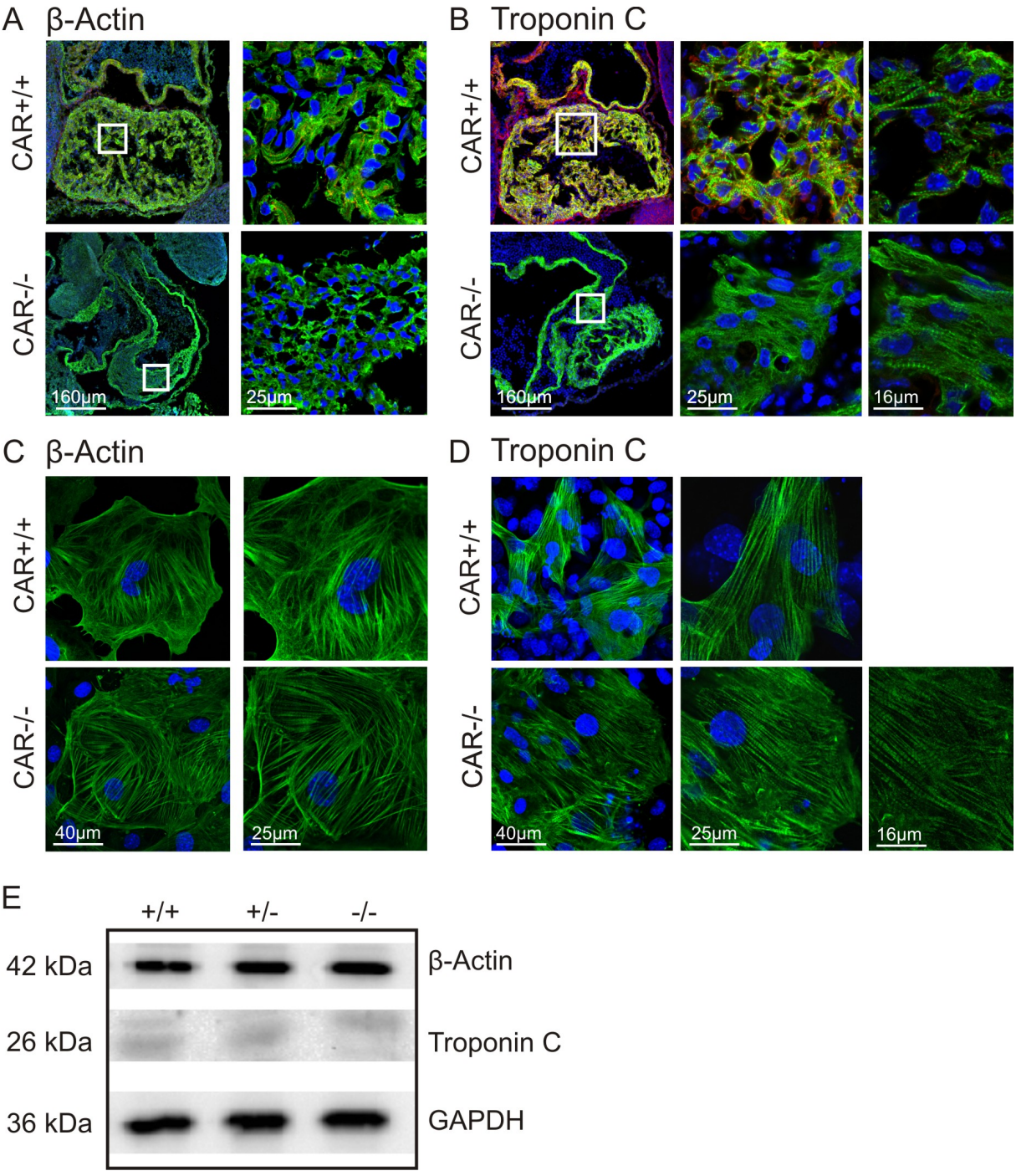

Figure 3.25: β-actin and troponin C were not altered in CAR KO hearts. E11 embryo cryostat sections were stained against β-actin or troponin C (green). No changes in CAR KO heart sections were observed for β-actin staining or troponin C (A, B). Higher magnifications in CAR KO sections revealed the same proper organisation of troponin C bundles as shown for CAR wt (B). E10.5 cultivated cardiomyocytes were also stained against β-actin and troponin C and no difference in staining for both proteins could be observed in CAR KO cardiomyocytes (C, D). β-actin and troponin C protein amount was determined by western blot analysis. For both genotypes the same band intensities of troponin C and β-actin were detected (E). green - β-actin or troponin C (as indicated), blue - DAPI, red - CAR.

3.2.12 AKT-GSK3β signaling in CAR KO cardiomyocytes

Dorner et al. (2005) showed an increase in stored glycogen in CAR KO heart sections. However, no statistical anaylsis of glycogen concentration in CAR wt and KO hearts was performed. Therefore, glyocgen concentration was measured and the upstream signalling pathway of glycogen synthesis was investigated. As illustrated in fig.3.26 D glycogen synthesis of glucose is catalyzed by glycogen synthase which is inhibited by glycogen synthase kinase 3 β (GSK3β) (Hardt, 2002; Sugden et al., 2008). Phosphorylation of GSK3β by protein kinase B (AKT) activates glycogen synthase (Sugden et al., 2008; Sussman et al., 2011). AKT is a major signalling molecule which is involved in many cellular processes like cell proliferation and growth, cell survival and metabolism and can be activated by various hormones, cytokines, integrins or other enzymes (Sussman et al., 2011). Further, activation of AKT in heart results in increased beating and Ca^{2+} cycling and hypertrophy (Catalucci et al., 2009; Condorelli et al., 2002).

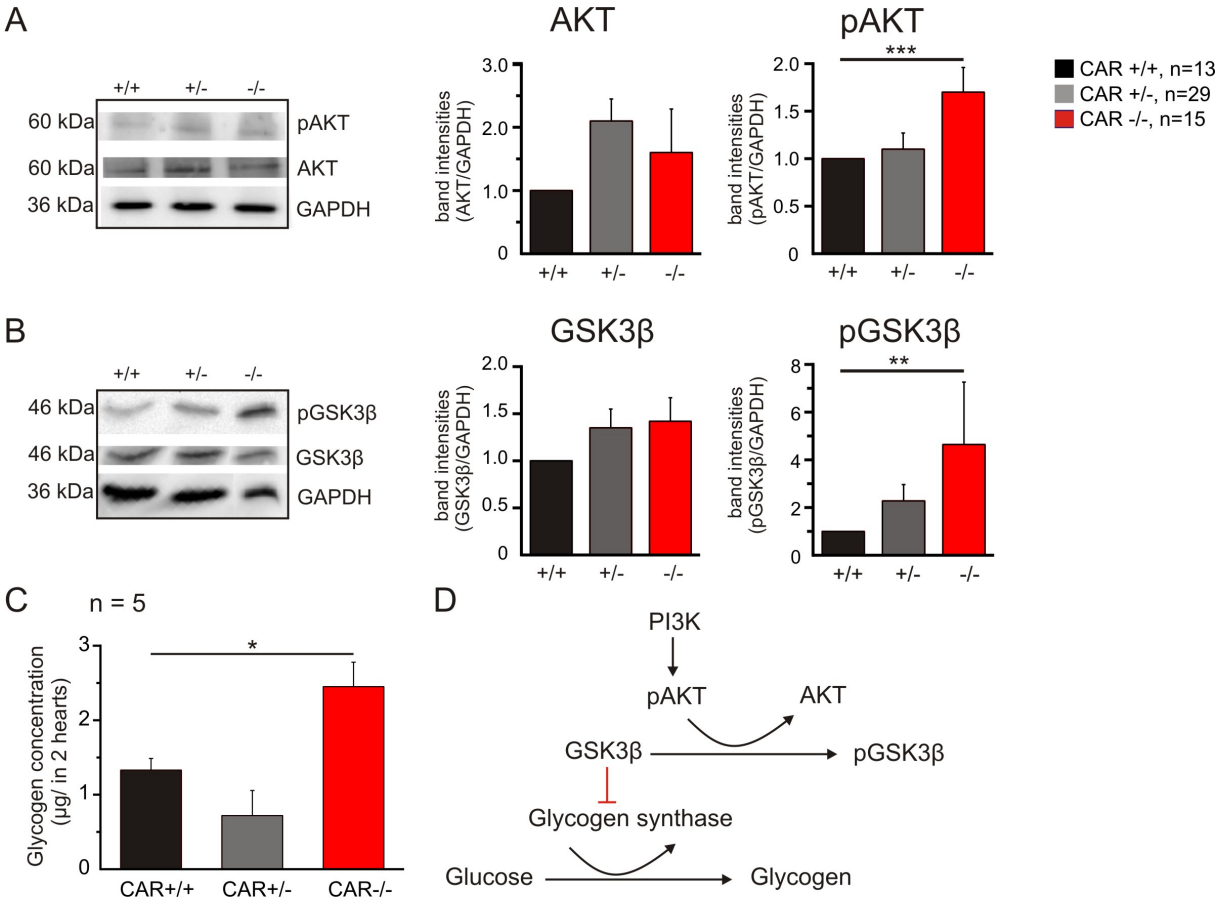

Figure 3.26: Increased phosphorylation of AKT and GSK3β induced glycogen synthesis. Western blot analysis of CAR wt and KO E11 hearts revealed a significant increase in band intensities for phospho-AKT (A) and phospho-GSK3β in CAR KO hearts (B). Total protein level of AKT and GSK3β was not changed in CAR KO hearts. Measurement of stored gylcogen in E11 hearts revealed a significant higher concentration for CAR KO (C). Signalling pathway of AKT and GSK3β directly influence gylcogen synthesis (D).* P<0.05, ** P<0.01, *** P<0.001

Comparison of phospho-AKT western blot band intensities showed that for E11 CAR KO hearts a significant higher phosphorylation of AKT was detected compared to wt hearts (fig.3.26 A). The induction in phospho-AKT is due to increased phosphorylation of AKT because western blot bands of total AKT protein did not revealed any significant change for CAR KO hearts. Further downstream, phosphorylation of GSK3β is also increased. CAR KO hearts showed significant higher western blot band intensities for phospho-GSK3β than measured for CAR wt hearts (fig.3.26 B). The total protein level of GSK3β was not altered in CAR KO hearts. Next, the glycogen concentration was determined and revealed a significant higher concentration for CAR KO compared to wt hearts (fig.3.26 C). These data indicates that probably induced AKT signalling via GSK3β increased glycogen synthesis in CAR KO hearts.

3.2.13 Induced coupling of neighbouring CAR KO cardiomyocytes

Correct and fast conduction of action potentials and excitation between neighbouring cardiomyocytes is called electrical coupling and mediated by gap junctions. Gap junctions are composed of two hemichannels one from each cell which consists of connexins (Jansen et al., 2010). In the heart mainly connexin 40, 43 and 45 (Cx40, Cx43, Cx45) are expressed whereby specific parts of the heart show unique connexin expression profiles (Desplantez et al., 2007; Hertzberg et al., 1991; Severs et al., 2008). In the mature heart the connexins are located at the intercalted disks and it was shown that CAR and Cx43 or Cx45 colocalize (Lim et al., 2008; Lisewski et al., 2008). Further, in adult CAR KO cardiomyocytes altered connexin expression was shown as well as induced intercellular coupling via gap junctions (Lisewski et al., 2008). However, no studies of the influence of CAR on connexins and gap junction function during early heart development was done. Therefore, for E10.5 CAR wt and KO cardiomyocytes Cx40, Cx43 and Cx45 expression and localisation of Cx and CAR was investigated. Also, the intercellular coupling was studied by using dye spreading with lucifer yellow and neurobiotin.

Gene expression analysis of CAR wt and KO hearts revealed a reduction of Cx40 which was not significant (fig.3.27 A). Also Cx43 expression was not altered in CAR KO hearts whereby wt hearts showed a high variation between the individual experiments. Surprisingly Cx45 expression was significant reduced in CAR KO hearts. Next, connexin protein concentration was determined by using western blot analysis (fig.3.27 B). The observed Cx43 western blot showed a double band indicating the phosphorylated Cx43 form (upper band) and the unphosphorylated form (lower band). CAR KO hearts revealed decreased band intensities for Cx43. Also Cx40 protein amount was reduced in CAR KO compared to CAR wt hearts. Comparison of the Cx40 and Cx43 western blot data with real-time PCR indicate that Cx40 and Cx43 protein amount was reduced although no significant reduction was observed at the mRNA level. As expected, Cx45 band intensities were reduced in CAR KO hearts as already indicated by decreasing Cx45 gene expression. Furthermore, colocalisation of CAR and Cx43 was investigated in embryonic E11

wt heart cryosections and cultivated cardiomyocytes (fig.3.27 C). The heart sections revealed a uniform expression of CAR in the myocardium. Cx43 is also widely expressed and colocalisation (indicated in yellow/orange in the merge picture) with CAR occurs. However, there are several parts of the tissue in which no colocalisation was found. Cultivated wt cardiomyocytes showed a higher amount of CAR-Cx43 colocalisation compared to heart cryosections. Especially connecting cell membranes to neighbouring cardiomyocytes revealed strong expression of CAR and Cx43. These date suggest that CAR and Cx43 also colocalise in embryonic hearts and therefore support electrical coupling between neighbouring cells.

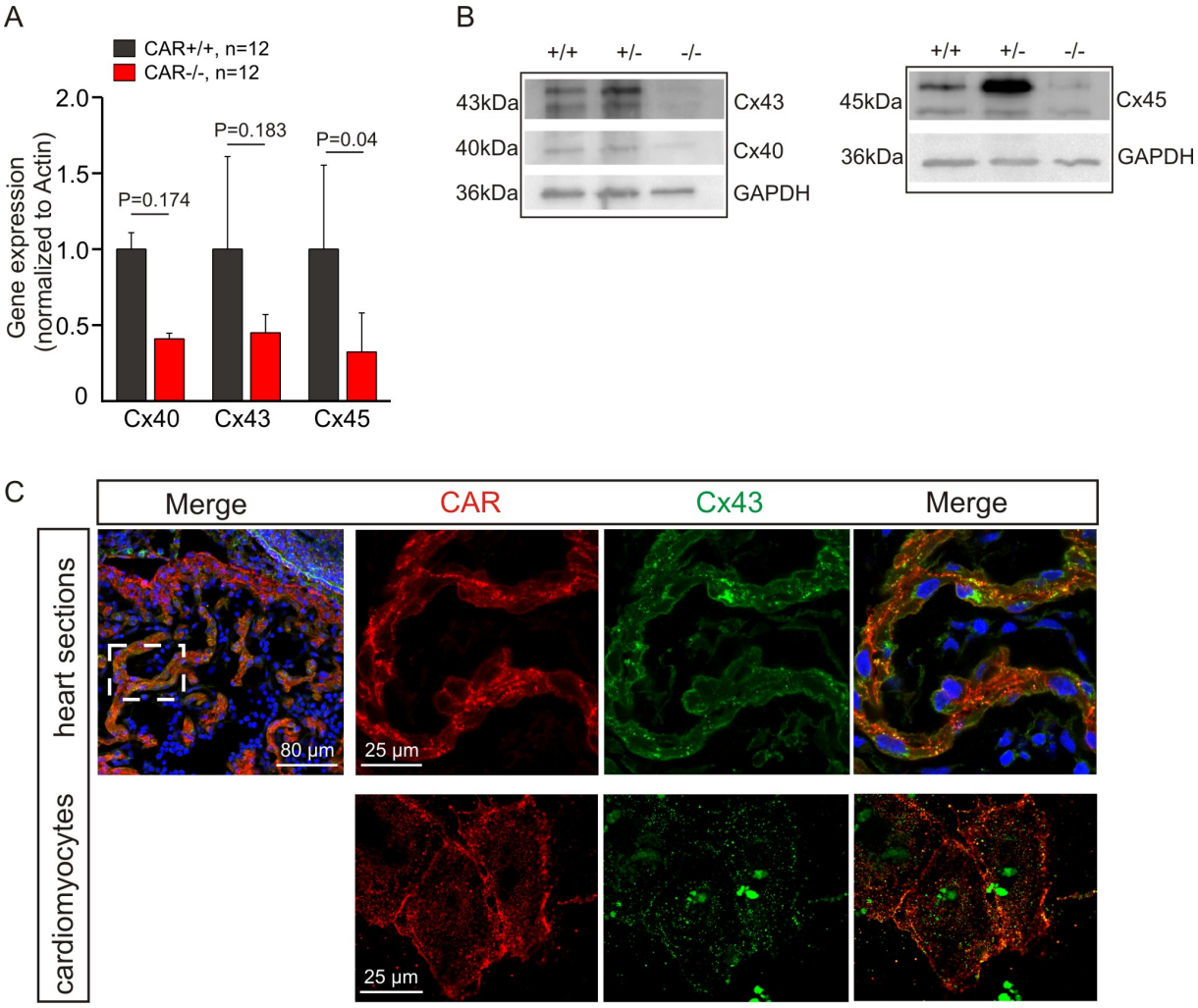

Figure 3.27: Connexin gene expression in CAR KO and wt hearts. E11 CAR wt and KO hearts were dissected and gene expression of Cx40, Cx43 and Cx45 was analysed by real-time PCR. Cx40 and Cx43 did not show a significant difference in CAR KO. Cx45 was significant reduced in hearts of CAR KO embryos (A). Protein concentration of cardiac Cx was determined by western blot and for Cx45 a slight reduction was observed (B). E11 CAR wt heart cryostat sections showed colocalisation of CAR and Cx43 (Blue - DAPI). Also in cultivated E11 cardiomyocytes colocalisation of CAR and Cx43 was observed (C).

To analyse the function of gap junction and its influence on electrical coupling in CAR KO cardiomyocytes lucifer yellow was injected in cardiomyocytes and the dye spreading to its neighbouring cardiomyocytes was determined. After 5 min of dye spreading the experiment was stopped and the complete lucifer yellow stained area was measured (fig.3.28 A). CAR wt and KO did not show a different lucifer yellow spreading. Analysis of the spreaded area revealed for both genotypes the same dimensions of ca. 6500 µm^2 (fig.3.28 B). However, comparison of the injected cell size indicated that CAR KO cardiomyocytes were significant smaller compared to CAR wt cardiomyocytes (CAR wt 2175 ± 365 µm^2 vs. CAR KO 1095 ± 85 µm^2). Furthermore, correction of the total spreaded lucifer yellow area by the injected cell area resulted in a significant increased lucifer yellow spreaded area in CAR KO cardiomocytes (fig.3.28 C). Also the percentage increase of lucifer yellow stained area from the injected cell (100%) to the final spreading area is significant higher in CAR KO cardiomyocytes: in CAR wt cardiomyocytes an increase of 460% was found. However, in CAR KO cardiomyocytes the lucifer yellow stained area raised about 842% after injection.

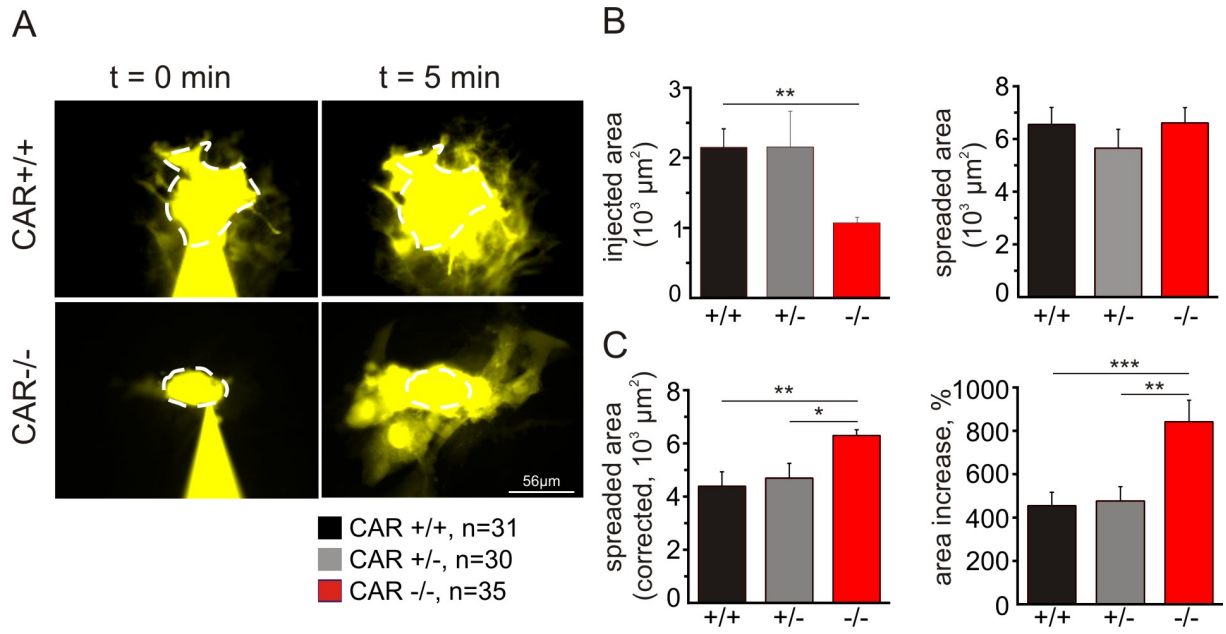

Figure 3.28: Increased dye spreading in CAR KO cardiomyocytes. E10.5 embryo hearts were dissociated and plated on pre-coated fibronectin glass dishes. At DIV4 lucifer yellow solution was injected in a cardiomyocyte by using a glass pipette and after 5 min of incubation lucifer yellow fluorescence intensity was detected (A). Analysis of the injected cell area revealed a significant smaller cell size for CAR KO cardiomyocytes. CAR wt and KO cardiomyocytes did not show a significant change in the final spreaded area dimensions (B). Correction of the total lucifer yellow spreaded area by the injected cell size indicated a significant increase in dye spreading for CAR KO cardiomyocytes. The percentaged increase of injected lucifer yellow area and spreaded stained area after 5 min was significant higher for CAR KO cardiomyocytes (C). * P<0.05, ** P<0.01, *** P<0.001

Next, a 2% neurobiotin/1% lucifer yellow was injected and the spreading was determined. Because neurobiotin has a smaller molecular weight of 358 g/mol compared to lucifer yellow (458 g/mol)

the spreaded area of neurobiotin was expected to be larger. However, analysis of the neurobiotin spreading showed a smaller stained area compared to lucifer yellow (for wt cardiomyocytes: 1380 ± 280 µm^2 vs. 6584 ± 560 µm^2, compare fig.3.29). CAR wt and KO neurobiotin staining did not differ dramatically whereby in CAR KO cardiomyocytes the neurobiotin spreaded area was slightly larger (CAR wt 1380 ± 280 µm^2 vs. CAR KO 1974 ± 350 µm^2).

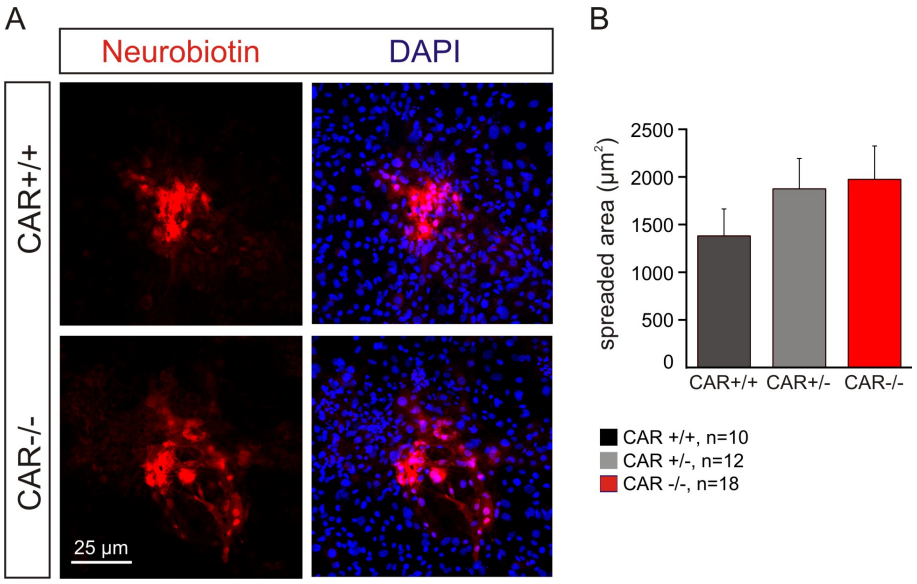

Figure 3.29: Neurobiotin spreading was not significant altered in CAR KO cardiomyocytes. E10.5 plated cardiomyocytes were injected with 2% neurobiotin/1% lucifer yellow by using a glass pipette. After incubation of 5 min, the cells were fixated and streptavidin-Cy5 antibody was applied to detect neurobiotin (A). Analysis of the neurobiotin stained area did not reveal any significant change in CAR KO cardiomyocytes compared to wt (B).

Application of the gap junction blocker carbenoxolone (CBX) or 5-nitro-2-(3-phenyl-propylamino)-benzoic acid (NPPB) should decrease the spreading of lucifer yellow. Also the organised coupled beating of the cultivated cardiomyocytes might be influenced by blocking the gap junctions. Therefore in the following experiment either 200 µM CBX or 100 µM NPPB was applied and afterwards lucifer yellow was injected to the cardiomyocytes to analyse the spreading of the fluorescence dye. Further, the influence of CBX or NPPB on beating frequency was determined. As expected, CBX treatment reduced lucifer yellow spreading in CAR wt and KO cardiomyocytes (fig.3.30 A, B). For both genotypes the final spreaded lucifer yellow area was significant smaller compared to untreated cardiomyocytes. Also NPPB application reduced the dye spreading in CAR wt and KO cardiomyocytes (fig.3.30 E, F). Compared to CBX the spreaded lucifer yellow area is still larger in NPPB treated cardiomocytes which suggest an incomplete gap junction block. Only in CAR KO cardiomyocytes a significant decrease in lucifer yellow spreaded area was determined after NPPB was applied (fig.3.30 E, F).

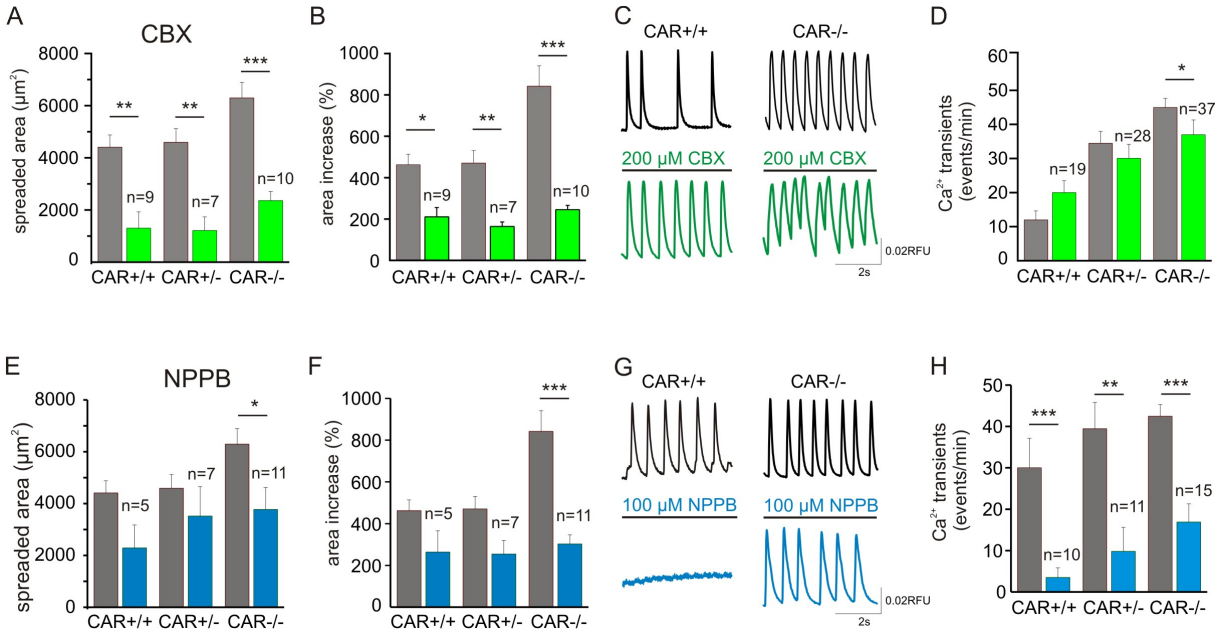

Figure 3.30: Application of gap junction blocker. E10.5 cardiomyocytes were treated with either 200 µM CBX (A-D) or 100 µM NPPB (E-H) and lucifer yellow was injected to analyse dye spreading. CBX treatment (green bars, A, B) resulted in significant decrease of dye spreading for CAR wt and KO cardiomyocytes compared to untreated cardiomyocytes (grey bars, A, B). Organised cardiomyocyte cluster beating and beating frequency was not strongly effected by CBX in wt and KO (C, D). NPPB application (blue bars, E, F) only slightly reduced lucifer yellow spreading in CAR KO cardiomyocytes (grey bars - untreated cardiomyocytes, E, F). In CAR wt and KO cardiomyocytes the beating frequency was decreased significant by NPPB but no effect on beating coupling was observed (G, H). * $P<0.05$, ** $P<0.01$, *** $P<0.001$

To analyse the influence of the gap junction blocker on the frequency of Ca^{2+} transients calcium imaging was performed. Therefore the plated cardiomyocytes were treated with 200 µM CBX or 100 µM NPPB and the Ca^{2+} transients were recorded. Surprisingly, application of either CBX or NPPB did not result in major disorganised beating as expected because gap junctions mainly mediate electrical coupling of neighbouring cardiomyocytes. However, in CAR wt cardiomyocytes CBX treatment resulted in a slight induction of beating frequency which was not significant. CAR KO cardiomyocytes significantly reduced their beating after CBX incubation (fig.3.30 C, D). In contrast, NPPB application resulted in significant slow down of beating in both genotypes whereby in CAR wt cardiomyocytes a lack of beating was observed (fig.3.30 G, H). CAR KO cardiomyocytes still beat after NPPB treatment, however a significant decrease in beating frequency was recorded. Further, no statistical difference in the beating frequency between CAR wt and KO cardiomyocytes was observed anymore (fig.3.30 H).

The analysis of gap junctions in the CAR KO cardiomyocytes revealed that the coupling between neighbouring KO cells is significant higher compared to CAR wt cardiomyocytes because lucifer yellow spreading was significant larger. Also KO cardiomyocytes responded more sensitive to gap junction blockers resulting in decreasing beating. Furthermore, the dye spreading experiments

illustrated a significant smaller cell size of CAR KO cardiomyocytes. Therefore, next the cell size of CAR KO cardiomyocytes was further investigated.

3.2.14 Decreased cell size of CAR KO cardiomyocytes compared to CAR wt

Analysis of cell size was performed by light transmission microscopy, lucifer yellow injection and dextran-rhodamine B injection to verify the measured cardiomyocyte cell sizes. The cell size was calculated by using Fiji/Image J.

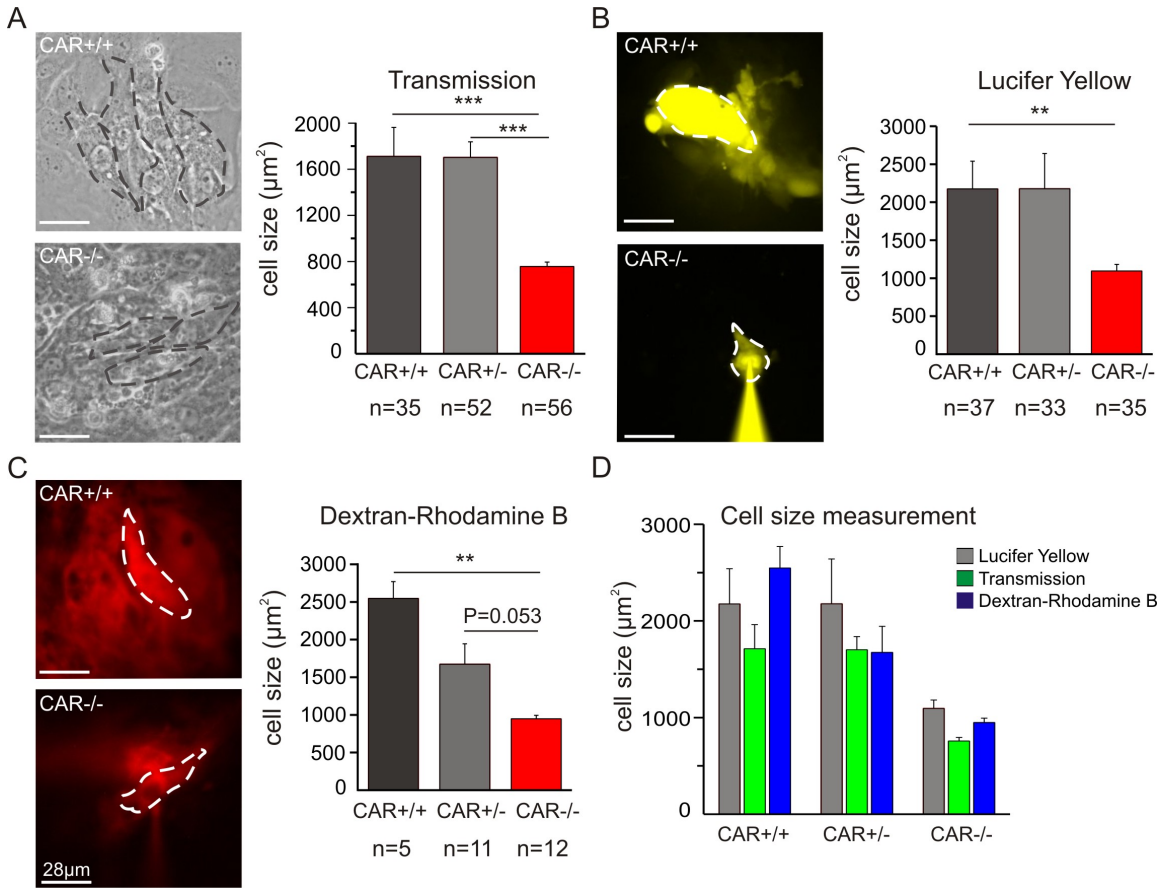

Figure 3.31: Cultivated CAR KO cardiomyocytes were significant smaller compared to CAR wt. Determination of cultivated cardiomyocyte cell size was done by light transmission microscopy (A), lucifer yellow injection (B) and dextran-rhodamine B injection (C). All methods revealed a significant smaller cell size for cultivated CAR KO cardiomyocytes (D.) ** P<0.01, *** P<0.001

The images obtained by light transmission microscopy revealed for CAR wt cardiomyocytes 1711 ± 250 µm^2 cell area. In contrast, CAR KO cardiomyocytes only have an actual size of 756 ± 37 µm^2 (fig.3.31 A). After lucifer yellow injection the CAR wt cardiomyocyte size of 2175 ± 365 µm^2 was calculated. CAR KO cell size was 1095 ± 85 µm^2 (fig. 3.31 B). Dextran-rhodamine B has a molecular weight of 10.000 g/mol which can not be transferred to neighbouring cells via gap

junctions. Therefore, dextran-rohodamine B injection is used to estimate the size of the injected cell. Also, CAR wt cardiomyocytes showed a significant higher cell size of 2546 ± 222 μm^2 compared to 948 ± 46 μm^2 in CAR KO cardiomyocytes (fig.3.31 C). The three used methods to determine the cardiomyocyte size did not differ significantly which verifies the obtained result that cultivated CAR KO cardiomyocytes were significant smaller than wt cardiomyocytes (fig. 3.31 D).

Next, the size of the cardiomyocytes in intact hearts was investigated. Therefore E11 hearts were dissected, embedded in plastic and 5 µm sections were prepared to perform a haematoxylin and eosin staining. This staining procedure allows to analyse the size and number of the cardiomyocytes in the embryonic heart. To obtain the correct cardiomycyte size and number light transmission microscopy was performed and the images were analysed by using Fiji/Image J.

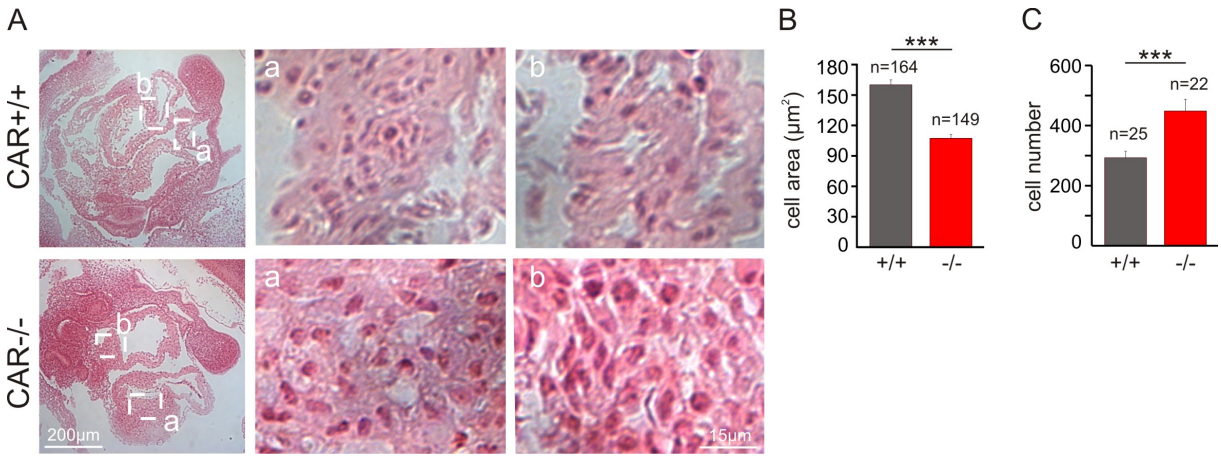

Figure 3.32: Cardiomyocytes of CAR KO hearts were significant smaller compared to CAR wt hearts. The cardiomyocyte cell size of E11 embryo heart sections was obtained by staining with haematoxylin and eosin (A). Afterwards the size and number of the cardiomyocytes was measured by using Fiji/ Image J (B, C). Compared to CAR wt hearts, CAR KO hearts revealed a significant smaller cardiomyocyte cell size and a significant higher number of cardiomyocytes in the investigated heart sections. *** P<0.001

Comparison of CAR wt and KO cardiomyocytes revealed for CAR KO cardiomyocytes a significant smaller cell size (fig.3.32 A, B). For CAR wt cardiomyocytes a cell area of 160 ± 5 μm^2 was detected. In contrast, for CAR KO cardiomyocytes a cell size of 107 ± 4 μm^2 was obtained (fig.3.32 B). Because the overall heart size was not changed it can be concluded from a significant smaller cell size that the number of cardiomyocytes in CAR KO hearts is increased. Indeed, analysis of the E11 CAR KO heart sections revealed a significant higher number of cardiomyocytes mainly located at the ventricle walls of the CAR KO hearts (fig.3.32 C). These data support the observed effect in cultivated CAR KO cardiomyocytes that the cell size of CAR KO cardiomyocytes is significantly reduced.

3.3 Cell Signaling pathways of CAR

3.3.1 Ad2 fiber knob binding to CAR increased intracellular Ca^{2+} and beating frequency in cultivated wt cardiomyocytes

To study whether CAR modulates intracellular signalling the fiber knob of the adenovirus 2, termed Ad2, or extracellular domains of CAR were applied to cultivated E15 wt cardiomyocytes. The fiber knob of the Ad2 virus binds to the extracellular CAR domain D1 and therefore may trigger the signaling pathways (Bewley, 1999). Schreiber (2009) showed an increase in intracellular Ca^{2+} concentration after Ad2 treatment on E10.5 neuronal cell culture. At first the effect of Ad2 on cytosolic Ca^{2+} concentration and beating frequency by recording the frequency of Ca^{2+} transients in E15 wt cardiomyocytes was investigated.

Ad2 application to beating cardiomyocytes increased significantly after 2 min the frequency of Ca^{2+} transients (fig.3.33 A-C). As shown in the example traces shortly after Ad2 treatment the intracellular Ca^{2+} concentration increased and the maximal beating frequency was obtained after 3 min (fig.3.33 A, C). Further the extracellular Ca^{2+} concentration was modified and independent of low (0.5 mM) or high (2 mM) extracellular Ca^{2+} the Ad2 effect could be measured. Unexpected, only 58-73% of all tested cardiomyocyte cell clusters responded positive to Ad2 and increased the frequency of Ca^{2+} transients. 14-22% reduced beating after Ad2 treatment and 12-20% did not show any reaction (fig.3.33 B). Only positive responding cell clusters were used for measuring the increase in beating frequency.

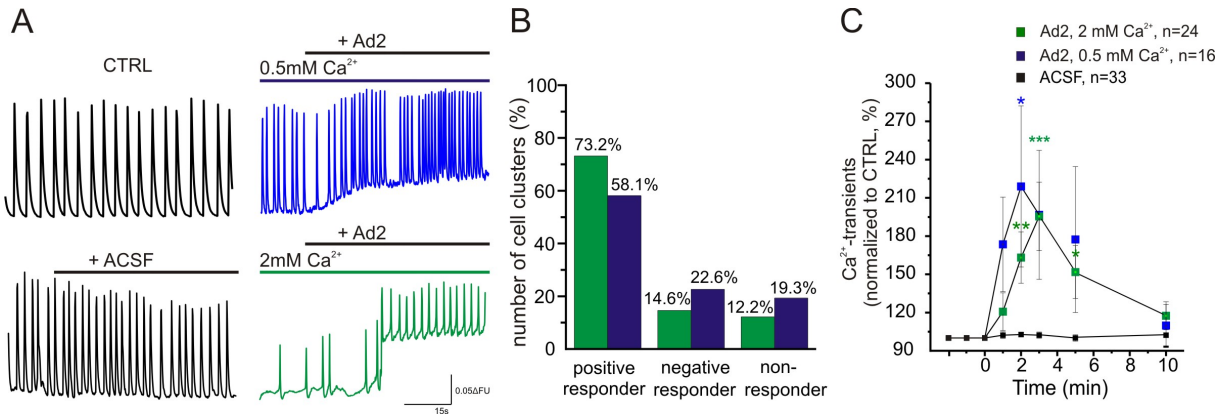

Figure 3.33: Ad2 fiber knob treatment increased intracellular Ca^{2+} concentration and beating frequency. E15 cardiomyocytes were treated with Ad2 fiber knob (final concentration 230 µg/ml) and flourescence intensity of Fura-2 was recorded (A). Ad2 application increased intracellular Ca^{2+} concentration and beating frequency independent of high (2 mM) or low (0.5 mM) extracellular Ca^{2+} concentration (A, C; CTRL and ACSF recordings were performed in 2 mM extracellular Ca^{2+} concentration). Ad2 did not induce the beating frequency in all cardiomyocyte cell clusters (B). 30-40% of the recorded cell clusters did not show any response or increase in beating. * $P<0.05$, ** $P<0.01$, *** $P<0.001$

To verify the specific effect of Ad2 on beating and intracellular Ca^{2+} in cardiomyocytes a binding assay was performed. Therefore the selective binding of Ad2 fiber knob and the extracellular CAR domains was investigated. Besides CAR also the related proteins CLMP and BT-IgSF were tested. CLMP and BT-IgSF are cell adhesion proteins highly related to CAR. Fc fragments of the extracellular mouse domains of CAR, CLMP and BT-IgSF were immobilized on microliter plates and Ad2 fiber knob was applied. The specific binding of Ad2 to the extracellular domains was detected by application of a monoclonal antibody against Ad2 (100 ng/ml) tagged with His-taq-HRP. Afterwards, o-phenylenediamine (OPD, 100 ng/ml) was applied to detect positive Ad2 binding by absorbance measurement (490 nm). As negative control the Fc fragment alone was used. Only for mCAR-Fc fragment a strong signal was obtained (fig.3.34 A). For mCLMP-Fc, mBT-IgSF-Fc and Fc fragments no signal was determined. This result indicates a strong and specific binding of Ad2 fiber knob to CAR.

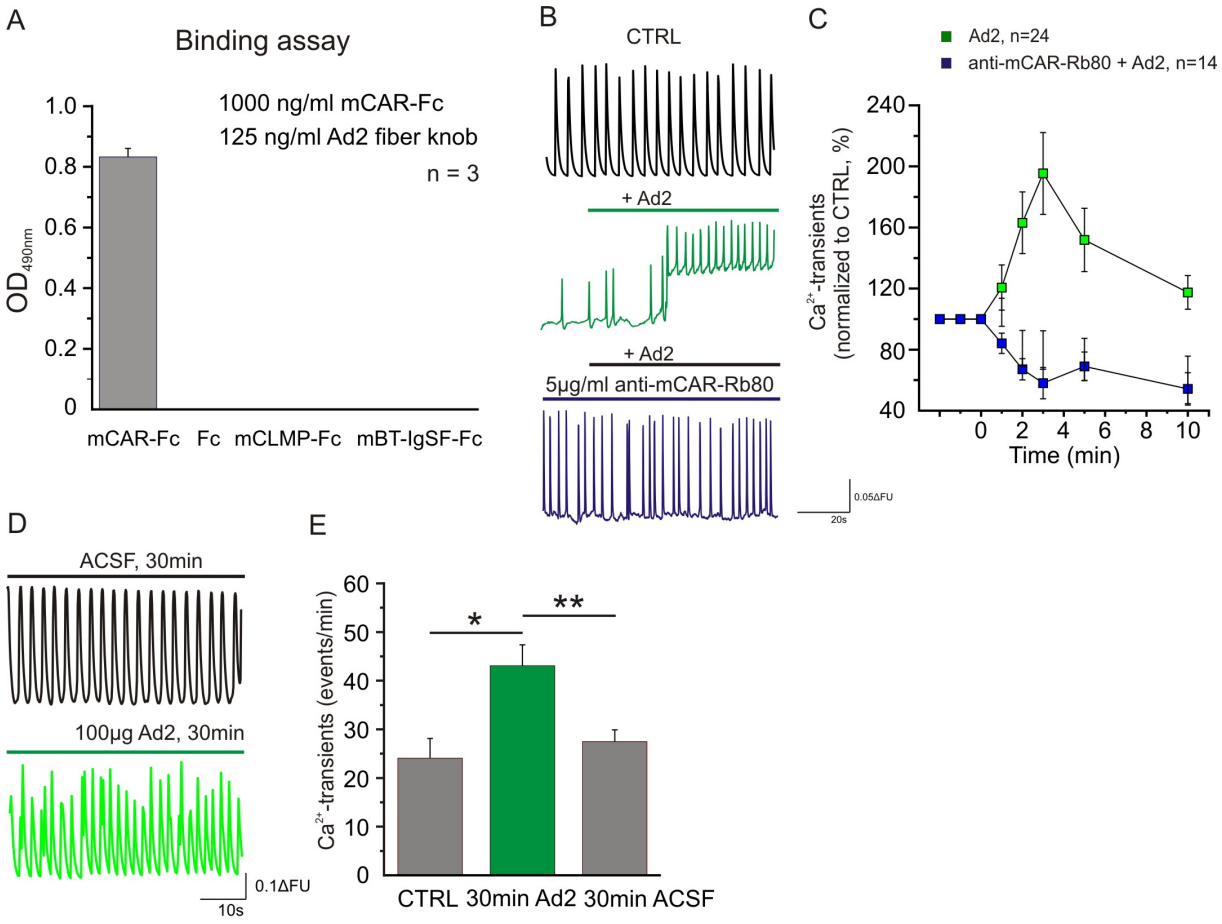

Figure 3.34: Ad2 binding is specific for CAR. To analyse the specific binding of CAR and Ad2 fiber knob extracellular mouse CAR, CLMP and BT-IgsF domains were immobilized on microliter plates and Ad2 was applied. Detection of binding was performed by using the HRP/OPD system. Only mCAR-Fc fragment showed a signal (A). The positive effect of Ad2 can be abolished by covering the CAR domains with the specific antibody mCAR-Rb80 (B, C). Ad2 long-term effect (30 min application) also revealed a significant increase in beating frequency compared to non-treated cells (D, E).* $P<0.05$, ** $P<0.01$

Further the effect of Ad2 on beating frequency can be abolished by masking the extracellular CAR domains. Before Ad2 application the cardiomyocytes were treated with an antibody against mCAR (3 µg/ml mCAR-Rb80) followed by Ad2 addition. No increase in beating frequency was determined (fig.3.34 B, C). Compared to the strong induction of beating after Ad2 treatment, no change in the frequency of spontaneous Ca^{2+} transients was noticed. Also the long-term effect of Ad2 was analysed by incubation of cardiomyocytes to Ad2 for 30 min. Afterwards the beating frequency was studied and revealed a significant increase compared to ACSF treated cells (fig.3.34 D, E).

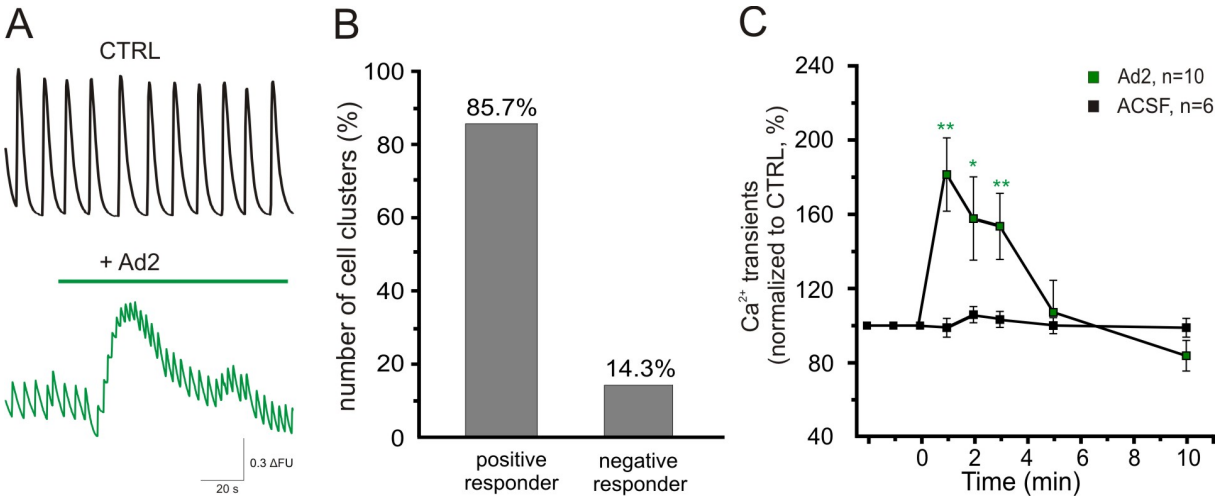

Figure 3.35: Treatment of HL-1 cells with Ad2 increased beating frequency. Cultivated HL-1 cells were loaded with Fura-2AM and beating was recorded by calcium imaging. After Ad2 application cytosolic Ca^{2+} and the frequency of spontaneous Ca^{2+} transients significantly increased (A, C). 85% of all tested HL-1 cells showed a positive response to Ad2 (B). * $P<0.05$, ** $P<0.01$

As an artificial cardiac cell culture system HL-1 cells were cultivated and used to analyse the effect of Ad2 on CAR induced cell signaling pathways. Application of Ad2 to beating HL-1 cells significantly increased beating frequency already after 1 min (fig.3.35 A-C). 85% of all tested HL-1 cells responded positive to Ad2 treatment and increased the cytosolic Ca^{2+} concentration and beating frequency of spontaneous Ca^{2+} transients (fig.3.35 B). Compared to E15 wt cardiomyocytes the effect of Ad2 occurred already shortly after application and lasted only for 4 min (fig.3.35 C).

3.3.2 Homophilic CAR binding increased intracellular Ca^{2+} and beating frequency

Besides the binding of the Ad2 fiber knob to CAR also homophilic interaction between extracellular CAR domains can occur (Patzke et al., 2010). To analyse if homophilic binding could also trigger the increase of the frequency of spontaneous Ca^{2+} transients cultivated E15 wt cardiomyocytes were treated with the extracellular mouse CAR domains D1 and D2 in the form of a Fc fusion

protein (0.78 mg/ml mD1D2-Fc) which bind to the extracellular part of CAR localized on the cell membrane of the cardiomyocytes. Application of mD1D2-Fc also increased the beating frequency and cytosolic Ca^{2+} concentration (fig.3.36 A-C). Compared to Ad2 mD1D2-Fc induced the maximal beating frequency of 160% after 1 min (fig.3.36 C). As already shown for Ad2 treatment not all investigated cardiomyocyte clusters reacted in a positive manner: 78% of the cardiomyocyte clusters increased the beating and 21% reduced the frequency (fig.3.36 B).

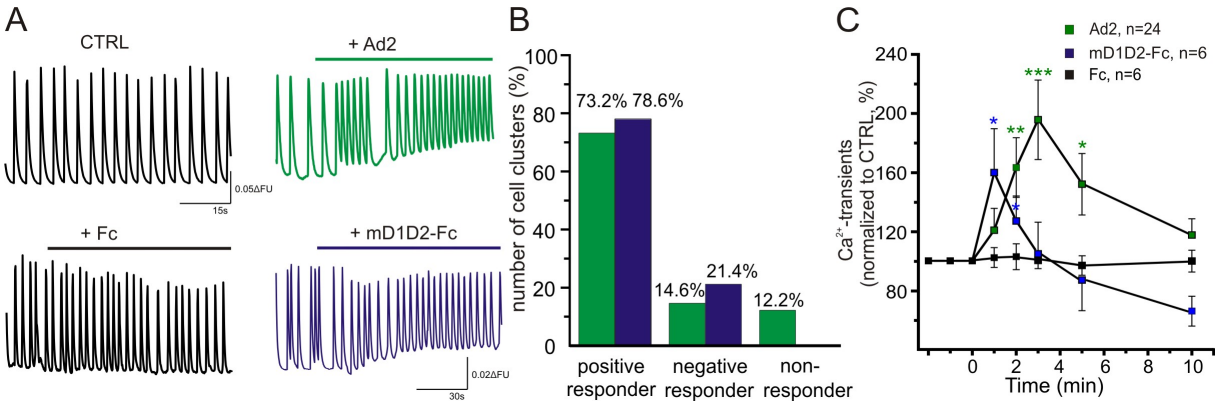

Figure 3.36: Homophilic CAR binding increased intracellular Ca^{2+} concentration and beating frequency. E15 cardiomyocytes were treated with Ad2 fiber knob (final concentration 230 µg/ml) or mD1D2-Fc (0.78 mg/ml) and fluorescence intensity of Fura-2 was recorded (A). Application of both fragments increased intracellular Ca^{2+} and beating frequency (A). 70-80% of all analysed cardiomyocytes indicated a significant increase in beating (B). Ad2 fiber knob treatment increased beating frequency in a stronger manner compared to mD1D2-Fc (C). * $P<0.05$, ** $P<0.01$, *** $P<0.001$

Application of the extracellular domains from chick (chD1D2-Fc) did not change the beating significantly (fig.3.37). Compared to the strong effect of mouse extracellular domains (mD1D2-Fc) only a slight induction in beating was obtained after the E15 wt cardiomyocytes were treated with chD1D2-Fc (fig.3.37 A, C). 66% of all analysed cardiomyocytes did not respond to chD1D2-Fc at all and the other 33% cardiomyocytes only slightly increased their beating frequency (fig.3.37 B, C). However, alignment (BLAST, (Altschul et al., 1990)) of mCAR against chCAR revealed an 58% identity and 74% positives (fig.3.37 D). Therefore similar results were expected. For homophilic binding mainly D1 and D2 domains are involved (Patzke et al., 2010) but only 40% identity and 62% positives were calculated for protein alignment of mD2 against chD2 domain. The lacking induction effect of chCAR on beating of E15 wt cardiomyocytes could be caused by structural differences.

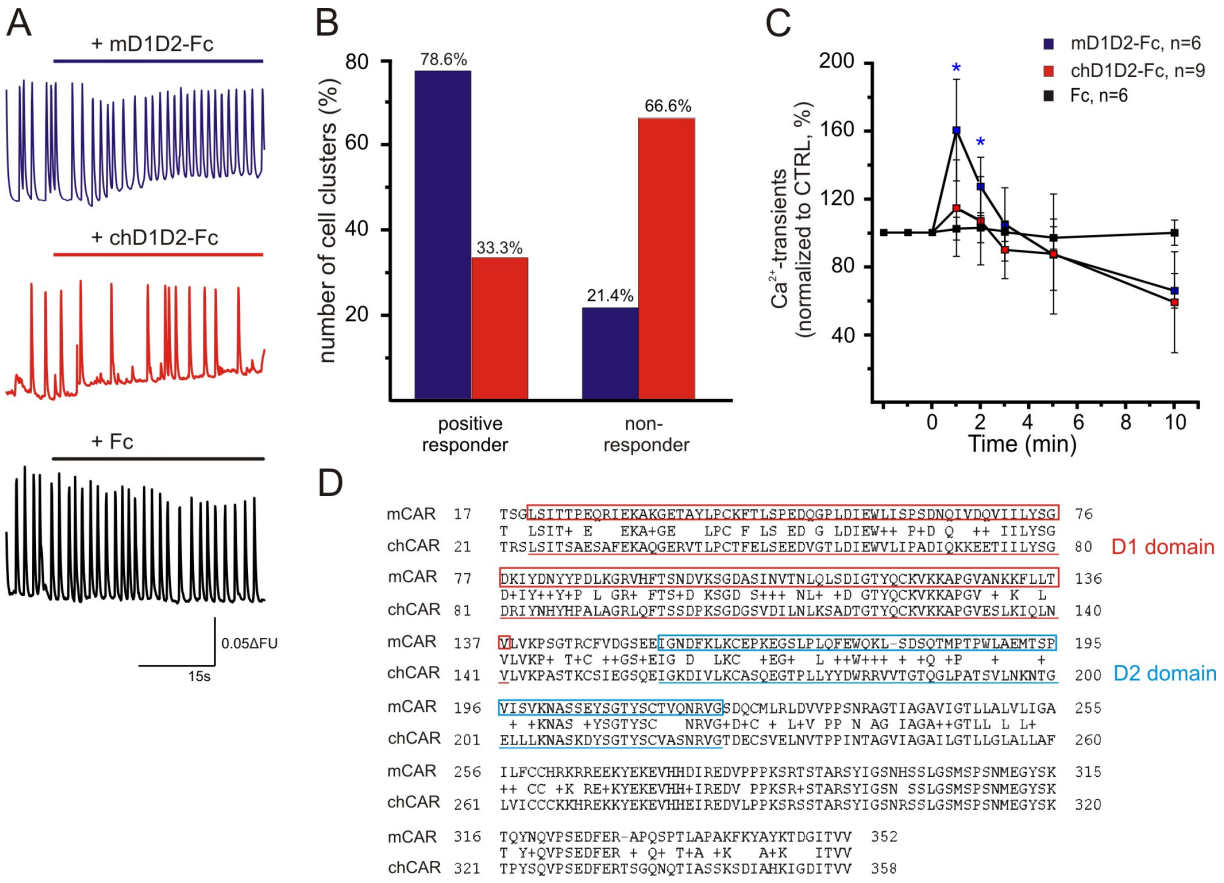

Figure 3.37: Application of chick CAR lacked induction of beating frequency in cardiomyocytes. E15 wt cardiomyocytes were treated with 0.83 mg/ml chD1D2-Fc and beating were anaylsed by calcium imaging (A). Only 33% of all investigated cardiomyocyte clusters responded slightly (B). No significant increase in beating frequency was measured after chD1D2-Fc application. In contrast, mD1D2-Fc strongly induced frequency of spontaneous Ca^{2+} transients and cytosolic Ca^{2+} concentration (C). BLAST of mCAR against chCAR revealed a 58% idendity and 74% positives (D). * P<0.05

Homophilic interaction of the D1 and D2 domains of mCAR increased the beating frequency and cytosolic Ca^{2+} in a similar manner like Ad2 fiber knob binding. To identify if both domains are required for induction of cytosolic Ca^{2+} E15 wt cortex neuronal cell culture was treated by either mD1-122 or mD2 (fig.3.38 A-C). Both fragments increased intracellular Ca^{2+} concentration whereby for mD2 application a non significant reduced Ca^{2+} response was recorded compared to mD1-122 treatment (fig.3.38 B). Further different concentration of mD1-122 were tested to analyse a concentration dependence. The strongest increase in cytosolic Ca^{2+} was found for 6.6 mg/ml. Reduction of mD1-122 concentration lead to a decreased response whereby no significant increase of intracellular Ca^{2+} concentration was determined anymore (fig.3.38 C).

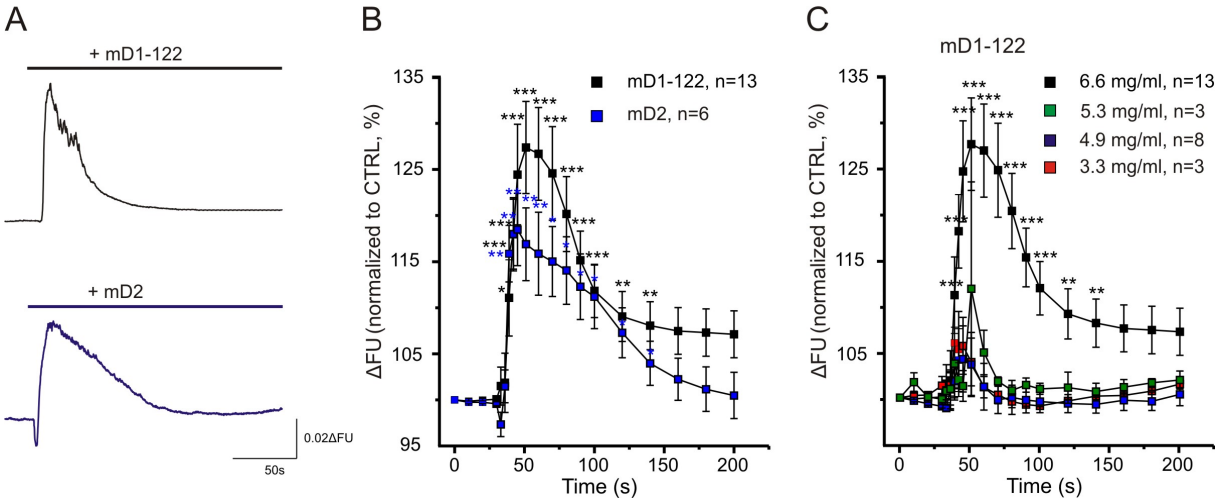

Figure 3.38: Application of D1 or D2 domain of CAR induced intracellular Ca^{2+} concentration. E15 wt cortex culture (DIV7) were treated with mD1-122 or mD2 fragment (A). For both fragments a significant increase in cytosolic Ca^{2+} was measured (B). Reduction of mD1-122 concentration from 6.6 mg/ml to 5.3 mg/ml already decreased the Ca^{2+} trigger (C). * P<0.05, ** P<0.01, *** P<0.001

3.3.3 Ad2 fiber knob binding triggers intracellular Ca^{2+} release

After binding of Ad2 fiber knob to CAR cytosolic Ca^{2+} increased whereby induction of intracellular Ca^{2+} results by either release of Ca^{2+} from sarcoplasmic reticulum or via calcium channels from outside the cell. To identify the Ca^{2+} source specific Ca^{2+} channel blocker or inhibitors for intracellular Ca^{2+} release were applied before Ad2 treatment (fig.3.39 A-C). Blocking all types of cardiac Ca^{2+} channels by incubation of the investigated cardiomyocytes with 1 µM verapamil (L-type), 1 µM nimodipine (L-type), 1 µM ω-conotoxin MVIIC and GVIA (L-, N- and T-type) and 1 µM ω-agatoxin (P-type) for 1 min resulted in lack of beating. However, shortly after Ad2 application a strong increase in cytosolic Ca^{2+} was determined (fig.3.39 A, red). Extracellular Ca^{2+} channels also can be inhibited by complete reduction of extracellular Ca^{2+} concentration (Ca^{2+}-free ACSF). Consequently the recorded cardiomyocytes did not beat anymore and after Ad2 treatment a strong increase in intracellular Ca^{2+} was recorded (fig.3.39 A, blue). Some cardiomyocyte cell clusters also showed short term bursts of Ca^{2+} transients.

These results indicated that Ad2 triggers intracellular Ca^{2+} release via ryanodine channels and IP_3 receptors. To verify this assumption intracellular Ca^{2+} store release was blocked by 50 µM 2-APB (IP_3 receptor) and 50 µM ryanodine (ryanodine receptor) for 5 min and afterwards Ad2 was applied. No increase in beating frequency or cytosolic Ca^{2+} could be detected anymore (fig.3.39 A, C). Compared to over 70% positive responders after Ad2 application 80% of all investigated cardiomyocytes which were incubated with intracellular Ca^{2+} store blockers showed no response to Ad2. In contrast, 70% of all tested cardiomyocytes treated with extracellular Ca^{2+}

channel inhibitors showed an increase in cytosolic Ca^{2+}. These results suggest that Ad2 after binding to the extracellular CAR domains somehow triggers an intracellular Ca^{2+} release which increases cytosolic Ca^{2+} concentration and therefore the beating frequency of wt cardiomyocytes.

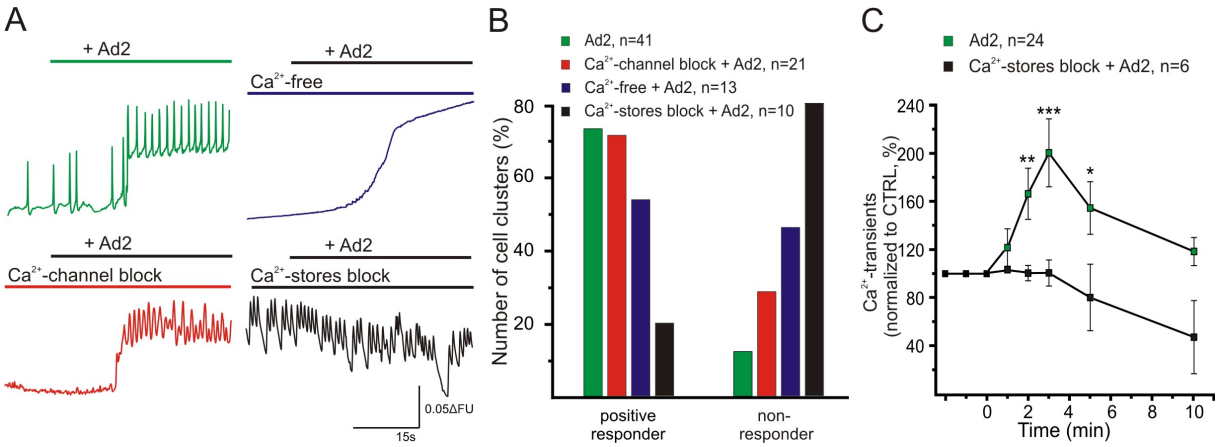

Figure 3.39: Ad2 fiber knob triggers intracellular Ca^{2+} release. E15 wt cardiomyocytes were treated before Ad2 application with extracellular Ca^{2+} channel blockers, placed in Ca^{2+} free ACSF or incubated with intracellular Ca^{2+} store release inhibitors (A). After incubation with the specific inhibitors Ad2 was applied and calcium imaging was performed to measure intracellular Ca^{2+} changes. Blocking of L-, T-, N- and P-type Ca^{2+} channels cardiomyocytes still showed an increase in cytosolic Ca^{2+} (A, red and blue graph). Cells in which intracellular Ca^{2+} store release was blocked no induction of intracellular Ca^{2+} and increase in beating was recorded (B, C). * P<0.05, ** P<0.01, *** P<0.001

3.3.4 Intracellular Ca^{2+} release is mediated by PI3K

Ad2 binding to CAR domains at the cell membrane triggers a signaling pathway which results in the release of Ca^{2+} from the sarcoplasmic reticulum to the cytosol. However, the signal transfer from the cell membrane (Ad2-CAR binding) to the intracellular Ca^{2+} store must be mediated by at least one or several signaling enzymes. To identify a related enzyme different inhibitors against specific signaling pathways were applied.

Blocking PI3K by wortmannin reduced beating of cardiomyocytes slightly (data not shown). Ad2 treatment after blocking of PI3K did not show an induction of beating frequency and cytosolic Ca^{2+} in E15 wt cardiomyocytes and HL-1 cells (fig.3.40 A-C). In calcium imaging recordings of E15 cardiomyocytes an increase of the fluorescence ratio appeared due to Fura-2 bleaching effects (fig.3.40 A, black). No increase in Ca^{2+} was detected. Further, the beating frequency of HL-1 cells and E15 wt cardiomyocytes did not rise after blocking PI3K and Ad2 treatment (fig.3.40 C). Therefore, Ad2 appears to trigger the activation of PI3K at the cell membrane of cardiomyocytes after binding to CAR. PI3K then activates the intracellular Ca^{2+} stores and the release of a high amounts of Ca^{2+}. However it is still unknown if PI3K alone or via other signaling enzymes triggers the release of Ca^{2+} from the sarcoplasmic reticulum which then induce

the beating frequency.

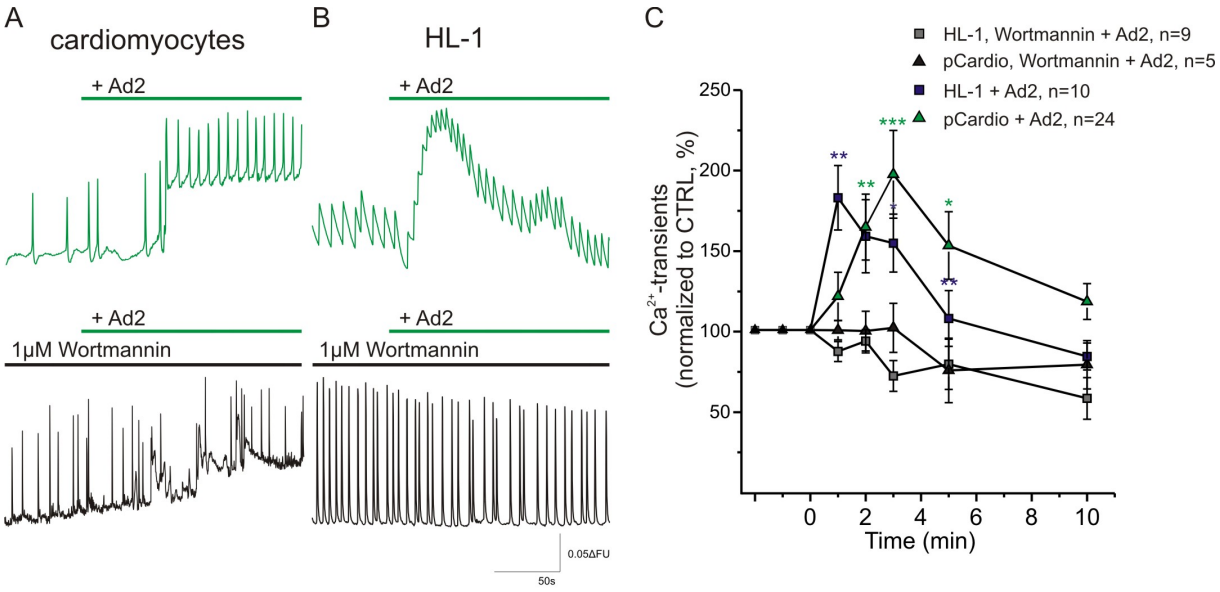

Figure 3.40: Ad2 induced intracellular Ca^{2+} release is mediated by PI3K. E15 wt cardiomyocytes and cultivated HL-1 cells were incubated with 1 µM wortmannin for 30 min. Afterwards Ad2 was applied and beating was recorded (A, B). For both cell types no increase in cytosolic Ca^{2+} was determined and the beating frequency did not change compared to wortmannin untreated cells (C). * $P<0.05$, ** $P<0.01$, *** $P<0.001$

4 Discussion

4.1 CAR KO cardiomyocytes and hearts beat significant faster than wt cardiomyocytes

Several studies showed that CAR is essential for correct embryonic heart development and therefore for survival of mouse embryos (Asher et al., 2005; Chen et al., 2006; Dorner et al., 2005). Furthermore, in the mature heart CAR is needed for correct electrical conduction in the AV node to transfer the excitation of the atrium to the working myocardium of the ventricles (Lim et al., 2008; Lisewski et al., 2008; Pazirandeh et al., 2011). An unregarded perspective of CAR during heart development is its role in early embryonic heart beating. Therefore in this study the influence of CAR on embryonic heart beats as well as on spontaneous Ca^{2+} transients in cardiomyocytes was investigated. First, a CAR KO mouse model (Dorner et al., 2005) was used to analyse beating frequency and Ca^{2+} cycling in CAR KO hearts and cardiomyocytes. Also CAR signaling in embryonic wt cardiomyocytes was studied.

The analysis of spontaneous beating frequency and the corresponding Ca^{2+} transients in cultivated E10.5 CAR KO cardiomyocytes showed a significant faster beating compared to wt cardiomyocytes. Also CAR KO hearts revealed a significant higher beating rate when investigated by eye. This effect of CAR disruption on beating frequency was also found by Lisewski et al. (2008, Supplement fig. 4). The authors showed an increase in heart rate after CAR expression was reduced by tamoxifen. Further, they observed a complete AV block in CAR KO mice suggesting that CAR is also essential for electrical conduction in the mature heart. The raised beating frequency in embryonic CAR KO cardiomyocytes found in this study showed that CAR also is involved in early heart beats. As component of tight and gap junctions CAR seems to promote the transmission of the electrical excitation between neighbouring cardiomyocytes. A loss of CAR may alter the cell-cell communication potentially due to changes in gap junction composition. Reduction of Cx45 was observed in embryonic CAR KO hearts and also in adult inducible CAR KO hearts (Lim et al., 2008; Lisewski et al., 2008). These data indicate that CAR regulates gap junctions and the transmission of electrical excitation.

The observed statistical difference in spontaneous beating frequency between CAR KO and wt was higher in E10.5 CAR wt and KO cardiomyocytes cultures compared to CAR wt and KO

whole heart cultures. This could be caused by experimental factors: the whole heart preparations were very sensitive to movement and temperature change. After removing the cultivated hearts from the incubator the hearts stopped to beat in some cases or reduced their beating frequency. Comparison of *in vivo* heart rates from E11 embryos in the uterus (124 ± 11 bpm (Gui et al., 1996)) with the used whole heart cultures also showed a slight reduction for CAR wt hearts (104 ± 10 bpm) after preparation and cultivation on the filter probably due to loss of sufficient nutrition, hormonal and neuronal regulation as well as tissue injuries generated during the preparation. This effect of reduction in heart rate after removal of the embryonic heart was also seen by Rapila et al. (2008). However, it can be assumed that for CAR wt as well as CAR KO hearts the beating rate *in vivo* is even higher and the difference between both genotypes more severe than observed in this study.

The beating frequency of cultivated cardiomyocytes was significant reduced compared to the observed heart rates of the whole heart preparations (for CAR wt 59 ± 5 bpm vs. 104 ±10 bpm). This reduction in cultivated cardiomyocytes could be caused by the loss of coordinated beating as found in the heart. Due to the dissociation of the hearts the intercellular communication and coordination of neighbouring cardiomyocytes get disrupted resulting in decrease of beating frequency in the plated cardiomyocytes cultures. Further, the recorded Ca^{2+} transients during calcium imaging experiments also showed a reduction compared to the eye counting of the beating of cultivated cardiomyocytes (for CAR wt 26 ± 3 bpm vs. 59 ± 5 bpm). The Ca^{2+} sensitive dye Fura-2AM used to measure spontaneous Ca^{2+} transients in cardiomyocytes was diluted in pluronic acid/DMSO whereby it was published that pluronic acid and DMSO can trigger leakage and partly damaging the cell membrane (Gurtovenko & Anwar, 2007; Yu & Quinn, 1994). Disruption in the cell membrane can alter the membrane potential and voltage-gated ion channels resulting in modified Ca^{2+} signaling. The reduced observed spontaneous beating rate of cardiomyocytes during calcium imaging could also be caused by temperature changes of the ACSF buffer.

Comparison of the CAR KO mouse model with various genetically modified mouse models of cell junction components revealed for N-cadherin and vinculin also dysfunction in the AV node (Kostetskii et al., 2005; Li et al., 2005; Zemljic-Harpf et al., 2007). However, investigation of heart rates in the adult KO mice could not represent an increase in beating frequency as observed in CAR KO adult and embryonic hearts. N-cadherin and vinculin KO mouse models showed a dis-organized structure of intercalated discs and myofibrils resulting in reduced or unaltered heart rate. These findings illustrate that CAR contains unique properties in correct heart beating among other cell junction proteins.

In summary, analysing the spontaneous beating frequency in cultivated E10.5 embryonic cardiomyocytes revealed a significant increase in beating frequency for CAR KO in comparison to wt. This effect was also seen in cultivated whole hearts suggesting that CAR is involved in the regulation of early embryonic heart beats. Therefore, next the cellular mechanism of the increased beating in CAR KO cardiomyocytes was further investigated.

4.2 Increased activity of NCX and SERCA2 results in faster Ca^{2+} decline in CAR KO cardiomyocytes

The analysis of spontaneous Ca^{2+} transients revealed a significant increase in frequency in CAR KO cardiomyocytes. However, the reason or underlying cellular mechanism for this raise in beating was not known. Closer investigation of the recorded Ca^{2+} transients revealed a different Ca^{2+} decline in CAR KO cardiomyocytes. Therefore, a kinetic analysis of the recorded Ca^{2+} transients was applied. Surprisingly, the first order exponential decay fit showed a significant smaller decay time constant of the observed Ca^{2+} decline in CAR KO cardiomyocytes compared to CAR wt. A smaller decay time constant results in faster systolic Ca^{2+} extrusion and therefore the CAR KO cardiomyocytes regenerate faster which then induces a new beating cycle. This observed effect of faster Ca^{2+} decline in CAR KO Ca^{2+} transients could be detected in all CAR KO calcium imaging recordings supporting the overall function of CAR as modulator for heart rate and electrical excitation in cardiomyocytes. However, it is not known if the same result for Ca^{2+} decline in mature CAR KO cardiomyocytes (by using a conditional CAR KO mouse model) will be obtained. But several similar results between the conventional CAR KO mouse model and the inducible CAR KO model suggest related decay time constants of recorded Ca^{2+} decline.

To verify this result, also the decay time constant of caffeine induced Ca^{2+} transients was calculated and revealed the same results: in CAR KO cardiomyocytes the Ca^{2+} decline of caffeine induced Ca^{2+} transients was significantly faster. Both experiments obtained a faster Ca^{2+} decline which indicates that the Ca^{2+} extrusion proteins or their activity are altered. The systolic Ca^{2+} extrusion is mainly carried out by SERCA2 and NCX while PMCA and mitochondria only play a minor role. Faster Ca^{2+} decline must be caused by higher activity or higher protein amount of SERCA2, NCX, PMCA or mitochondria. Therefore, next the activity of these Ca^{2+} extrusion proteins was measured by analysing the rate constants. For each Ca^{2+} extrusion protein the rate constant was measured and surprisingly for SERCA2 and NCX a significant higher rate constant was obtained in CAR KO Ca^{2+} transients.

During systolic Ca^{2+} decline the SERCA rate constant was significant increased in CAR KO compared to CAR wt cardiomyocytes. However, comparison of the specific proportions of Ca^{2+} amount which is extruded from the cytosol back to the SR was for both CAR wt and KO cardiomyocytes 90% of the total systolic Ca^{2+}. The increased SERCA rate constant in CAR KO cardiomyocytes implies a faster removal of cytosolic Ca^{2+} that means in the same time more Ca^{2+} is transferred by SERCA in CAR KO compared to the slower removal observed in CAR wt cardiomyocytes. But, if only one beating cycle is investigated, the proportion of removed Ca^{2+} from the cytosol into the SR by SERCA is the same for CAR wt and KO cardiomyocytes (90%). No difference between CAR wt and KO is found for the proportion of the removed Ca^{2+} but in CAR KO the needed time to transfer this amount of cytosolic Ca^{2+} is significant shorter than in

CAR wt cardiomyocytes resulting in the faster Ca^{2+} decline. For evaluation of the Ca^{2+} stored in the SR and the amount of released Ca^{2+} during the beating, the amplitude of the recorded caffeine induced Ca^{2+} transients can be measured and analysed. No significant change in the amount of released Ca^{2+} from the SR could be determined for CAR KO cardiomyocytes. These data suggest that in CAR KO cardiomyocytes the SERCA2 activity is increased whereby the same proportion of cytosolic Ca^{2+} is transferred by SERCA in CAR KO and wt but in CAR KO cardiomyocytes the needed time for the Ca^{2+} removal is faster. Further, comparison with published values of proportions of extruded Ca^{2+} by SERCA2 in mice revealed the same amount of ca. 90% (Bers, 2002; Voigt et al., 2012). The reported values always represent Ca^{2+} extrusion in adult cardiomyocytes so it can be concluded from the observed data in this study that already in early embryonic cardiomyocytes the Ca^{2+} extrusion system is fully developed.

Besides SERCA2 also the rate constant of NCX was significant increased in CAR KO cardiomyocytes (CAR wt 0.1 s^{-1} vs. CAR KO 0.28 s^{-1}) suggesting that in CAR KO cardiomyocytes the NCX activity is increased because NCX removes more Ca^{2+} in the same time compared to CAR wt. Further, an increase in the proportion of the extruded Ca^{2+} amount via NCX during every beating cycle could be measured. In CAR wt cardiomyocytes 5% of the systolic Ca^{2+} is removed by NCX from the cytosol across the cell membrane. A slight induction to 7% in CAR KO cardiomyocytes was determined. However, the analysis of caffeine induced Ca^{2+} transients revealed a strong increase from approx. 53% for CAR wt to 67% in CAR KO in the proportion of the Ca^{2+} amount that is extruded by NCX suggesting that the activity of NCX is strongly induced in CAR KO cardiomyocytes. To further verify this result the NCX activity and expression was closer investigated. Surprisingly, after blocking NCX by Ni^{2+} which is an unspecific blocker of NCX or application of Na^{+}- and Ca^{2+}-free ACSF buffer the caffeine induced Ca^{2+} transients showed the same Ca^{2+} decline in CAR wt and KO cardiomyocytes. For both genotypes similar decay time constants of the Ca^{2+} decline were measured. The strong prolongation of the Ca^{2+} decline is caused by the NCX block because afterwards only the slower Ca^{2+} extrusion mechanisms PMCA and mitochondria remove cytosolic Ca^{2+}. These observations were consistent with various published data that showed similar prolongation in Ca^{2+} decline after NCX block (Bassani et al., 1992; Pott et al., 2005; Yao et al., 1998). Because CAR wt and KO cardiomyocytes did not beat after complete block of NCX the activity was altered by changing the extracellular Na^{+} concentration. Raise from normal physiological Na^{+} concentration of 130 mM to 180 mM increased the activity for Ca^{2+} transport across the membrane expecting an increase in beating frequency. Both CAR wt and KO cardiomyocytes increased their beating frequency after raise of extracellular Na^{+} concentration but CAR wt showed a higher percentaged increase which was not significant. However, CAR KO cardiomyocytes revealed a significant increase in beating and still beat significant faster compared to CAR wt suggesting that NCX activity or protein level of NCX is increased in CAR KO cardiomyocytes. Analog findings were obtained after overexpression of NCX whereby the faster Ca^{2+} extrusion, due to higher activity of NCX, can be dimished by blocking NCX with Ni^{2+} (Pott et al., 2004; Reuter et al., 2004;

Terracciano et al., 2001). The same result was found in this study. The decrease of extracellular Na^{+} concentration revealed for CAR wt and KO a significant reduction in beating frequency but compared to wt CAR KO cardiomyocytes still beat significant faster. This result further promotes the suggested idea of induced NCX activity or raised NCX protein level in CAR KO cardiomyocytes. Surprisingly, NCX gene expression analysis and protein determination did not show any change of NCX in CAR KO compared to wt. Therefore it can be concluded that the activity of NCX is significant increased in CAR KO hearts which results in faster Ca^{2+} decline and therefore faster systolic recovery of the CAR KO cardiomyocytes.

As described above, also the SERCA2 rate constant was significant increased in CAR KO cardiomyocytes. Therefore further investigation of SERCA2 during spontaneous embryonic beating in CAR KO cardiomyocytes was done. Blocking of SERCA2 by thapsigargin is expected to result in complete loss of spontaneous beating of embryonic cardiomyocytes (Fu et al., 2006; Rapila et al., 2008; Viatchenko-Karpinski et al., 1999). This effect was only observed partly in CAR wt cardiomyocytes. As expected CAR wt cardiomyocytes reacted very sensitive to 10 µM thapsigargin treatment leading to long periods of complete loss of beating or sudden bursts of short term beating. The observed calcium imaging recordings suggest that after SERCA2 blocking CAR wt cardiomyocytes still can beat spontaneously, however the regular recorded Ca^{2+} transients before thapsigargin treatment were not determined anymore. This result support the mechanism of embryonic beating reported by Rapila et al. (2008) in which blocking of SERCA2 reduce beating frequency but for a certain period of time the cardiomyocytes can beat further due to voltage-gated L-type channels and NCX. Surprisingly, CAR KO cardiomyocytes did not alter their beating at all. There was a slight induction of spontaneous Ca^{2+} transient frequency but this effect was not significant. To verify the observed effect of thapsigargin a second SERCA2 blocker (CPA) was applied. CAR wt cardiomyocytes stopped beating shortly after CPA application. In contrast to thapsigargin, also CAR KO cardiomyocytes decreased their beating frequency. However, compared to CAR wt CAR KO cardiomyocytes still beat significant faster even after 30 min of CPA treatment. This conflicting results between thapsigargin and CPA treatment can be explained by closer investigation of the chemical structures and properties of thapsigargin and CPA. Thapsigargin has a molecular weight of 650 g/mol whereby CPA only 336 g/mol has and therefore the binding at the SERCA2 molecule differs: as a smaller molecule CPA can reach in more inner parts of the transmembrane domain of SERCA2 (Michelangeli & East, 2011; Moncoq et al., 2007; Winther et al., 2010; Xu et al., 2004). However, the inhibition constant of thapsigargin is 0.2 - 12 nM which suggest a higher sensitivity and specificity for proper blocking SERCA2. In contrast, CPA revealed an inhibition constant of 90 - 2500 nM resulting in less sensitivity and less specificity. Assuming that CPA could also trigger several side effects on other cardiac proteins (for example: voltage-gated channels, NCX, RyR or IP3R) within the cardiomyocytes which results in the stronger reduction of beating frequency compared to thapsigargin treatment. However, the significant raised decay time constant after CPA application calculated for CAR KO Ca^{2+} transients showed successful blocking of SERCA2.

Blocking SERCA2 by thapsigargin or CPA revealed for CAR KO continuously beating compared to partly or complete loss of spontaneous beating in CAR wt cardiomyocytes. This surprising effect can be explained by either a gene expression change of SERCA2/PLB or other Ca^{2+} extrusion proteins can rescue the SERCA2 block. Gene expression analysis, western blot and staining of E11 CAR wt and KO against SERCA2 and PLB did not reveal any change for CAR KO hearts. Therefore it can be concluded that the induced activity of NCX in CAR KO can rescue the SERCA block resulting in continuously beating. This suggest that both, the significant increased activity of SERCA2 and NCX maintain a significant faster Ca^{2+} decline resulting in higher beating frequency in CAR KO hearts and cardiomyocytes.

The rate constant of the slower Ca^{2+} extrusion proteins PMCA and the mitochondrial Ca^{2+} uniporter were also investigated and the analysis revealed only a minor proportion of Ca^{2+} amount that is removed by PMCA or into mitochondria (also published by Bers, 2002). No significant change in the calculated rate constants between CAR KO and wt could be observed. However, up to date the role of mitochondria and PMCA was not investigated for embryonic beating. Blocking the Ca^{2+} uptake into the mitochondria CAR wt cardiomyocytes increased their spontaneous beating frequency probably because mitochondria Ca^{2+} cycling is slower compared to re-uptake of Ca^{2+} via SERCA2 into the SR (Dedkova & Blatter, 2013). However, CAR KO cardiomyocytes did not change their beating after blocking mitochondrial Ca^{2+} uptake but still beat significant faster than wt cardiomyocytes suggesting that the CAR KO cardiomyocytes already carried their maximal beating rate. Inhibition of Ca^{2+} release from the mitochondria to the cytosol revealed for both genotypes a complete loss in beating shortly after application of the specific blocker CGP-37157 indicating that mitochondria already at this early embryonic time point play an important role as Ca^{2+} buffer system for correct generation of heart beats. A second reason for the prompt loss of spontaneous beating could be the fast change of mitochondrial membrane potential due to the block of mNCX. The main function of mitochondria is the production of ATP via the oxidative phosphorylation process which is highly dependent on the correct mitochondrial membrane potential. Therefore a change of the membrane potential of mitochondria could induce stop of ATP generation and therefore a loss of contraction as well as the opening of the mitochondrial permeability transition pore (Lemasters et al., 2010; Ruiz-Meana et al., 2007). Furthermore the size of the mitochondria in cultivated CAR KO cardiomyocytes was investigated because Dorner et al. (2005) published an increase in mitochondria size in E11 CAR KO heart sections. However, no significant difference could be found for CAR KO mitochondria in cultivated cardiomyocytes by this method. Also Lisewksi et al. (2008) could not observe any change in the structure and size of mitochondria in CAR KO hearts suggesting that this discrepancy might be explained by a difference between cultivated cardiomyocytes and intact hearts or by the methods applied.

4.3 Altered cell size of CAR KO cardiomyocytes and induced cell coupling trigger faster beating of CAR KO

Lim et al. (2008) and Lisewski et al. (2008) reported that in adult CAR KO hearts the protein level of Cx45 was strongly reduced, but furthermore the coupling of neighbouring adult cardiomyocytes was enhanced in CAR KO. However, up to date no investigation of embryonic CAR KO cardiomyocytes in regard of gap junction and cell coupling was done. Gene expression analysis and western blot also showed for embryonic E11 CAR KO hearts a significant reduction of Cx45 whereas Cx40 and Cx43 expression is not changed significantly. In E10.5 cultivated CAR KO cardiomyocytes increased dye coupling was determined. These observed results agree with the published data for adult conditional CAR KO hearts suggesting that CAR also influence gap junctions in the embryonic heart. Further, colocalisation with Cx43 could be shown for E11 embryo cryostat sections and in cultivated E10.5 wt cardiomyocytes. Changes in connexin expression and remodelling of gap junctions is often related to arrhythmia in various heart diseases due to altered electrical pulse propagation (Severs et al., 2008). Particularly, changes in Cx45 expression can strongly influence cell coupling and intracellular Ca^{2+} transients. Overexpression of Cx45 in mature cardiomyocytes results in reduced dye spreading with lucifer yellow (Betsuyaku et al., 2006). In Cx45 knockout the frequency of intracellular Ca^{2+} transients was increased but the decay time constant of the Ca^{2+} decline was increased (Egashira et al., 2004). These similar result of increased beating frequency in Cx45 KO hearts and CAR KO hearts could suggest a strong interplay between CAR and Cx45 in which both proteins can influence each other. Both proteins show the same expression regulation of high protein levels during embryonic development and strong reduction and strict localisation in the intercalated discs in mature hearts whereby mainly CAR and Cx45 is found in the sinoatrial and atrioventricular node (Jansen et al., 2010; Lisewski et al., 2008; Kumai et al., 2000; Matthäus et al., 2014). Colocalisation of CAR and Cx45 in the heart was shown by Lim et al. (2008) and both proteins contain a PDZ binding site at their cytoplasmic domain which promotes colocalisation with ZO-1 (Lim et al., 2008; Kopanic et al., 2014). Cx45 KO mouse die around E10.5 due to strong malformation inside the heart whereby again similarities to the CAR KO mouse model can be found: both KO models showed a AV conduction block in mature stages, malformations in the endocardial cushions but generation of first heart beats was possible (Kumai et al., 2000). In CAR KO, both embryonic and adult cardiomyocytes revealed a downregulation of Cx45 expression and similar observations of increased Ca^{2+} transient frequency and reduction of Ca^{2+} decline as recorded for Cx45 KO cardiomyocytes. Taken these data together, it could be suggested that Cx45 and CAR together as gap junction - tight junction protein complex in which also ZO-1 is involved can regulate electrical coupling of cardiomyocytes and therefore can influence intracellular Ca^{2+} transients. As a next step, the Cx45 KO mouse model should be further investigated in regard of a possible reduction of CAR expression.

Significant increased dye spreading of lucifer yellow in CAR KO cardiomyocytes was obtained after correction of the final spreaded lucifer yellow area by the injected cell size. Comparison of the total detected lucifer yellow area did not reveal a difference between CAR wt and KO cardiomyocytes but the number of coupled lucifer yellow stained cardiomyocytes was increased for CAR KO cardiomyocyte cultures. The same result was observed when neurobiotin was used to analyse the coupling of neighbouring cardiomyocytes. However, for technical reasons in the neurobiotin experiments the injected cell could not be identified afterwards and therefore no correction could be applied resulting in no significant difference for neurobiotin cell coupling in CAR KO cardiomyocytes. But also the number of coupled neurobiotin stained cardiomyocytes was higher in CAR KO than for wt. Further, neurobiotin is positively charged in contrast to the negatively charged lucifer yellow but mainly Cx45 containing gap junctions are able to transfer positively charged molecules. Lucifer yellow is transferred by gap junctions containing Cx40 and Cx43. Due to the decreased Cx45 expression in CAR KO hearts the transfer of neurobiotin from cell to cell could also be altered leading to no significant increase in neurobiotin spreaded area for CAR KO cardiomyocytes as observed during lucifer yellow experiments. Similar conflicting results were observed in a Cx45 overexpressing study by Betsuyaku et al. (2006) in which lucifer yellow spreading was reduced and neurobiotin spreading was increased due to higher amounts of Cx45 containing gap junctions.

This strong increase in CAR KO cardiomyocyte cell coupling could explain the increased beating frequency. Due to fast cell coupling the electrical excitation pulse can be transferred faster that results in faster depolarization of the surrounding cardiomyocytes. The more frequent depolarizations in CAR KO cardiomyocytes can only occur when the cardiomyocytes are faster regenerated from the beat before and its corresponding Ca^{2+} cycle which is carried out by the significant faster Ca^{2+} extrusion due to higher NCX and SERCA2 activity. The systolic Ca^{2+} must be removed before the next beat because otherwise the Ca^{2+} sensitivity of the cardiac myofilaments is decreased and no further contraction can occur (Janssen, 2010; Keurs, 2011). The increased cell coupling in CAR KO cardiomyocytes could be explained by the decreased Cx45 expression because Cx45 consisting gap junctions show the slowest conduction velocity and density (Desplantez et al., 2007; Söhl & Willecke, 2004; Van Veen et al., 2000). A reduction in Cx45 containing gap junctions and remodelling of Cx40 and Cx43 gap junctions can increase intercellular coupling in CAR KO cardiomyocytes. Remodelling of gap junctions may occur in CAR KO cardiomyocyte cultures because no lack in adhesion and connection between neighbouring cardiomyocytes was observed and cell density in E10.5 CAR KO cardiomyocyte cultures was not altered.

After blocking gap junctions by a specific blocker the lucifer yellow dye spreading was reduced for both CAR wt and KO cardiomyocytes. Blocking by 200 µM CBX decreased cell coupling more extensively compared to 100 µM NPPB treatment probably due to concentration changes and different specificity or side effects. However, in all determined gap junction blocking experiments

the final lucifer yellow spreaded area was strongly reduced and no significant difference between CAR wt and KO cardiomyocytes was observed anymore. Furthermore, the influence of gap junction blocker on spontaneous beating frequency and the coordination of Ca^{2+} transients in cardiomyocyte clusters was investigated. As expected, NPPB treatment completely abolished the beating in CAR wt cardiomyocytes. Also in CAR KO cardiomyocytes the beating frequency was significantly reduced whereby still spontaneous Ca^{2+} transients could be recorded that were highly coordinated. Also CBX application did not alter the coordination of spontaneous Ca^{2+} in neighbouring CAR wt or KO cardiomyocytes. Surprisingly, the beating frequency was increased in CAR wt cardiomyocytes after CBX treatment, in contrast to a significant reduction in CAR KO cardiomyocytes whereby the beating frequency was still significant faster compared to wt. The induction in beating as observed for CAR wt could be probably caused by side effects of CBX because several published studies of CBX treatment in cardiomyocytes measured a strong reduction of beating (De Groot et al., 2003; Howarth & Qureshi, 2006). However, all recorded data of CBX were received from adult cardiomyoctes. No publication could be found in which embryonic cardiomyocytes were studied in regard of blocking gap junctions with CBX. Therefore the observed converse effect could be provoked by the difference of development and in the excitation contraction system. Still, the lack of unorganised less coordinated Ca^{2+} transients in neighbouring cardiomyocytes can not be explained because blocking of gap junction should result in uncoordinated beating of cardiomyocyte cell clusters (Li et al., 2012; Suadicani et al., 2000). The differing results could be induced by the applied concentration of the gap junction blocker because Suadicani et al. (2000) measured lack of synchronisation in beating only after strong increase in heptanol (also a gap junction blocker) concentration from 0.3 M to 3 M. Furthermore, knockout mouse models of Cx43 did not show any loss of coordinated beating suggesting that only little amount of coupling is needed for correct synchronisation which probably can be rescued in embryonic cardiomyocytes (Jansen et al., 2010; Suadicani et al., 2000; Wilders et al., 1996).

The calculation of the lucifer yellow injected cell size revealed that CAR KO cardiomyocytes were significant smaller than wt cardiomyocytes. To verify this effect light transmission pictures of cultivated E10.5 CAR wt and KO cardiomyocytes were obtained and the cardiomyocyte cell dimensions were analysed. The same result of significant smaller CAR KO cardiomyocyte cell size was observed. Next, dextran was injected in cardiomyocytes and due to its very huge molecular weight no transfer to neighbouring cells can be maintained which makes dextran a very good molecule to investigate the size of the injected cardiomyocyte. Also this method showed the strong reduction in size of CAR KO cardiomyocytes. This surprising result was further verified in sections of E11 CAR KO embryos that revealed the same decrease in cardiomyocyte size. Because the CAR KO heart is not reduced in the overall size the cardiomyocyte number should be increased as observed for CAR KO heart sections whereby mainly the ventricle walls increased their cardiomyocyte cell numbers. This increase in cardiomyocyte cell number in CAR KO embryo hearts was also observed from Asher et al. (2005), Chen et al. (2006) and Dorner et al. (2005). In their published CAR KO heart sections an increased cardiomyocyte

cell number mainly in the atria and ventricle walls can be observed, but none of the authors analysed the exact number of cardiomyocytes. Furthermore, the thickening of ventricle walls was also determined in adult CAR KO hearts (Lisewski et al., 2008). The increased cardiomyocyte number can be related to a smaller cell size because the total dimensions of the CAR KO hearts independently of embryonic or adult conditional CAR KO is not changed. These results indicate that CAR is able to influence cell size maybe via ZO-1 and E-cadherin as published for epithel cells (Morton et al., 2013; Palatinus et al., 2011). Reduction of CAR and Cx45 expression in the cell membrane of the cardiomyocytes may reduce correct and sufficient localisation of ZO-1 at cell-contact sites as shown for heart failure patients in which decreased Cx43 expression resulted in reduction of ZO-1 localisation at the membrane (Kostin, 2007). ZO-1 is a scaffolding protein which is found at junctional sites and is involved in large protein complexes that can influence cell migration, cell-cell-communication, cell growth and proliferation (Bauer et al., 2010). In primary endothel cells a lack of ZO-1 led to tight junction disruption and induced the reorganisation of the actin-myosin cytoskeleton suggesting that ZO-1 is able to influence the overall cell shape (Tornavaca et al., 2015). Another group found interaction of ZO-1 with α-actinin 4 in cultivated cells of heart, brain and liver (Chen et al., 2006). Furthermore, ZO proteins (ZO-1-3) are able to directly influence transcription by nuclear trafficking or interaction with several associated nucleic acid binding proteins (Bauer et al., 2010). For example, ZO-2 interacts with the transcription factor *Myc* that can regulate cyclin D1 expression and therefore influence proliferation (Huerta et al., 2007). Taken these data together, the reduced size of CAR KO cardiomyocytes could be caused by altered ZO-1 localisation that triggers reorganisation of the cytoskeleton and maybe modulate transcription.

4.4 Other important cardiac beating regulators were not changed in CAR KO hearts and cardiomyocytes

The observed effect of increased beating frequency in CAR KO cardiomyocytes could also be caused by several other major cardiac regulators like cAMP, HCN channels and its corresponding *funny current* or the cytosolic and SR Ca^{2+} concentration. Therefore main important regulators of the beating frequency were analysed. However, in every investigated beating regulator no significant difference between CAR wt and KO cardiomyocytes or hearts could be determined.

The strong increase of beating frequency of CAR KO cardiomyocytes at first indicated a raise in cytosolic cAMP level because altered beating as observed in CAR KO cardiomyocytes is found under physiological conditions only shortly after β-adrenergic stimulation with isoproterenol. Measurement of cAMP concentration in CAR wt and KO hearts did not reveal any difference and therefore cAMP was excluded to cause the raised beating.

Next, the HCN channel and its influence on the spontaneous beating frequency was determined. As already published HCN channel expression starts already at early embryonic development (E9.5) and was considered as initiator for the first heart beats (Liang et al., 2010; Stieber et al., 2003; Yasui et al., 2001). Further, HCN channels are expressed in cardiac adult pacemaker cells and are able to beat spontaneously as also observed in embryonic cardiomyocytes suggesting that probably overexpression of HCN could further induce the beating frequency in CAR KO hearts. First, HCN channel expression was investigated but did not show any change in CAR KO hearts compared to CAR wt. Next, the influence of HCN on the spontaneous beating frequency was analysed by application of a specific HCN channel blocker. Surprisingly, the beating of CAR wt and KO cardiomyocytes did not completely stopped indicating that HCN does not initiate the early heart beating by itself but could be involved. This effect of HCN inhibition on spontaneous Ca^{2+} transients was also reported by Rapila et al. (2008) and Wang et al. (2013) whereby the authors did not observe any change in the frequency of spontaneous Ca^{2+} transients probably due to the less used concentration and incubation time of the blocker. For both genotypes, the cardiomyocytes reacted in a similar manner to the HCN inhibitor, hence the HCN channel can be excluded as potential source of the increased beating frequency in CAR KO cardiomyocytes. Nevertheless, to further verify these results the *funny current* should be measured by using the patch clamp method in cultivated CAR wt and KO cardiomyocytes.

The cytosolic Ca^{2+} concentration was measured for systole and diastole of the cardiomyocytes because higher amounts of free Ca^{2+} could also induce contraction in CAR KO hearts. However, no significant change in CAR KO compared to wt cardiomyocytes was observed. The measured intracellular Ca^{2+} concentrations varied between 120 nM - 130 nM for diastole in both genotypes. Published values of cytosolic Ca^{2+} concentration in adult cardiomyocytes revealed a range

between 110 nM - 181 nM for the diastolic state (Doeller & Wittenberg, 1990; Jaskova et al., 2012; Saini & Dhalla, 2006; Sheu et al., 1984; Thompson et al., 2000). So the measured Ca^{2+} concentrations conform to the published data. Furthermore, the cytosolic Ca^{2+} concentration in E12.5 embryonic cardiomyocytes was determined to 150 nM in the resting state and raising up to 600 nM for the systolic beat (Korhonen et al., 2010). The measured intracellular Ca^{2+} concentrations in this study increased during beating only up to 350 nM - 450 nM. This can be caused by the specific used Ca^{2+} calibration method (Ca^{2+} calibration using a Ca^{2+} sensitive fluorescence dye, Ca^{2+} sensitive electrode, analysis of mathematical models of cardiac beating) and embryonic development stage of the investigated cardiomyocytes. Further, Korhonen et al. (2010) induced beating of the investigated E12.5 cardiomyocytes by electrical pacing (0.5, 1 and 2 Hz) resulting in Ca^{2+} transients with probably higher amplitudes compared to spontaneous Ca^{2+} transients. Since no dramatically difference between CAR wt and KO cardiomyocytes was found the cytosolic Ca^{2+} concentration was discarded as potential origin for the increased beating in CAR KO cardiomyocytes.

As the most important Ca^{2+} store the SR and its corresponding receptors and proteins were also investigated. At first, the maximal amount of Ca^{2+} which could be released was measured by caffeine application. For CAR wt and KO the same Ca^{2+} transient amplitudes were recorded suggesting that the Ca^{2+} amount stored inside the SR is the same and that the release do not differ. Ca^{2+} release from the SR to the cytosol is maintained mainly by RyR2 and to a minor manner by IP3R2. As expected, gene expression analysis of RyR2 and IP3R2 did not reveal any significant change. CAR KO hearts showed a reduction in expression of RyR2 but no significant decrease was observed. This reduction in RyR2 mRNA could be caused during embryo preparation due to tissue damaging, insufficient cDNA synthesis or loss of isolated RNA. Next, the Ca^{2+} leak in cultivated CAR wt and KO cardiomyocytes was determined after the method published by Shannon et al. (2002) and Voigt et al. (2012). An increased Ca^{2+} leak is related to sudden, spontaneous Ca^{2+} sparks which could induce arrhythmias and heart failure (Bers, 2014; Neef et al., 2010; Voigt et al., 2012). However, in CAR KO compared to CAR wt cardiomyocytes no increased Ca^{2+} leak was observed. Inhibition of either PKA or CamKII which can induce the Ca^{2+} leak revealed no change in the observed SR Ca^{2+} leak in CAR wt and KO cardiomyocytes. This result indicates that probably the complete signaling cascade between PKA or CamKII to RyR and SR is not fully developed or that phosphorylation of RyR does not influence spontaneous SR Ca^{2+} release as observed for adult cardiomyocytes. Furthermore, calsequestrin expression was investigated by using western blot. In both, CAR wt and KO hearts an equal amount of calsequestrin was detected. In summary, the SR and its related proteins did not show any change in CAR KO hearts and cardiomyocytes and therefore also this potential cause of increased beating frequency could be rejected. Nevertheless, intracellular IP3 concentration should be measured for CAR KO hearts because an increase in IP3 in embryonic cardiomyocytes induces the frequency of spontaneous SR Ca^{2+} releases (Rapila et al., 2008) and therefore could trigger the increased CAR KO beating.

4.5 CAR mediates intracellular Ca^{2+} release via PI3K signaling pathway

To study the function of CAR further the fiber knob Ad2 of the adenovirus 2 and extracellular domains of CAR were applied to cultivated embryonic wt cardiomyocytes. Therefore specific ligands of CAR were applied and the spontaneous beating frequency and the cytosolic Ca^{2+} concentration was determined. In cultivated embryonic neurons CAR binding triggers Ca^{2+} release from the SR whereby the signaling cascade from CAR to the SR is not understood (Schreiber, 2009). Embryonic cardiomyocytes are very sensitive to cytosolic Ca^{2+} change which provides this cell type as a good working model. Application of the Ad2 fiber knob or extracellular CAR domains (mouse/chick D1D2-Fc) to cultivated E15 wt cardiomyocytes induced a strong intracellular Ca^{2+} raise and the spontaneous beating frequency of Ca^{2+} transients was significant increased whereby the Ad2 fiber knob could increase the beating frequency the most. Also the observed induction in cytosolic Ca^{2+} concentration was higher after Ad2 fiber knob treatment probably due to the 1000-fold higher binding affinity of the fiber knob to the extracellular CAR domains compared to homophilic CAR-CAR binding (Kirby et al., 2000; van Raaij et al., 2000). The same effect was observed when cultivated HL-1 cells were treated with Ad2 fiber knob. However, there was no uniform response to Ad2 or the extracellular CAR domains determined. Between 20-40% of all investigated cardiomyocytes did not increase their spontaneous beating or the cytosolic Ca^{2+}. This variations in the results could be caused by the experimental set up because application of Ad2 or mD1D2-Fc was performed by a glass pipette which was localised near the studied cardiomyocytes. In some cases the exact positioning of the glass pipette was missed that probably caused a reduced ligand concentration resulting in lack of induction of cytosolic Ca^{2+}. Further, cultivated embryonic cardiomyocytes are very sensitive to movement, temperature change and mechanical influences like flow which also could lead to no response after Ad2 treatment. Comparison of mouse and chick D1D2-Fc revealed for chD1D2-Fc a reduced induction in beating frequency and cytosolic Ca^{2+} increase. Furthermore, only 33% of all investigated cardiomyocyte clusters did show any response suggesting that chD1D2-Fc has structural difference compared to mD1D2-Fc that in contrast triggers an intracellular Ca^{2+} increase in 80% of all measured cardiomyocytes. BLAST analysis of mouse CAR against chick CAR measured 58% identity suggesting a high similarity in the protein structure. For correct homophilic binding the D1 and D2 domains of CAR are needed whereby the D2 domain promotes the overall organisation of CAR (Carson, 2001; van Raaij et al., 2000). The measured identity of the mouse and chick D2 domain is only 40% indicating more severe structural changes in chick D2 which probably could cause the observed difference in raise of spontaneous beating and cytoslic Ca^{2+}. Also Patzke et al. (2010) determined a reduction of NIH 3T3 cell adhesion when the cells were applied to immobilized chD1D2 compared to higher cell adhesion with mD1D2 promoting the idea that the slight change in chick CAR protein structure already is enough for loss or reduction of CAR intracellular signaling. Surprisingly, treatment of E15 wt cortex

neurons with mouse D2 domain alone also induced a significant increase in intracellular Ca^{2+} concentration that compared to mouse D1 domain application was reduced. However, this result further promotes the idea that the structural difference in the D2 domain of chick CAR compared to mouse D2 CAR could cause the observed lack of increased beating in E15 wt cardiomyocytes. To further verify this assumption also E15 wt cardiomyocytes should be treated with mouse and chick D2 CAR domain to investigate different response on spontaneous beating frequency and cytosolic Ca^{2+} concentration.

Next, the source of the observed intracellular Ca^{2+} increase was investigated. Schreiber (2009) found in embryonic wt neurons treated with Ad2 fiber knob a release of intracellular Ca^{2+} from the SR. Therefore the same mechanism was suggested in embryonic wt cardiomyocytes. After blocking all types of voltage-gated Ca^{2+} channels Ad2 fiber knob was applied but still an induction in beating and intracellular Ca^{2+} was observed. The same result was found when the extracellular ACSF buffer was changed to Ca^{2+}-free buffer. In contrast, blocking of RyR and IP3R resulted in a complete loss of increase in beating frequency and cytosolic Ca^{2+} after Ad2 application. This result further verifies the proposed CAR signaling mechanism reported by Schreiber (2009). However, there is still a missing link between CAR binding and the determined Ca^{2+} release from the SR. Surprisingly, blocking of phosphatidylinositol 3-kinase (PI3K) by wortmannin revealed a complete loss of the expected response after Ad2 treatment in E15 wt cardiomyocytes suggesting that PI3K is involved in CAR signaling. Indeed, Verdino et al. (2010) published an interaction between junctional adhesion molecule-like (JAML) and CAR in epithel T cells that recruits PI3K for further signaling of JAML. However, in the heart or in cardiomyocytes no family members of the JAM subgroup of the junctional adhesion molecules is expressed (Bazzoni, 2003; Ebnet et al., 2004; Guo et al., 2009; Martìn-Padura et al., 1998). Probably another tight junction or gap junction molecule can recruit and bind to PI3K. After activation of PI3K phosphatidylinositol 3,4,5-trisphosphate (PtdIns-3,4,5-P_3) is generated that also can activate phospholipase C (PLC) resulting in induced IP3 concentration and SR Ca^{2+} release (Bony et al., 2001; Rameh et al., 1998). PI3Kγ is suggested as important cardiac regulator because it negatively regulates cAMP concentrations in cardiomyocytes (Guo et al., 2011; Kerfant et al., 2006; Leblais et al., 2004). Therefore, it can be suggested that CAR binding triggers PI3K activation resulting in PtdIns-3,4,5-P_3 production and PLC activation and afterwards IP3 generation (Bae et al., 1998; Falasca et al., 1998). However, to further promote the proposed CAR signaling mechanism IP3 concentration should be measured after Ad2 fiber knob treatment. Further, western blot analysis should be performed to observe the activation (phosphorylation) of PLC and PI3K after Ad2 fiber knob-CAR binding. First calcium imaging recordings of Ad2 fiber knob application after blocking PLC by a specific inhibitor (U-73122) indicated a loss of increased cytosolic Ca^{2+} and induction in spontaneous beating (data not shown) that also promotes the suggested CAR signaling mechanism.

4.6 Conclusion and future perspective

The aim of the study was to analyse the function of CAR during embryonic heart beating and its potential intracellular signaling in cardiomyocytes. By using a global CAR KO mouse model a significant increased beating frequency in E11 CAR KO hearts and E10.5 cultivated cardiomyocytes was found. This increased beating frequency is facilitated by accompanied faster Ca^{2+} decline due to a significant induced NCX and SERCA2 activity in CAR KO cardiomyocytes. Further, a reduction in Cx45 expression was observed. However, increased cell coupling and uniformed looking CAR KO cardiomyocyte cultures suggesting no lack of cell adhesion and cell-cell-communication probably due to remodelling of gap junction by Cx40 and Cx43. The cell size of CAR KO cardiomyocytes in cultures and hearts was measured and revealed a significant decrease compared to CAR wt cardiomyocytes that is possibly caused by reduced ZO-1 localisation at the cardiomyocyte membrane due to loss in Cx45 and CAR expression. These results indicate that CAR plays an essential role during embryonic heart beating. Due to the strong coexpression with Cx43 and Cx45 it can be suggested that CAR is localised in a larger protein complex involved with ZO-1 at the junctional sites. There, CAR may promote correct localisation of Cx45 and ZO-1 to regulate cell-to-cell coupling. This function of CAR is not only observed in embryonic hearts, also in adult hearts CAR is localised at junctional sites inside the intercalated discs where it promotes correct transmission of electrical excitation and cell coupling. CAR is not needed to trigger the first embryonic heart beats because also in CAR KO embryos a constant heart beat is observed. However, CAR seems to regulate the cell-cell communication in the developing embryonic and adult myocardium and loss of CAR may induce remodelling of gap junctions resulting in altered transmission and cell coupling. Binding of CAR-specific ligands to its receptor triggers a strong Ca^{2+} release from the SR whereby the signaling mechanism includes PI3K.

To further understand the role of CAR in cell coupling, closer investigation in CAR induced gap junction remodelling should be carried out in CAR KO cardiomyocytes. Therefore at first, correct measurement of the gap junction composition must be done in embryonic and adult CAR KO hearts. Gene expression analysis did not show any significant change for Cx43 and Cx40 expression but also the protein level of these connexins must be analysed by western blot. Moreover, the exact localisation of Cx40 and Cx43 should be determined in cultivated CAR KO cardiomyocytes as well as in CAR KO heart sections. Variations in gap junction composition can alter cell coupling as observed in CAR KO cardiomyocytes. Probably, electron microscopy or atomic force microscopy analysis of gap and tight junctions in CAR KO embryos and adult CAR KO hearts (intercalated disc) could be useful to determine changes. Furthermore, functional investigation of gap junctions and cell coupling in CAR KO embryonic whole hearts should be carried out to indicate if electrical excitation and conduction is altered. Both, calcium imaging and cell coupling by injecting lucifer yellow could be done to investigate the electrical conduction.

However, the murine mouse models could be very difficult to analyse due to the size of the heart and fluorescence loss after injecting the dyes. Therefore the zebrafish as *in vivo* working model would be a better choice because of its fast developmental cycle, the reduced size and its paleness which promotes *in vivo* fluorescence recordings (Chi et al., 2010; Hou et al., 2014). To further verify that cell coupling is faster in CAR KO hearts also the velocity of lucifer yellow spreading should be determined. The function of gap junctions can be altered by phosphorylation of several kinases like PKC, extracellular signal-regulated kinase (ERK), the tyrosin kinase src, casein kinase 1, PKA or AKT (Jeyaraman et al., 2012; Márquez-Rosado et al., 2012; Solan & Lampe, 2009). Potentially, changes in phosphorylation of Cx43 or Cx40 in CAR KO hearts further influence cell coupling. Problematic could be the high numbers of possible phosphorylation sites (7 for Cx43, Solan et al., 2009) and the lack of very precise antibodies which may result in non-specific analysis. Besides these general investigations of all connexins, the Cx45 KO mouse model should also be further considered. First of all, the expression of CAR must be determined to monitor if Cx45 and CAR expression is coordinated. Next, calcium imaging in embryonic Cx45 KO cardiomyocytes should be performed to identify the Ca^{2+} extrusion mechanism and clarify if Cx45 KO and CAR KO probably have similar effects on Ca^{2+} decline.

ZO-1 as scaffolding protein highly colocalises with CAR and Cx45 and therefore this protein should be closer investigated. As reduction in CAR and Cx45 expression in the membrane of CAR KO cardiomyocytes was shown, it is very interesting to analyse the localisation. Probably due to loss of colocalisation with CAR and Cx45 no correct arrangement of ZO-1 in the cell membrane is found anymore resulting in nuclear trafficking and gene transcription regulation. Expression of ZO-1 is not changed in embryonic CAR KO hearts (data not shown) suggesting that only localisation could be altered. To investigate ZO-1 localisation cultivated CAR KO embryonic cardiomyocytes and E11 embryo sections should be stained against ZO-1. Lim et al. (2008) found in adult CAR KO hearts a significant reduction in ZO-1 protein level that was also observed in heart sections. Besides ZO-1, the authors measured a reduction in β-catenin whereby the exact localisation was not analysed. Increased nuclear translocalisation from the membrane into the nucleus suggest altered gene transcription. However, in embryonic CAR KO cardiomyocytes no nuclear translocalisation of β-catenin could be determined. These data indicate that in CAR KO hearts the gene expression is altered probably via ZO-1 or the β-catenin pathway. Fast analysis of various gene expression can be done by using the micro array technique. To identify potential up- or downregulation of specific genes in the CAR KO mouse model embryonic and adult CAR KO hearts should be determined. This allows to indicate developmental differences of CAR in the heart. Troponin C, actin and α-actinin staining revealed that the overall localisation and generation of the cardiac cytoskeleton in embryonic CAR KO hearts is not altered. However, the cell size was significant reduced probably due to ZO-1 alterations in localisation and transcription regulation. Therefore, a micro array would be an elegant method to identify potential altered expression of genes that are involved in cell growth and proliferation.

A significant increased NCX activity was observed for CAR KO cardiomyocytes by using calcium imaging. To verify this result also the inward Na^+ current could be measured using the patch clamp method. Furthermore, the membrane resistance could be determined to confirm the obtained reduced cell size for CAR KO cardiomyocytes. The increased heart beat was also found in adult CAR KO mice suggesting that in mature CAR KO cardiomyocytes the Ca^{2+} decline is probably faster. Calcium imaging of adult CAR KO cardiomyocytes could be clarify if Ca^{2+} extrusion is significant faster in KO compared to wt cardiomyocytes as observed for embryonic CAR KO cardiomyocytes. Furthermore, the influence on spontaneous beating and Ca^{2+} cycling in specific CAR overexpressing hearts should be investigated. Due to the results of this CAR KO study it can be speculated that overexpression of CAR results in loss of beating or reduction in spontaneous beating, slowing of Ca^{2+} cycling and reduced cell coupling. CAR overexpressing mature hearts showed increased heart size and dilated ventricles (Caruso et al., 2010). 4 weeks after birth a severe cardiomyopathy was observed in CAR overexpressing mice (Caruso et al., 2010; Yuen et al., 2011). This surprising result can be related to clinical studies of patients suffering from dilated cardiomyopathy in which CAR is significant higher expressed (Noutsias et al., 2001; Toivonen et al., 2010). As a next step, Ca^{2+} cycling, beating frequency and cell coupling of cardiomyocytes from dilated cardiomyopathy patients should be anaylsed to verify the role of CAR. It can be expected that due to the raised CAR expression gap and tight junctions are altered resulting in decreased cell coupling and slowing of Ca^{2+} cycling that than generates cardiomyopathies.

5 Summary

The coxsackie- and adenovirus receptor (CAR) is a cell adhesion protein of the Ig superfamily which serves as receptor for different coxsackie- and adenoviruses. CAR is strongly expressed throughout the developing heart and in contrast, during adulthood CAR is concentrated found at the intercalated discs. CAR knockout mouse models show malformation of the heart which leads to death between embryonic days E11.5 and E12.5 indicating an important function of CAR during heart development. Conditional CAR KO mouse models revealed impairment during excitation conduction in the mature heart. The aim of this study was to investigate the physiological function of CAR during early heart beats with regard to intercellular communication and Ca^{2+} cycling in embryonic cardiomyocytes. By using a global CAR KO mouse model, the investigation of cultivated E10.5 CAR KO cardiomyocytes and E11 CAR KO hearts revealed a significant higher beating frequency. Calcium imaging recordings of spontaneous Ca^{2+} transients in CAR KO cardiomyocytes showed a significant faster systolic Ca^{2+} decline compared to wt. The analysis of the cardiac Ca^{2+} extrusion mechanisms revealed a higher activity for NCX and SERCA2 in CAR KO cardiomyocytes. Gene expression and protein level of both NCX and SERCA2 was not changed in CAR KO hearts. Dye spreading studies with lucifer yellow indicated increased cell coupling of cultivated E10.5 CAR KO cardiomyocytes. Further, a significant reduction of the cell size of the CAR KO cardiomyocytes was found in culture and in embryonic heart sections. Cx45 expression was downregulated in CAR KO hearts, however the observed increased cell coupling suggested in CAR KO hearts a remodelling of gap junctions that increases intercellular communication and excitation conduction resulting in the increased embryonic heart beat as recorded for CAR KO embryos. Due to the strong coexpression with Cx43 and Cx45 it can be suggested that CAR is localised in a larger protein complex involved with ZO-1 at the junctional sites. There, CAR may promote correct localisation of Cx45 and ZO-1 and cell-to-cell coupling. Taken together, CAR regulates intercellular communication between embryonic cardiomyocytes, is able to influence spontaneous Ca^{2+} cycling and is therefore an important regulator for embryonic heart beating.

6 Zusammenfassung

Der Coxsackie- und Adenovirusrezeptor (CAR) ist ein Zelladhäsionsmolekül aus der Superfamilie der Immunglobuline, welches als Rezeptor für verschiedene Coxsackie- und Adenoviren entdeckt wurde. Weitere Untersuchungen zeigten, dass CAR sehr stark während der embryonalen Entwicklung des Herzens exprimiert wird. Hingegen wird CAR in adulten Herzen vorwiegend in den Glanzstreifen zwischen benachbarten Kardiomyozyten gefunden. CAR KO Mausmodelle zeigen starke Herzentwicklungsfehler, welche zwischen Entwicklungsstufe E11.5 und E12.5 zum Tode der betroffenen Embryonen führen und darauf hindeuten, dass CAR eine bedeutende Funktion während der Entwicklung des Herzen hat. Bei Untersuchungen von konditionellen CAR KO Mausmodellen wurde eine Beeinträchtigung der Erregungsweiterleitung im adulten Herzen beobachtet. Ziel dieser Arbeit war es zu untersuchen, inwiefern CAR das spontane Schlagen des embryonalen Herzens in Hinblick auf intrazelluläres Ca^{2+} und Zell-Zell Kommunikation beeinflusst. Dazu wurde ein globales CAR KO Mausmodell verwendet, welches für kultivierte E10.5 CAR KO Kardiomyozyten sowie für E11 CAR KO Herzen eine signifikant erhöhte spontane Schlagfrequenz aufzeigte. Bei Messungen von spontanen Ca^{2+} Transienten in CAR KO Kardiomyozyten wurde eine schnellere systolische Ca^{2+} Abnahme beobachtet im Gegensatz zu den deutlich langsameren Ca^{2+} Abnahmen im wt Kardiomyozyten. Die weitere Analyse von systolischen Ca^{2+} Abbaumechanismen zeigte eine höhere Aktivität für NCX und SERCA2 in CAR KO Kardiomyozyten. Die Genexpression sowie die gemessene Proteinmenge war jedoch für NCX und SERCA2 nicht verändert. Die Beobachtung von *lucifer yellow* Diffusion zwischen benachbarten Kardiomyozyten machte für CAR KO Kardiomyozyten eine stärkere Verbreitung des Farbstoffes deutlich, was auf eine bessere Zell-Zell Kommunikation deutet. Außerdem wurde eine geringere Zellgröße in kultivierten CAR KO Kardiomyozyten und in Gewebeschnitten der embryonalen CAR KO Herzen gefunden. Des Weiteren ist die Expression von Cx45 herunter reguliert, wobei die erhöhte Zell-Zell Kommunikation zwischen CAR KO Kardiomyozyten auf eine Veränderung und Remodellierung der Connexine und *gap junctions* hinweist, die wiederum eine verstärkte Interaktion und Erregungsweiterleitung zwischen den Kardiomyozyten induziert und dadurch die Schlagfrequenz erhöht. Die beobachtete Ko-expression von CAR mit Cx43 und Cx45 unterstützt die Annahme, dass CAR in einen größeren Proteinkomplex zusammen mit Cx43, Cx45 und ZO-1 involviert ist und dieser an Zell-Zell-Kontakten lokalisiert ist. In diesem Proteinkomplex könnte CAR die korrekte Lokalisierung von Cx45 und ZO-1 fördern und somit die Erregungsweiterleitung und interzelluläre Kommunikation unterstützen. Zusammenfassend, CAR reguliert die Interaktion und Kommunikation zwischen benachbarten Kardiomyozyten

im embryonalen Herzen, beeinflusst dadurch die spontanen Ca^{2+} Transienten und ist somit möglicherweise ein weiterer Regulator für das embryonale Herzschlagen.

Bibliography

Adachi-Akahane, S., Lu, L., Li, Z., Frank, J. S., Philipson, K. D., & Morad, M. (1997). Calcium signaling in transgenic mice overexpressing cardiac Na(+)-Ca2+ exchanger. *The Journal of general physiology*, 109(6), 717–29.

Altschul, S. F., Gish, W., Miller, W., Myers, E. W., & Lipman, D. J. (1990). Basic local alignment search tool. *Journal of molecular biology*, 215(3), 403–410.

Anderson, R. H., Webb, S., Brown, N. a., Lamers, W., & Moorman, A. (2003). Development of the heart: (2) Septation of the atriums and ventricles. *Heart (British Cardiac Society)*, 89(8), 949–958.

Aronsen, J. M., Swift, F., & Sejersted, O. M. (2013). Cardiac sodium transport and excitation-contraction coupling. *Journal of molecular and cellular cardiology*, 61, 11–19.

Asher, D. R., Cerny, A. M., Weiler, S. R., Horner, J. W., Keeler, M. L., Neptune, M. a., Jones, S. N., Bronson, R. T., Depinho, R. a., & Finberg, R. W. (2005). Coxsackievirus and adenovirus receptor is essential for cardiomyocyte development. *Genesis (New York, N.Y. : 2000)*, 42(2), 77–85.

Bae, Y. S., Cantley, L. G., Chen, C.-s., Kim, S.-r., Kwon, K.-s., & Rhee, S. G. (1998). Activation of Phospholipase C- âŘě by Phosphatidylinositol. *THE JOURNAL OF BIOLOGICAL CHEMISTRY*, 273(8), 4465–4469.

Barry, D. M. & Nerbonne, J. M. (1996). Myocardial potassium channels: electrophysiological and molecular diversity. *Annual review of physiology*, 58, 363–394.

Baruscotti, M., Barbuti, A., & Bucchi, A. (2010). The cardiac pacemaker current. *Journal of molecular and cellular cardiology*, 48(1), 55–64.

Bassani, B. Y. R. A., Bassani, J. W. M., & Bers, D. M. (1992). MITOCHONDRIAL AND SARCOLEMMAL Ca2+ TRANSPORT REDUCE Ca2+ DURING CAFFEINE CONTRACTURES IN RABBIT CARDIAC MYOCYTES. *Journal of Phy*, 453, 591–608.

Bassani, J. W., Bassani, R. a., & Bers, D. M. (1994). Relaxation in rabbit and rat cardiac cells: species-dependent differences in cellular mechanisms. *The Journal of physiology*, 476(2), 279–293.

Bauer, H., Zweimueller-Mayer, J., Steinbacher, P., Lametschwandtner, a., & Bauer, H. C. (2010). The dual role of zonula occludens (ZO) proteins. *Journal of Biomedicine and Biotechnology*, 2010(Figure 1).

Bazzoni, G. (2003). The JAM family of junctional adhesion molecules. *Current Opinion in Cell Biology*, 15(5), 525–530.

Beard, N. a., Laver, D. R., & Dulhunty, a. F. (2004). Calsequestrin and the calcium release channel of skeletal and cardiac muscle. *Progress in biophysics and molecular biology*, 85(1), 33–69.

Beard, N. a., Wei, L., & Dulhunty, A. F. (2009). Ca2+ signaling in striated muscle: The elusive roles of triadin, junctin, and calsequestrin. *European Biophysics Journal*, 39(1), 27–36.

Bergelson, J. M., Cunningham, J. A., Droguett, G., Kurt-Jones, E. A., Krithivas, A., Hong, J. S., Horwitz, M. S., Crowell, R. L., & Finberg, R. W. (1997). Isolation of a common receptor for Coxsackie B viruses and adenoviruses 2 and 5. *Science*, 275(5304), 1320–3.

Berridge, M. J. (2009). Inositol trisphosphate and calcium signalling mechanisms. *Biochimica et Biophysica Acta - Molecular Cell Research*, 1793(6), 933–940.

Berridge, M. J., Bootman, M. D., & Roderick, H. L. (2003). Calcium signalling: dynamics, homeostasis and remodelling. *Nature reviews. Molecular cell biology*, 4(7), 517–529.

Berridge, M. J., Lipp, P., & Bootman, M. D. (2000). The versatility and universality of calcium signalling. *Nature reviews. Molecular cell biology*, 1(1), 11–21.

Bers, D. (2002). Cardiac excitation contraction coupling. *Nature*, 415, 198–205.

Bers, D. M. (2014). Cardiac sarcoplasmic reticulum calcium leak: basis and roles in cardiac dysfunction. *Annual review of physiology*, 76, 107–27.

Bers, D. M. & Despa, S. (2006). Cardiac Myocytes Ca2+ and Na+ Regulation in Normal and Failing Hearts. *Journal of Pharmacological Sciences*, 100(5), 315–322.

Bers, D. M. & Perez-Reyes, E. (1999). Ca channels in cardiac myocytes: Structure and function in Ca influx and intracellular Ca release. *Cardiovascular Research*, 42(2), 339–360.

Bers, D. M. & Shannon, T. R. (2013). Calcium movements inside the sarcoplasmic reticulum of cardiac myocytes. *Journal of Molecular and Cellular Cardiology*, 58(1), 59–66.

Betsuyaku, T., Nnebe, N. S., Sundset, R., Patibandla, S., Krueger, C. M., & Yamada, K. a. (2006). Overexpression of cardiac connexin45 increases susceptibility to ventricular tachyarrhythmias in vivo. *American journal of physiology. Heart and circulatory physiology*, 290(1), H163–H171.

Bewley, M. C. (1999). Structural Analysis of the Mechanism of Adenovirus Binding to Its Human Cellular Receptor, CAR. *Science*, 286(5444), 1579–1583.

Biel, M., Schneider, A., & Wahl, C. (2002). Cardiac HCN channels: structure, function, and modulation. *Trends in cardiovascular medicine*, 12(5), 206–12.

Biel, M., Wahl-schott, C., Michalakis, S., & Zong, X. (2009). Hyperpolarization-Activated Cation Channels : From Genes to Function. *Physiol Rev*, 89, 847–885.

Blaustein, M. P. & Lederer, W. J. (1999). Sodium/calcium exchange: its physiological implications. *Physiological reviews*, 79(3), 763–854.

Bony, C., Roche, S., Shuichi, U., Sasaki, T., Crackower, M. a., Penninger, J., Mano, H., & Pucéat, M. (2001). A specific role of phosphatidylinositol 3-kinase gamma. A regulation of autonomic Ca(2)+ oscillations in cardiac cells. *The Journal of cell biology*, 152(4), 717–28.

Bosanac, I., Michikawa, T., Mikoshiba, K., & Ikura, M. (2004). Structural insights into the regulatory mechanism of IP 3 receptor. *Biochimica et Biophysica Acta - Molecular Cell Research*, 1742(1-3), 89–102.

Boukens, B. J. & Christoffels, V. M. (2012). Electrophysiological patterning of the heart. *Pediatric Cardiology*, 33(6), 900–906.

Bowles, K. R., Gibson, J., Wu, J., Shaffer, L. G., Towbin, J. a., & Bowles, N. E. (1999). Genomic organization and chromosomal localization of the human Coxsackievirus B-adenovirus receptor gene. *Human genetics*, 105(4), 354–9.

Bowles, N. E., Javier Fuentes-Garcia, F., Makar, K. a., Li, H., Gibson, J., Soto, F., Schwimmbeck, P. L., Schultheiss, H. P., & Pauschinger, M. (2002). Analysis of the coxsackievirus B-adenovirus receptor gene in patients with myocarditis or dilated cardiomyopathy. *Molecular Genetics and Metabolism*, 77(3), 257–259.

Brade, T., Pane, L. S., Moretti, A., Chien, K. R., & Laugwitz, K. L. (2013). Embryonic heart progenitors and cardiogenesis. *Cold Spring Harbor perspectives in medicine*, 3(10), 1–18.

Brini, M. & Carafoli, E. (2011). The Plasma Membrane Ca2+ ATPase and the Plasma Membrane Sodium Calcium Exchanger Cooperate in the Regulation of Cell Calcium. *Cold Spring Harbor Perspectives in Biology*, 3(2), a004168–a004168.

Brittsan, a. G. (2000). Maximal Inhibition of SERCA2 Ca2+ Affinity by Phospholamban in Transgenic Hearts Overexpressing a Non-phosphorylatable Form of Phospholamban. *Journal of Biological Chemistry*, 275(16), 12129–12135.

Bustin, S. a. & Nolan, T. (2004). Pitfalls of Quantitative Real-time PCR. *Journal of Biomolecular Techniques*, 15(3), 155–166.

Cai, C. L., Liang, X., Shi, Y., Chu, P. H., Pfaff, S. L., Chen, J., & Evans, S. (2003). Isl1 identifies a cardiac progenitor population that proliferates prior to differentiation and contributes a majority of cells to the heart. *Developmental Cell*, 5(6), 877–889.

Carson, S. D. (2001). Receptor for the group B coxsackieviruses and adenoviruses : CAR. *Reviews in Medical Virology*, 11, 219–226.

Caruso, L., Yuen, S., Smith, J., Husain, M., & Opavsky, M. A. (2010). Cardiomyocyte-targeted overexpression of the coxsackie-adenovirus receptor causes a cardiomyopathy in association with beta-catenin signaling. *Journal of molecular and cellular cardiology*, 48(6), 1194–205.

Catalucci, D., Latronico, M. V. G., Ceci, M., Rusconi, F., Young, H. S., Gallo, P., Santonastasi, M., Bellacosa, A., Brown, J. H., & Condorelli, G. (2009). Akt increases sarcoplasmic reticulum Ca2+ cycling by direct phosphorylation of phospholamban at Thr17. *The Journal of biological chemistry*, 284(41), 28180–7.

Chaudhry, B., Ramsbottom, S., & Henderson, D. J. (2014). *Genetics of cardiovascular development.*, volume 124. Elsevier Inc., 1 edition.

Chen, J.-W., Ghosh, R., Finberg, R. W., & Bergelson, J. M. (2003). Structure and chromosomal localization of the murine coxsackievirus and adenovirus receptor gene. *DNA and cell biology*, 22(4), 253–9.

Chen, J.-W., Zhou, B., Yu, Q.-C., Shin, S. J., Jiao, K., Schneider, M. D., Baldwin, H. S., & Bergelson, J. M. (2006). Cardiomyocyte-specific deletion of the coxsackievirus and adenovirus receptor results in hyperplasia of the embryonic left ventricle and abnormalities of sinuatrial valves. *Circulation research*, 98(7), 923–30.

Chi, N. C., Bussen, M., Brand-Arzamendi, K., Ding, C., Olgin, J. E., Shaw, R. M., Martin, G. R., & Stainier, D. Y. R. (2010). Cardiac conduction is required to preserve cardiac chamber morphology. *Proceedings of the National Academy of Sciences of the United States of America*, 107(33), 14662–14667.

Christoffels, V. M., Smits, G. J., Kispert, A., & Moorman, A. F. M. (2010). Development of the pacemaker tissues of the heart. *Circulation research*, 106(2), 240–54.

Clapham, D. E. (2007). Calcium Signaling. *Cell*, 131(6), 1047–1058.

Claycomb, W., Lanson, N., STALLWORTH, B., EGELAND, D., Delcarpio, J. O. B. D., Ahinski, A. N. B., & Zzo, N. I. J. I. (1998). HL-1 cells : A cardiac muscle cell line that contracts and retains phenotypic characteristics of the adult cardiomyocyte. *Proc. Natl. Acad. Sci. USA*, 95(March), 2979–2984.

Cohen, C. J., Shieh, J. T., Pickles, R. J., Okegawa, T., Hsieh, J. T., & Bergelson, J. M. (2001). The coxsackievirus and adenovirus receptor is a transmembrane component of the tight junction. *Proceedings of the National Academy of Sciences of the United States of America*, 98(26), 15191–6.

Condorelli, G., Drusco, A., Stassi, G., Bellacosa, A., Roncarati, R., Iaccarino, G., Russo, M. a., Gu, Y., Dalton, N., Chung, C., Latronico, M. V. G., Napoli, C., Sadoshima, J., Croce, C. M.,

& Ross, J. (2002). Akt induces enhanced myocardial contractility and cell size in vivo in transgenic mice. *Proceedings of the National Academy of Sciences of the United States of America*, 99(19), 12333–8.

Connor, N. O. & Silver, R. B. (2007). Ratio Imaging: Practical Considerations for Measuring Intracellular Ca2+ and pH in Living Cells. In *Digital Microscopy, 3rd Edition*, volume 81 (pp. 415–433).

Coyne, C. B. & Bergelson, J. M. (2005). CAR: A virus receptor within the tight junctions. *Advanced Drug Delivery Reviews*, 57, 869–882.

Coyne, C. B., Voelker, T., Pichla, S. L., & Bergelson, J. M. (2004). The coxsackievirus and adenovirus receptor interacts with the multi-PDZ domain protein-1 (MUPP-1) within the tight junction. *The Journal of biological chemistry*, 279(46), 48079–84.

De Groot, J. R., Veenstra, T., Verkerk, A. O., Wilders, R., Smits, J. P. P., Wilms-Schopman, F. J. G., Wiegerinck, R. F., Bourier, J., Belterman, C. N. W., Coronel, R., & Verheijck, E. E. (2003). Conduction slowing by the gap junctional uncoupler carbenoxolone. *Cardiovascular Research*, 60(2), 288–297.

Dedkova, E. N. & Blatter, L. a. (2013). Calcium signaling in cardiac mitochondria. *Journal of molecular and cellular cardiology*, 58, 125–33.

Desplantez, T., Dupont, E., Severs, N. J., & Weingart, R. (2007). Gap junction channels and cardiac impulse propagation. *The Journal of membrane biology*, 218(1-3), 13–28.

DiFrancesco, D. (2010). The role of the funny current in pacemaker activity. *Circulation research*, 106(3), 434–46.

Doeller, J. E. & Wittenberg, B. A. (1990). Intracellular calcium and high-energy in isolated cardiac myocytes. *American Physiological Society*, (51), H1851–H1859.

Dorner, A. a., Wegmann, F., Butz, S., Wolburg-Buchholz, K., Wolburg, H., Mack, A., Nasdala, I., August, B., Westermann, J., Rathjen, F. G., & Vestweber, D. (2005). Coxsackievirus-adenovirus receptor (CAR) is essential for early embryonic cardiac development. *Journal of cell science*, 118(Pt 15), 3509–21.

Doroudgar, S. & Glembotski, C. C. (2013). New concepts of endoplasmic reticulum function in the heart: Programmed to conserve. *Journal of Molecular and Cellular Cardiology*, 55(1), 85–91.

Duchen, M. R. (2000). Mitochondria and Ca(2+)in cell physiology and pathophysiology. *Cell calcium*, 28(5-6), 339–48.

Ebnet, K., Suzuki, A., Ohno, S., & Vestweber, D. (2004). Junctional adhesion molecules (JAMs): more molecules with dual functions? *Journal of cell science*, 117(Pt 1), 19–29.

Egashira, K., Nishii, K., Nakamura, K. I., Kumai, M., Morimoto, S., & Shibata, Y. (2004). Conduction abnormality in gap junction protein connexin45-deficient embryonic stem cell-derived cardiac myocytes. *Anatomical Record - Part A Discoveries in Molecular, Cellular, and Evolutionary Biology*, 280(2), 973–979.

Endoh, M. (2004). Force-frequency relationship in intact mammalian ventricular myocardium: Physiological and pathophysiological relevance. *European Journal of Pharmacology*, 500(1-3 SPEC. ISS.), 73–86.

Evenas, J., Malmendal, A., & Forsen, S. (1998). Calcium. *Current Opinion in Chemical Biology*, 2, 293–302.

Excoffon, K., Gansemer, N. D., Mobily, M. E., Karp, P. H., Parekh, K. R., & Zabner, J. (2010). Isoform-specific regulation and localization of the coxsackie and adenovirus receptor in human airway epithelia. *PloS one*, 5(3), e9909.

Excoffon, K. A., Hruska-Hageman, A., Klotz, M., Traver, G. L., & Zabner, J. (2004). A role for the PDZ-binding domain of the coxsackie B virus and adenovirus receptor (CAR) in cell adhesion and growth. *Journal of cell science*, 117(Pt 19), 4401–9.

Excoffon, K. J. D. a., Traver, G. L., & Zabner, J. (2005). The role of the extracellular domain in the biology of the coxsackievirus and adenovirus receptor. *American journal of respiratory cell and molecular biology*, 32(6), 498–503.

Falasca, M., Logan, S. K., Lehto, V. P., Baccante, G., Lemmon, M. a., & Schlessinger, J. (1998). Activation of phospholipase Cγ by PI 3-kinase- induced PH domain-mediated membrane targeting. *The EMBO journal*, 17(2), 414–422.

Farman, G. P., Allen, E. J., Schoenfelt, K. Q., Backx, P. H., & De Tombe, P. P. (2010). The role of thin filament cooperativity in cardiac length-dependent calcium activation. *Biophysical Journal*, 99(9), 2978–2986.

Fechner, H. (2003). Induction of Coxsackievirus-Adenovirus-Receptor Expression During Myocardial Tissue Formation and Remodeling: Identification of a Cell-to-Cell Contact-Dependent Regulatory Mechanism. *Circulation*, 107(6), 876–882.

Fechner, H., Haack, a., Wang, H., Wang, X., Eizema, K., Pauschinger, M., Schoemaker, R., Veghel, R., Houtsmuller, a., Schultheiss, H. P., Lamers, J., & Poller, W. (1999). Expression of coxsackie adenovirus receptor and alphav-integrin does not correlate with adenovector targeting in vivo indicating anatomical vector barriers. *Gene therapy*, 6(9), 1520–1535.

Fechner, H., Pinkert, S., Wang, X., Sipo, I., Suckau, L., Kurreck, J., Dörner, A., Sollerbrant, K., Zeichhardt, H., Grunert, H.-P., Vetter, R., Schultheiss, H.-P., & Poller, W. (2007). Coxsackievirus B3 and adenovirus infections of cardiac cells are efficiently inhibited by vector-mediated RNA interference targeting their common receptor. *Gene Therapy*, 14(12), 960–971.

Fischer, T. H., Maier, L. S., & Sossalla, S. (2013). The ryanodine receptor leak: how a tattered receptor plunges the failing heart into crisis. *Heart failure reviews*, 18(4), 475–83.

Foskett, J. K., White, C., Cheung, K.-h., & Mak, D.-o. D. (2007). Inositol Trisphosphate Receptor Ca 2+ Release Channels. *Physiological Reviews*, 87(2), 593–658.

Frank, K. & Kranias, E. G. (2000). Phospholamban and cardiac contractility. *Ann Med*, 32, 572–578.

Frank, K. F., Bölck, B., Erdmann, E., & Schwinger, R. H. G. (2003). Sarcoplasmic reticulum Ca2+-ATPase modulates cardiac contraction and relaxation. *Cardiovascular research*, 57(1), 20–7.

Freire, A. G., Resende, T. P., & Pinto-Do-Ó, P. (2014). Building and repairing the heart: What can we learn from embryonic development? *BioMed Research International*, 2014.

Fu, J.-D., Li, J., Tweedie, D., Yu, H.-M., Chen, L., Wang, R., Riordon, D. R., Brugh, S. a., Wang, S.-Q., Boheler, K. R., & Yang, H.-T. (2006). Crucial role of the sarcoplasmic reticulum in the developmental regulation of Ca2+ transients and contraction in cardiomyocytes derived from embryonic stem cells. *FASEB journal : official publication of the Federation of American Societies for Experimental Biology*, 20(1), 181–3.

Gaffin, S. L. (1999). Simplified calcium transport and storage pathways. *J Therm Biology*, 24, 251–264.

Gessert, S. & Kühl, M. (2010). The multiple phases and faces of Wnt signaling during cardiac differentiation and development.

Glembotski, C. C. (2012). Roles for the sarco-/endoplasmic reticulum in cardiac myocyte contraction, protein synthesis, and protein quality control. *Physiology (Bethesda)*, 27(6), 343–350.

Gordon, A. M., Homsher, E., & Regnier, M. (2000). Regulation of contraction in striated muscle. *Physiological reviews*, 80(2), 853–924.

Grynkiewicz, G., Poenie, M., & Tsien, R. Y. (1985). A new generation of Ca2+ indicators with greatly impoved fluorescence properties. *Journal of Biological Chemistry*, 260(6), 3440–3450.

Gui, Y., Linask, K., Khowsathit, P., & Huhta, J. (1996). Doppler Echocardiography of Normal and Abnormal Embryonic Mouse Heart. *Pediatric Research*, 40, 633–642.

Guo, D., Thiyam, G., Bodiga, S., Kassiri, Z., & Oudit, G. Y. (2011). Uncoupling between enhanced excitation-contraction coupling and the response to heart disease: lessons from the PI3Kγ knockout murine model. *Journal of molecular and cellular cardiology*, 50(4), 606–12.

Guo, Y.-L., Bai, R., Chen, C. X.-J., Liu, D.-Q., Liu, Y., Zhang, C.-Y., & Zen, K. (2009). Role of junctional adhesion molecule-like protein in mediating monocyte transendothelial migration. *Arteriosclerosis, thrombosis, and vascular biology*, 29(1), 75–83.

Gurtovenko, A. & Anwar, J. (2007). Modulating the structure and properties of cell membranes: the molecular mechanism of action of dimethyl sulfoxide. *J Phys Chem Biology*, 111, 10453–60.

Gustafsson, A. B. & Gottlieb, R. a. (2008). Heart mitochondria: gates of life and death. *Cardiovascular research*, 77(2), 334–43.

Gwathmey, J. K., Slawsky, M. T., Hajjar, R. J., Briggs, G. M., & Morgan, J. P. (1990). Role of intracellular calcium handling in force-interval relationships of human ventricular myocardium. *The Journal of clinical investigation*, 85(5), 1599–1613.

Györke, S., Stevens, S. C. W., & Terentyev, D. (2009). Cardiac calsequestrin: quest inside the SR. *The Journal of physiology*, 587(Pt 13), 3091–3094.

Hammes, A., Oberdorf-Maass, S., Rother, T., Nething, K., Gollnick, F., Linz, K. W., Meyer, R., Hu, K., Han, H., Gaudron, P., Ertl, G., Hoffmann, S., Ganten, U., Vetter, R., Schuh, K., Benkwitz, C., Zimmer, H. G., & Neyses, L. (1998). Overexpression of the sarcolemmal calcium pump in the myocardium of transgenic rats. *Circulation research*, 83(9), 877–888.

Hardt, S. E. (2002). Glycogen Synthase Kinase-3beta: A Novel Regulator of Cardiac Hypertrophy and Development. *Circulation Research*, 90(10), 1055–1063.

Harrell, M. D., Harbi, S., Hoffman, J. F., Zavadil, J., & Coetzee, W. a. (2007). Large-scale analysis of ion channel gene expression in the mouse heart during perinatal development. *Physiological genomics*, 28(3), 273–83.

Harvey, R. P. (1998). Cardiac looping–an uneasy deal with laterality. *Seminars in cell & developmental biology*, 9(1), 101–108.

Hayashi, H. & Miyata, H. (1994). Fluorescence imaging of intracellular Ca2+. *Journal of pharmacological and toxicological methods*, 31(1), 1–10.

He, Y., Chipman, P. R., Howitt, J., Bator, C. M., Whitt, M. A., Baker, T. S., Kuhn, R. J., Anderson, C. W., Freimuth, P., & Rossmann, M. G. (2001). Interaction of coxsackievirus B3 with the full length coxsackievirus- adenovirus receptor. *Nature structural biology*, 8(10), 874–878.

Henderson, S. A., Goldhaber, J. I., So, J. M., Han, T., Motter, C., Ngo, A., Chantawansri, C., Ritter, M. R., Friedlander, M., Nicoll, D. A., Frank, J. S., Jordan, M. C., Roos, K. P., Ross, R. S., & Philipson, K. D. (2004). Functional Adult Myocardium in the Absence of Na+ -Ca2+ Exchange Cardiac-Specific Knockout of NCX1. *Circ Res*, 95, 604–611.

Herrmann, S., Layh, B., & Ludwig, A. (2011). Novel insights into the distribution of cardiac HCN channels: an expression study in the mouse heart. *Journal of molecular and cellular cardiology*, 51(6), 997–1006.

Hertzberg, E. L., Spray, D. C., & Leinwand, L. A. (1991). Expression of Connexin43 in the Developing Rat Heart. *Circulation research*, 68, 782–787.

Hilgemann, D. W. (2004). New insights into the molecular and cellular workings of the cardiac Na+/Ca2+ exchanger. *American journal of physiology. Cell physiology*, 287(5), C1167–72.

Holroydes, M. J., Robertson, S. P., Johnsong, J. D., Solarosgl, R. J., & James, D. (1980). The Calcium and Magnesium Binding Sites on Cardiac Troponin and I t a. *The Journal of biological chemistry*, 255(24), 11688–11693.

Honda, T., Saitoh, H., Masuko, M., Katagiri-Abe, T., Tominaga, K., Kozakai, I., Kobayashi, K., Kumanishi, T., Watanabe, Y. G., Odani, S., & Kuwano, R. (2000). The coxsackievirus-adenovirus receptor protein as a cell adhesion molecule in the developing mouse brain. *Brain research. Molecular brain research*, 77(1), 19–28.

Hotta, Y., Honda, T., Naito, M., & Kuwano, R. (2003). Developmental distribution of coxsackie virus and adenovirus receptor localized in the nervous system. *Developmental Brain Research*, 143(1), 1–13.

Hou, J. H., Kralj, J. M., Douglass, A. D., Engert, F., & Cohen, A. E. (2014). Simultaneous mapping of membrane voltage and calcium in zebrafish heart in vivo reveals chamber-specific developmental transitions in ionic currents. *Frontiers in Physiology*, 5(September), 1–10.

Howarth, F. C. & Qureshi, M. a. (2006). Effects of carbenoxolone on heart rhythm, contractility and intracellular calcium in streptozotocin-induced diabetic rat. *Molecular and Cellular Biochemistry*, 289(1-2), 21–29.

Howitt, J., Anderson, C. W., & Freimuth, P. (2003). Adenovirus interaction with its cellular receptor CAR. *Current topics in microbiology and immunology*, 272, 331–64.

Huang, K.-C., Yasruel, Z., Guérin, C., Holland, P. C., & Nalbantoglu, J. (2007). Interaction of the Coxsackie and adenovirus receptor (CAR) with the cytoskeleton: binding to actin. *FEBS letters*, 581(14), 2702–8.

Huerta, M., Munoz, R., Tapia, R., Soto-Reyes, E., Ramirez, L., Recillas-Targa, F., Gonzales-Mariscal, L., & Lopez-Bayghen, E. (2007). Cyclin D1 Is Transcriptionally Down-Regulated by ZO-2 via an E Box and the Transcription Factor c-Myc. *Molecular biology of the cell*, 18(1), 4826–4836.

Ito, M., Kodama, M., Masuko, M., Yamaura, M., Fuse, K., Uesugi, Y., Hirono, S., Okura, Y., Kato, K., Hotta, Y., Honda, T., Kuwano, R., & Aizawa, Y. (2000). Expression of Coxsackievirus

and Adenovirus Receptor in Hearts of Rats With Experimental Autoimmune Myocarditis. *Circulation Research*, 86(3), 275–280.

Janowski, E., Cleemann, L., Sasse, P., & Morad, M. (2006). Diversity of Ca2+ signaling in developing cardiac cells. *Annals of the New York Academy of Sciences*, 1080, 154–64.

Jansen, J. a., van Veen, T. a. B., de Bakker, J. M. T., & van Rijen, H. V. M. (2010). Cardiac connexins and impulse propagation. *Journal of molecular and cellular cardiology*, 48(1), 76–82.

Janssen, P. M. L. (2010). Myocardial contraction-relaxation coupling. *American Journal Physiology Heart*, 299(6), 1741–1749.

Jaskova, K., Pavlovicova, M., & Jurkovicova, D. (2012). Calcium transporters and their role in the development of neuronal disease and neuronal damage. *General physiology and biophysics*, 31(4), 375–382.

Jeyaraman, M. M., Srisakuldee, W., Nickel, B. E., & Kardami, E. (2012). Connexin43 phosphorylation and cytoprotection in the heart. *Biochimica et Biophysica Acta - Biomembranes*, 1818(8), 2009–2013.

Ju, Y.-K., Woodcock, E. a., Allen, D. G., & Cannell, M. B. (2012). Inositol 1,4,5-trisphosphate receptors and pacemaker rhythms. *Journal of molecular and cellular cardiology*, 53(3), 375–81.

Kadambi, V. J., Ponniah, S., Harrer, J. M., Hoit, B. D., Ii, G. W. D., Walsh, R. A., & Kranias, E. G. (1996). Cardiac-specific Overexpression of Phospholamban Alters Calcium Kinetics and Resultant Cardiomyocyte Mechanics in Transgenic Mice. *J. Clin. Invest.*, 97, 533–539.

Kashimura, T., Kodama, M., Hotta, Y., Hosoya, J., Yoshida, K., Ozawa, T., Watanabe, R., Okura, Y., Kato, K., Hanawa, H., Kuwano, R., & Aizawa, Y. (2004). Spatiotemporal changes of coxsackievirus and adenovirus receptor in rat hearts during postnatal development and in cultured cardiomyocytes of neonatal rat. *Virchows Archiv : an international journal of pathology*, 444(3), 283–92.

Kattman, S. J., Huber, T. L., & Keller, G. M. (2006). Multipotent Flk-1+ Cardiovascular Progenitor Cells Give Rise to the Cardiomyocyte, Endothelial, and Vascular Smooth Muscle Lineages. *Developmental Cell*, 11(5), 723–732.

Kaur, T., Mishra, B., Saikia, U. N., Sharma, M., Bahl, A., & Ratho, R. K. (2012). Expression of coxsackievirus and adenovirus receptor and its cellular localization in myocardial tissues of dilated cardiomyopathy. *Experimental and clinical cardiology*, 17(4), 183–6.

Kelly, R. G. (2012). *Heart Development*, volume 100. Elsevier Inc.

Kerfant, B.-G., Rose, R. a., Sun, H., & Backx, P. H. (2006). Phosphoinositide 3-kinase gamma regulates cardiac contractility by locally controlling cyclic adenosine monophosphate levels. *Trends in cardiovascular medicine*, 16(7), 250–6.

Keurs, H. E. D. J. (2011). Electromechanical coupling in the cardiac myocyte; Stretch-arrhythmia feedback. *Pflugers Archiv European Journal of Physiology*, 462(1), 165–175.

Kirby, I., Davison, E., Beavil, a. J., Soh, C. P., Wickham, T. J., Roelvink, P. W., Kovesdi, I., Sutton, B. J., & Santis, G. (2000). Identification of contact residues and definition of the CAR-binding site of adenovirus type 5 fiber protein. *Journal of virology*, 74(6), 2804–13.

Kobayashi, T. & Solaro, R. J. (2005). Calcium, thin filaments, and the integrative biology of cardiac contractility. *Annual review of physiology*, 67, 39–67.

Kolawole, A. O., Sharma, P., Yan, R., Lewis, K. J. E., Xu, Z., Hostetler, H. A., & Ashbourne Excoffon, K. J. D. (2012). The PDZ1 and PDZ3 domains of MAGI-1 regulate the eight-exon isoform of the coxsackievirus and adenovirus receptor. *Journal of virology*, 86(17), 9244–54.

Kopanic, J. L., Al-Mugotir, M. H., Kieken, F., Zach, S., Trease, A. J., & Sorgen, P. L. (2014). Characterization of the connexin45 carboxyl-terminal domain structure and interactions with molecular partners. *Biophysical Journal*, 106(10), 2184–2195.

Korhonen, T., Rapila, R., Ronkainen, V.-P., Koivumäki, J. T., & Tavi, P. (2010). Local Ca2+ releases enable rapid heart rates in developing cardiomyocytes. *The Journal of physiology*, 588(Pt 9), 1407–17.

Korhonen, T., Rapila, R., & Tavi, P. (2008). Mathematical model of mouse embryonic cardiomyocyte excitation-contraction coupling. *The Journal of general physiology*, 132(4), 407–19.

Kostetskii, I., Li, J., Xiong, Y., Zhou, R., Ferrari, V. a., Patel, V. V., Molkentin, J. D., & Radice, G. L. (2005). Induced deletion of the N-cadherin gene in the heart leads to dissolution of the intercalated disc structure. *Circulation Research*, 96(3), 346–354.

Kostin, S. (2007). Zonula occludens-1 and connexin 43 expression in the failing human heart. *Journal of Cellular and Molecular Medicine*, 11(4), 892–895.

Kranias, E. G. & Hajjar, R. J. (2012). Modulation of cardiac contractility by the phospholamban/SERCA2a regulatome. *Circulation research*, 110(12), 1646–60.

Kubalak, S. W., Miller-Hance, W. C., O'Brien, T. X., Dyson, E., & Chien, K. R. (1994). Chamber specification of atrial myosin light chain-2 expression precedes septation during murine cardiogenesis. *Journal of Biological Chemistry*, 269(24), 16961–16970.

Kumai, M., Nishii, K., Nakamura, K., Takeda, N., Suzuki, M., & Shibata, Y. (2000). Loss of connexin45 causes a cushion defect in early cardiogenesis. *Development (Cambridge, England)*, 127(16), 3501–3512.

Lanner, J. T., Georgiou, D. K., Joshi, A. D., & Hamilton, S. L. (2001). Ryanodine Receptors: Structure, Expression, Molecular Details, and Function in Calcium Release. *Cold Spring Harbor Perspectives in Biology*, (pp. 1–22).

Law, L. K. & Davidson, B. L. (2005). What does it take to bind CAR? *Molecular therapy : the journal of the American Society of Gene Therapy*, 12(4), 599–609.

Leblais, V., Jo, S.-H., Chakir, K., Maltsev, V., Zheng, M., Crow, M. T., Wang, W., Lakatta, E. G., & Xiao, R.-P. (2004). Phosphatidylinositol 3-kinase offsets cAMP-mediated positive inotropic effect via inhibiting Ca2+ influx in cardiomyocytes. *Circulation research*, 95(12), 1183–90.

Lemasters, J., Theruvath, T., Zhong, Z., & Nieminen, A. (2010). Mitochondrial Calcium and the Permeability Transition in Cell Death. *Biochimica et biophysica acta*, 1787(11), 1395–1401.

Li, C., Meng, Q., Yu, X., Jing, X., Xu, P., & Luo, D. (2012). Regulatory Effect of Connexin 43 on Basal Ca2+ Signaling in Rat Ventricular Myocytes. *PLoS ONE*, 7(4), e36165.

Li, J., Patel, V. V., Kostetskii, I., Xiong, Y., Chu, A. F., Jacobson, J. T., Yu, C., Morley, G. E., Molkentin, J. D., & Radice, G. L. (2005). Cardiac-specific loss of N-cadherin leads to alteration in connexins with conduction slowing and arrhythmogenesis. *Circulation Research*, 97(5), 474–481.

Liang, H., Halbach, M., Hannes, T., Bernd, K., Tang, M., Schunkert, H., Hescheler, J., & Reppel, M. (2010). Electrophysiological Basis of the First Heart Beats. *Cellular Physiology Biochemistry and Biochemistr y*, 25, 561–570.

Lim, B.-k., Xiong, D., Dorner, A., Youn, T.-j., Yung, A., Liu, T. I., Gu, Y., Dalton, N. D., Wright, A. T., Evans, S. M., Chen, J., Peterson, K. L., Mcculloch, A. D., Yajima, T., & Knowlton, K. U. (2008). Coxsackievirus and adenovirus receptor (CAR) mediates atrioventricular-node function and connexin 45 localization in the murine heart. *The Journal of Clinical Investigation*, 118(8), 2758–2770.

Lipp, P., Laine, M., Tovey, S. C., Burrell, K. M., Berridge, M. J., Li, W., & Bootman, M. D. (2000). Functional InsP 3 receptors that may modulate excitation contraction coupling in the heart. *Current Biology*, (July), 939–942.

Lisewski, U., Shi, Y., Wrackmeyer, U., Fischer, R., Chen, C., Schirdewan, A., Jüttner, R., Rathjen, F., Poller, W., Radke, M. H., & Gotthardt, M. (2008). The tight junction protein CAR regulates cardiac conduction and cell-cell communication. *The Journal of experimental medicine*, 205(10), 2369–79.

Liu, W., Yasui, K., Opthof, T., Ishiki, R., Lee, J.-K., Kamiya, K., Yokota, M., & Kodama, I. (2002). Developmental changes of Ca(2+) handling in mouse ventricular cells from early embryo to adulthood. *Life sciences*, 71(11), 1279–92.

Luo, W., Grupp, I. L., Harrer, J., Ponniah, S., Grupp, G., Duffy, J. J., Doetschman, T., & Kranias, E. G. (1994). Targeted ablation of the phospholamban gene is associated with markedly enhanced myocardial contractility and loss of beta-agonist stimulation. *Circulation Research*, 75(3), 401–409.

Lytton, J. (2007). Na+/Ca2+ exchangers: three mammalian gene families control Ca2+ transport. *The Biochemical journal*, 406(3), 365–82.

MacLennan, D. H. & Kranias, E. G. (2003). Phospholamban: a crucial regulator of cardiac contractility. *Nature reviews. Molecular cell biology*, 4(7), 566–77.

Mamidi, R., Gresham, K. S., & Stelzer, J. E. (2014). Length-dependent changes in contractile dynamics are blunted due to cardiac myosin binding protein-C ablation. 5(December), 1–11.

Männer, J. (2009). The anatomy of cardiac looping: A step towards the understanding of the morphogenesis of several forms of congenital cardiac malformations. *Clinical Anatomy*, 22(1), 21–35.

Márquez-Rosado, L., Solan, J. L., Dunn, C. a., Norris, R. P., & Lampe, P. D. (2012). Connexin43 phosphorylation in brain, cardiac, endothelial and epithelial tissues. *Biochimica et Biophysica Acta - Biomembranes*, 1818(8), 1985–1992.

Martìn-Padura, I., Lostaglio, S., Schneemann, M., Williams, L., Romano, M., Fruscella, P., Panzeri, C., Stoppacciaro, a., Ruco, L., Villa, a., Simmons, D., & Dejana, E. (1998). Junctional adhesion molecule, a novel member of the immunoglobulin superfamily that distributes at intercellular junctions and modulates monocyte transmigration. *The Journal of cell biology*, 142(1), 117–27.

Matthäus, C., Schreiber, J., Jüttner, R., & Rathjen, F. (2014). The Ig CAM CAR is Implicated in Cardiac Development and Modulates Electrical Conduction in the Mature Heart. *Journal of Cardiovascular Development and Disease*, 1(1), 111–120.

Mesirca, P., Torrente, A. G., & Mangoni, M. E. (2015). Functional role of voltage gated Ca2+ channels in heart automaticity. *Frontiers in Physiology*, 6(February), 1–13.

Michalak, M. & Opas, M. (2009). Endoplasmic and sarcoplasmic reticulum in the heart. *Trends in Cell Biology*, 19(6), 253–259.

Michelangeli, F. & East, J. M. (2011). A diversity of SERCA Ca2+ pump inhibitors. *Biochemical Society transactions*, 39(3), 789–97.

Mirza, M., Hreinsson, J., Strand, M.-L., Hovatta, O., Söder, O., Philipson, L., Pettersson, R. F., & Sollerbrant, K. (2006). Coxsackievirus and adenovirus receptor (CAR) is expressed in male germ cells and forms a complex with the differentiation factor JAM-C in mouse testis. *Experimental cell research*, 312(6), 817–30.

Mirza, M., Raschperger, E., Philipson, L., Pettersson, R. F., & Sollerbrant, K. (2005). The cell surface protein coxsackie- and adenovirus receptor (CAR) directly associates with the Ligand-of-Numb Protein-X2 (LNX2). *Experimental cell research*, 309(1), 110–20.

Moncoq, K., Trieber, C. a., & Young, H. S. (2007). The molecular basis for cyclopiazonic acid inhibition of the sarcoplasmic reticulum calcium pump. *The Journal of biological chemistry*, 282(13), 9748–57.

Moore, E. D., Becker, P. L., Fogarty, K. E., Williams, D. a., & Fay, F. S. (1990). Ca2+ imaging in single living cells: theoretical and practical issues. *Cell calcium*, 11(2-3), 157–179.

Moorman, A., Webb, S., Brown, N. a., Lamers, W., & Anderson, R. H. (2003). Development of the heart: (1) formation of the cardiac chambers and arterial trunks. *Heart (British Cardiac Society)*, 89(7), 806–814.

Moorman, A. F. M. & Christoffels, V. M. (2003). Cardiac chamber formation: development, genes, and evolution. *Physiological reviews*, 83(4), 1223–1267.

Moorman, A. F. M., Vermeulen, J. L. M., Koban, M. U., Schwartz, K., Lamers, W. H., & Boheler, K. R. (1995). Patterns of Expression of Sarcoplasmic Reticulum Ca2+-ATPase and Phospholamban mRNAs During Rat Heart Development. *Circulation Research*, 76, 616–625.

Moretti, A., Caron, L., Nakano, A., Lam, J. T., Bernshausen, A., Chen, Y., Qyang, Y., Bu, L., Sasaki, M., Martin-Puig, S., Sun, Y., Evans, S. M., Laugwitz, K. L., & Chien, K. R. (2006). Multipotent Embryonic Isl1+ Progenitor Cells Lead to Cardiac, Smooth Muscle, and Endothelial Cell Diversification. *Cell*, 127(6), 1151–1165.

Morton, P. E., Hicks, A., Nastos, T., Santis, G., & Parsons, M. (2013). CAR regulates epithelial cell junction stability through control of E-cadherin trafficking. *Scientific reports*, 3, 2889.

Neef, S., Dybkova, N., Sossalla, S., Ort, K. R., Fluschnik, N., Neumann, K., Seipelt, R., Schöndube, F. a., Hasenfuss, G., & Maier, L. S. (2010). CaMKII-dependent diastolic SR Ca2+ leak and elevated diastolic Ca2+ levels in right atrial myocardium of patients with atrial fibrillation. *Circulation research*, 106(6), 1134–44.

Nerbonne, J. M. & Kass, R. S. (2005). Molecular Physiology of Cardiac Repolarization. *Physiol Rev*, 85, 1205–1253.

Noutsias, M., Fechner, H., Jonge, H. D., Wang, X., Dekkers, D., Pauschinger, M., Bergelson, J., Warraich, R., Yacoub, M., Lamers, J., Schultheiss, H.-p., & Poller, W. (2001). Human Coxsackie-Adenovirus Receptor Is Colocalized With Integrins and Upregulated in Dilated Cardiomyopathy Implications for Cardiotropic Viral Infections v 3 and v 5 on the Cardiomyocyte Sarcolemma. *Circulation*, 104, 275–280.

Oceandy, D., Stanley, P. J., Cartwright, E. J., & Neyses, L. (2007). The regulatory function of plasma-membrane Ca(2+)-ATPase (PMCA) in the heart. *Biochemical Society transactions*, 35(Pt 5), 927–30.

Ottolia, M., Torres, N., Bridge, J. H. B., Philipson, K. D., & Goldhaber, J. I. (2013). Na/Ca exchange and contraction of the heart. *Journal of molecular and cellular cardiology*, 61, 28–33.

Palatinus, J. a., O'Quinn, M. P., Barker, R. J., Harris, B. S., Jourdan, J., & Gourdie, R. G. (2011). ZO-1 determines adherens and gap junction localization at intercalated disks. *American journal of physiology. Heart and circulatory physiology*, 300(2), H583–H594.

Pan, X., Liu, J., Nguyen, T., Liu, C., Sun, J., Teng, Y., Fergusson, M. M., Rovira, I. I., Allen, M., Springer, D. a., Aponte, A. M., Gucek, M., Balaban, R. S., Murphy, E., & Finkel, T. (2013). The physiological role of mitochondrial calcium revealed by mice lacking the mitochondrial calcium uniporter. *Nature cell biology*, 15(12), 1464–72.

Patzke, C., Max, K. E. a., Behlke, J., Schreiber, J., Schmidt, H., Dorner, A. a., Kröger, S., Henning, M., Otto, A., Heinemann, U., & Rathjen, F. G. (2010). The coxsackievirus-adenovirus receptor reveals complex homophilic and heterophilic interactions on neural cells. *The Journal of neuroscience*, 30(8), 2897–910.

Pazirandeh, A., Sultana, T., Mirza, M., Rozell, B., Hultenby, K., Wallis, K., Vennström, B., Davis, B., Arner, A., Heuchel, R., Löhr, M., Philipson, L., & Sollerbrant, K. (2011). Multiple phenotypes in adult mice following inactivation of the Coxsackievirus and Adenovirus Receptor (Car) gene. *PloS one*, 6(6), e20203.

Periasamy, M., Bhupathy, P., & Babu, G. J. (2008). Regulation of sarcoplasmic reticulum Ca 21 ATPase pump expression and its relevance to cardiac muscle physiology and pathology. *Cardiovascular Research*, 77, 265–273.

Petrella, J., Cohen, C. J., Gaetz, J., & Bergelson, J. M. (2002). A zebrafish coxsackievirus and adenovirus receptor homologue interacts with coxsackie B virus and adenovirus. *Journal of virology*, 76(20), 10503–10506.

Pfaffl, M. W. (2004). Quantification strategies in real-time PCR. In *A-Z of quantitative PCR* (pp. 87–112).

Pfaffl, M. W., Physiologie, L., & Weihenstephan, W. (2004). Real-time RT-PCR : Neue Ansätze zur exakten mRNA Quantifizierung. *BIOspektrum*, 1/04 10. J, 92–95.

Pfeiffer, E. R., Tangney, J. R., Omens, J. H., & McCulloch, A. D. (2014). Biomechanics of cardiac electromechanical coupling and mechanoelectric feedback. *Journal of biomechanical engineering*, 136(2), 021007.

Pinkert, S., Klingel, K., Lindig, V., Dorner, A., Zeichhardt, H., Spiller, O. B., & Fechner, H. (2011). Virus-Host Coevolution in a Persistently Coxsackievirus B3-Infected Cardiomyocyte Cell Line. *Journal of Virology*, 85(24), 13409–13419.

Poelmann, R. E., Mikawa, T., & Gittenberger-De Groot, a. C. (1998). Neural crest cells in outflow tract septation of the embryonic chicken heart: Differentiation and apoptosis. *Developmental Dynamics*, 212(3), 373–384.

Poláková, E., Zahradníková, A., Pavelková, J., Zahradník, I., & Zahradníková, A. (2008). Local calcium release activation by DHPR calcium channel openings in rat cardiac myocytes. *The Journal of physiology*, 586(16), 3839–3854.

Poller, W., Fechner, H., Noutsias, M., Tschoepe, C., & Schultheiss, H.-P. (2002). Highly variable expression of virus receptors in the human cardiovascular system. Implications for cardiotropic viral infections and gene therapy. *Zeitschrift für Kardiologie*, 91(12), 978–91.

Pott, C., Goldhaber, J. I., & Philipson, K. D. (2004). Genetic manipulation of cardiac Na+/Ca2+ exchange expression. *Biochemical and biophysical research communications*, 322(4), 1336–40.

Pott, C., Philipson, K. D., & Goldhaber, J. I. (2005). Excitation-contraction coupling in Na+-Ca2+ exchanger knockout mice: reduced transsarcolemmal Ca2+ flux. *Circulation research*, 97(12), 1288–95.

Prall, O. W. J., Menon, M. K., Solloway, M. J., Watanabe, Y., Zaffran, S., Bajolle, F., Biben, C., McBride, J. J., Robertson, B. R., Chaulet, H., Stennard, F. a., Wise, N., Schaft, D., Wolstein, O., Furtado, M. B., Shiratori, H., Chien, K. R., Hamada, H., Black, B. L., Saga, Y., Robertson, E. J., Buckingham, M. E., & Harvey, R. P. (2007). An Nkx2-5/Bmp2/Smad1 Negative Feedback Loop Controls Heart Progenitor Specification and Proliferation. *Cell*, 128(5), 947–959.

Qu, Y., Whitaker, G. M., Hove-Madsen, L., Tibbits, G. F., & Accili, E. a. (2008). Hyperpolarization-activated cyclic nucleotide-modulated 'HCN' channels confer regular and faster rhythmicity to beating mouse embryonic stem cells. *The Journal of physiology*, 586(3), 701–16.

Quednau, B. D., Nicoll, D. A., & Philipson, K. D. (2004). The sodium / calcium exchanger family SLC8. *Eur J Physio*, 447, 543–548.

Rajabi, M., Kassiotis, C., Razeghi, P., & Taegtmeyer, H. (2007). Return to the fetal gene program protects the stressed heart: A strong hypothesis. *Heart Failure Reviews*, 12(3-4), 331–343.

Rameh, L. E., Rhee, S. G., Spokes, K., Kazlauskas, a., Cantley, L. C., & Cantley, L. G. (1998). Phosphoinositide 3-kinase regulates phospholipase Cgamma-mediated calcium signaling. *The Journal of biological chemistry*, 273(37), 23750–7.

Rapila, R., Korhonen, T., & Tavi, P. (2008). Excitation-contraction coupling of the mouse embryonic cardiomyocyte. *The Journal of general physiology*, 132(4), 397–405.

Raschperger, E., Engstrom, U., Pettersson, R. F., & Fuxe, J. (2004). CLMP, a novel member of the CTX family and a new component of epithelial tight junctions. *The Journal of biological chemistry*, 279(1), 796–804.

Raschperger, E., Thyberg, J., Pettersson, S., Philipson, L., Fuxe, J., & Pettersson, R. F. (2006). The coxsackie- and adenovirus receptor (CAR) is an in vivo marker for epithelial tight junctions,

with a potential role in regulating permeability and tissue homeostasis. *Experimental cell research*, 312(9), 1566–80.

Reed, T. D., Babu, G. J., Ji, Y., Zilberman, A., Heyen, M. V., Wuytack, F., & Periasamy, M. (2002). ATPase and the Na / Ca Exchanger are Antithetically Regulated During Mouse Cardiac Development and in Hypo / hyperthyroidism. *J Mol Cell Cardiol*, 32, 453–464.

Renken, C., Hsieh, C. E., Marko, M., Rath, B., Leith, A., Wagenknecht, T., Frank, J., & Mannella, C. a. (2009). Structure of frozen-hydrated triad junctions: A case study in motif searching inside tomograms. *Journal of Structural Biology*, 165(2), 53–63.

Reppel, M., Fleischmann, B. K., Reuter, H., Sasse, P., Schunkert, H., & Hescheler, J. (2007a). Regulation of the Na+/Ca2+ exchanger (NCX) in the murine embryonic heart. *Cardiovascular research*, 75(1), 99–108.

Reppel, M., Igelmund, P., Egert, U., Hescheler, J., & Drobinskaya, I. (2007b). Effect of Cardioactive Drugs on Action Potential Generation and Propagation in Embryonic Stem. *Cellular Physiology Biochemistry and Biochemistr y*, 19, 213–224.

Reppel, M., Sasse, P., Malan, D., Nguemo, F., Reuter, H., Bloch, W., Hescheler, J., & Fleischmann, B. K. (2007c). Functional expression of the Na+/Ca2+ exchanger in the embryonic mouse heart. *Journal of molecular and cellular cardiology*, 42(1), 121–32.

Reuter, H. (2002). Knockout Mice for Pharmacological Screening: Testing the Specificity of Na+-Ca2+ Exchange Inhibitors. *Circulation Research*, 91(2), 90–92.

Reuter, H., Han, T., Motter, C., Philipson, K. D., & Goldhaber, J. I. (2004). Mice overexpressing the cardiac sodium-calcium exchanger: defects in excitation-contraction coupling. *The Journal of physiology*, 554(Pt 3), 779–89.

Risebro, C. a. & Riley, P. R. (2006). Formation of the ventricles. *TheScientificWorldJournal*, 6, 1862–1880.

Robert, V., Gurlini, P., Tosello, V., Nagai, T., Miyawaki, a., Di Lisa, F., & Pozzan, T. (2001). Beat-to-beat oscillations of mitochondrial [Ca2+] in cardiac cells. *The EMBO journal*, 20(17), 4998–5007.

Rochais, F., Mesbah, K., & Kelly, R. G. (2009). Signaling pathways controlling second heart field development. *Circulation Research*, 104(8), 933–942.

Rossi, A. E. & Dirksen, R. T. (2006). Sarcoplasmic reticulum: The dynamic calcium governor of muscle. *Muscle and Nerve*, 33(6), 715–731.

Rossi, D., Barone, V., Giacomello, E., Cusimano, V., & Sorrentino, V. (2008). The sarcoplasmic reticulum: An organized patchwork of specialized domains. *Traffic*, 9(7), 1044–1049.

Ruiz-Meana, M., Abellán, A., Miró-Casas, E., & Garcia-Dorado, D. (2007). Opening of mitochondrial permeability transition pore induces hypercontracture in Ca2+ overloaded cardiac myocytes. *Basic research in cardiology*, 102(6), 542–52.

Saini, H. K. & Dhalla, N. S. (2006). Modification of intracellular calcium concentration in cardiomyocytes by inhibition of sarcolemmal Na+/H+ exchanger. *American journal of physiology. Heart and circulatory physiology*, 291(6), H2790–H2800.

Sasse, P., Zhang, J., Cleemann, L., Morad, M., Hescheler, J., & Fleischmann, B. K. (2007). Intracellular Ca2+ oscillations, a potential pacemaking mechanism in early embryonic heart cells. *The Journal of general physiology*, 130(2), 133–44.

Schreiber, J. (2009). *The cell adhesion molecule coxsackie virus and adenovirus receptor (CAR) modulates intracellular Ca2+ concentration and Cl- conductance in cultivated mouse cortical neurons.* PhD thesis.

Seki, S., Nagashima, M., Yamada, Y., & Tsutsuura, M. (2003). Fetal and postnatal development of Ca2+ transients and Ca2+ sparks in rat cardiomyocytes. *Cardiovascular Research*, 58, 535–548.

Severs, N. J., Bruce, A. F., Dupont, E., & Rothery, S. (2008). Remodelling of gap junctions and connexin expression in diseased myocardium. *Cardiovascular research*, 80(1), 9–19.

Shannon, T. R. (2002). Quantitative Assessment of the SR Ca2+ Leak-Load Relationship. *Circulation Research*, 91(7), 594–600.

Shaw, C. a., Holland, P. C., Sinnreich, M., Allen, C., Sollerbrant, K., Karpati, G., & Nalbantoglu, J. (2004). Isoform-specific expression of the Coxsackie and adenovirus receptor (CAR) in neuromuscular junction and cardiac intercalated discs. *BMC cell biology*, 5(1), 42.

Sheu, S. S., Sharma, V. K., & Banerjee, S. P. (1984). Measurement of cytosolic free calcium concentration in isolated rat ventricular myocytes with quin 2. *Circulation research*, 55(6), 830–834.

Simmerman, H. K. & Jones, L. R. (1998). Phospholamban: protein structure, mechanism of action, and role in cardiac function. *Physiological reviews*, 78(4), 921–47.

Snyders, D. J. (1999). Structure and function of cardiac potassium channels. *Cardiovascular research*, 42(2), 377–390.

Söhl, G. & Willecke, K. (2004). Gap junctions and the connexin protein family. *Cardiovascular Research*, 62(2), 228–232.

Solan, J. L. & Lampe, P. D. (2009). Connexin43 phosphorylation: structural changes and biological effects. *The Biochemical journal*, 419(2), 261–272.

Sollerbrant, K., Raschperger, E., Mirza, M., Engstrom, U., Philipson, L., Ljungdahl, P. O., & Pettersson, R. F. (2003). The Coxsackievirus and adenovirus receptor (CAR) forms a complex with the PDZ domain-containing protein ligand-of-numb protein-X (LNX). *The Journal of biological chemistry*, 278(9), 7439–44.

Stieber, J., Herrmann, S., Feil, S., Löster, J., Feil, R., Biel, M., Hofmann, F., & Ludwig, A. (2003). The hyperpolarization-activated channel HCN4 is required for the generation of pacemaker action potentials in the embryonic heart. *Proceedings of the National Academy of Sciences of the United States of America*, 100(25), 15235–40.

Strehler, E. E., Filoteo, A. G., Penniston, J. T., & Caride, A. J. (2008). Plasma membrane Ca2+ -pumps:. *Biochem Soc trans*, 35(Pt 5), 919–922.

Suadicani, S. O., Vink, M. J., Spray, D. C., Sylvia, O., & David, C. (2000). Slow intercellular Ca2+ signaling in wild-type and Cx43-null neonatal mouse cardiac myocytes. *Am J Physiol Heart Circ Physiol*, 279, 3076–3088.

Sugden, P. H., Fuller, S. J., Weiss, S. C., & Clerk, a. (2008). Glycogen synthase kinase 3 (GSK3) in the heart: a point of integration in hypertrophic signalling and a therapeutic target? A critical analysis. *British journal of pharmacology*, 153 Suppl, S137–53.

Sussman, M. a., Völkers, M., Fischer, K., Bailey, B., Cottage, C. T., Din, S., Gude, N., Avitabile, D., Alvarez, R., Sundararaman, B., Quijada, P., Mason, M., Konstandin, M. H., Malhowski, A., Cheng, Z., Khan, M., & McGregor, M. (2011). Myocardial AKT: the omnipresent nexus. *Physiological reviews*, 91(3), 1023–70.

Taber, L. a. (2006). Biophysical mechanisms of cardiac looping. *International Journal of Developmental Biology*, 50(2-3), 323–332.

Tadross, M. R., Ben Johny, M., & Yue, D. T. (2010). Molecular endpoints of Ca2+/calmodulin- and voltage-dependent inactivation of Ca(v)1.3 channels. *The Journal of general physiology*, 135(3), 197–215.

Takahashi, A., Camacho, P., Lechleiter, J. D., & Herman, B. (1999). Measurement of intracellular calcium. *Physiological reviews*, 79(4), 1089–125.

Takeshima, H., Komazaki, S., Hirose, K., Nishi, M., Noda, T., & Iino, M. (1998). Embryonic lethality and abnormal cardiac myocytes in mice lacking ryanodine receptor type 2. *The EMBO journal*, 17(12), 3309–3316.

Takeshima, H., Nishimura, S., Matsumoto, T., Ishida, H., Kangawa, K., Minamino, N., Ueda, M., Hanaoka, M., Hirose, T., & Numa, S. (1989). Primary structure and expression from complementary DNA of skeletal muscle ryanodine receptor. *Nature*, 339, 439–445.

Terentyev, D., Viatchenko-Karpinski, S., Valdivia, H. H., Escobar, A. L., & Györke, S. (2002). Luminal Ca2+ controls termination and refractory behavior of Ca2+-induced Ca2+ release in cardiac myocytes. *Circulation Research*, 91(5), 414–420.

Terracciano, C. M., Philipson, K. D., & MacLeod, K. T. (2001). Overexpression of the Na(+)/Ca(2+) exchanger and inhibition of the sarcoplasmic reticulum Ca(2+)-ATPase in ventricular myocytes from transgenic mice. *Cardiovascular research*, 49(1), 38–47.

Thoelen, I., Keyaerts, E., Lindberg, M., & Van Ranst, M. (2001a). Characterization of a cDNA encoding the bovine coxsackie and adenovirus receptor. *Biochemical and biophysical research communications*, 288(4), 805–808.

Thoelen, I., Magnusson, C., Tå gerud, S., Polacek, C., Lindberg, M., & Van Ranst, M. (2001b). Identification of alternative splice products encoded by the human coxsackie-adenovirus receptor gene. *Biochemical and biophysical research communications*, 287(1), 216–222.

Thompson, M., Kliewer, A., Maass, D., Becker, L., White, D., Bryant, D., Arteaga, G., Horton, J., & Giroir, B. (2000). Increased Cardiomyocyte Intracellular Calcium during Endotoxin-Induced Cardiac Dysfunction in Guinea Pigs. *Pediatric research*, 47, 669–676.

Toivonen, R., Mäyränpää, M. I., Kovanen, P. T., & Savontaus, M. (2010). Dilated cardiomyopathy alters the expression patterns of CAR and other adenoviral receptors in human heart. *Histochemistry and cell biology*, 133(3), 349–57.

Tomko, R. P., Johansson, C. B., Totrov, M., Abagyan, R., Frisén, J., & Philipson, L. (2000). Expression of the adenovirus receptor and its interaction with the fiber knob. *Experimental cell research*, 255(1), 47–55.

Tomko, R. P., Xu, R., & Philipson, L. (1997). HCAR and MCAR: the human and mouse cellular receptors for subgroup C adenoviruses and group B coxsackieviruses. *Proceedings of the National Academy of Sciences of the United States of America*, 94(7), 3352–6.

Tornavaca, O., Chia, M., Dufton, N., Almagro, L. O., Conway, D. E., Randi, a. M., Schwartz, M. a., Matter, K., & Balda, M. S. (2015). ZO-1 controls endothelial adherens junctions, cell-cell tension, angiogenesis, and barrier formation. *The Journal of Cell Biology*, 208(6), 821–838.

Trafford, W., Díaz, M. E., & Eisner, D. a. (1999). A novel, rapid and reversible method to measure Ca buffering and time-course of total sarcoplasmic reticulum Ca content in cardiac ventricular myocytes. *Pflugers Archiv : European journal of physiology*, 437(3), 501–503.

van den Hoff, M. J., Moorman, a. F., Ruijter, J. M., Lamers, W. H., Bennington, R. W., Markwald, R. R., & Wessels, a. (1999). Myocardialization of the cardiac outflow tract. *Developmental biology*, 212(2), 477–490.

Van Petegem, F. (2012). Ryanodine Receptors: Structure and Function. *Journal of Biological Chemistry*, 287(38), 31624–31632.

Van Petegem, F. (2015). Ryanodine Receptors: Allosteric Ion Channel Giants. *Journal of Molecular Biology*, 427(1), 31–53.

van Raaij, M. J., Chouin, E., van der Zandt, H., Bergelson, J. M., & Cusack, S. (2000). Dimeric structure of the coxsackievirus and adenovirus receptor D1 domain at 1.7 A resolution. *Structure (London, England : 1993)*, 8(11), 1147–55.

Van Veen, T. a. B., Van Rijen, H. V. M., & Jongsma, H. J. (2000). Electrical conductance of mouse connexin45 gap junction channels is modulated by phosphorylation. *Cardiovascular Research*, 46(3), 496–510.

Varian, K. D. & Janssen, P. M. L. (2007). Frequency-dependent acceleration of relaxation involves decreased myofilament calcium sensitivity. *American journal of physiology. Heart and circulatory physiology*, 292(5), H2212–H2219.

Verdino, P., Witherden, D. a., Havran, W. L., & Wilson, I. a. (2010). The molecular interaction of CAR and JAML recruits the central cell signal transducer PI3K. *Science (New York, N.Y.)*, 329(5996), 1210–4.

Vervloessem, T., Yule, D. I., Bultynck, G., & Parys, J. B. (2014). The type 2 inositol 1,4,5-trisphosphate receptor, emerging functions for an intriguing Ca2+-release channel. *Biochimica et Biophysica Acta (BBA) - Molecular Cell Research*.

Viatchenko-Karpinski, S., Fleischmann, B. K., Liu, Q., Sauer, H., Gryshchenko, O., Ji, G. J., & Hescheler, J. (1999). Intracellular Ca2+ oscillations drive spontaneous contractions in cardiomyocytes during early development. *Proceedings of the National Academy of Sciences of the United States of America*, 96(14), 8259–64.

Voigt, N., Li, N., Wang, Q., Wang, W., Trafford, A. W., Abu-Taha, I., Sun, Q., Wieland, T., Ravens, U., Nattel, S., Wehrens, X. H. T., & Dobrev, D. (2012). Enhanced sarcoplasmic reticulum Ca2+ leak and increased Na+-Ca2+ exchanger function underlie delayed afterdepolarizations in patients with chronic atrial fibrillation. *Circulation*, 125(17), 2059–70.

Wallukat, G. (2002). The beta-adrenergic receptors. *Herz*, 27(7), 683–90.

Wang, P., Tang, M., Gao, L., Luo, H., Wang, G., Ma, X., & Duan, Y. (2013). Roles of I(f) and intracellular Ca(2+) release in spontaneous activity of ventricular cardiomyocytes during murine embryonic development. *Journal of cellular biochemistry*, (February), 1–25.

Wei, L., Hanna, A. D., Beard, N. a., & Dulhunty, A. F. (2009). Unique isoform-specific properties of calsequestrin in the heart and skeletal muscle. *Cell Calcium*, 45(5), 474–484.

White, S. M., Constantin, P. E., & Claycomb, W. C. (2004). Cardiac physiology at the cellular level: use of cultured HL-1 cardiomyocytes for studies of cardiac muscle cell structure and function. *American journal of physiology. Heart and circulatory physiology*, 286(3), H823–9.

Wilders, R., Verheijck, E. E., Kumar, R., Goolsby, W. N., van Ginneken, a. C., Joyner, R. W., & Jongsma, H. J. (1996). Model clamp and its application to synchronization of rabbit sinoatrial node cells. *The American journal of physiology*, 271(5 Pt 2), H2168–H2182.

Winther, A.-M. L., Liu, H., Sonntag, Y., Olesen, C., le Maire, M., Soehoel, H., Olsen, C.-E., Christensen, S. B. g., Nissen, P., & Mø ller, J. V. (2010). Critical roles of hydrophobicity and orientation of side chains for inactivation of sarcoplasmic reticulum Ca2+-ATPase with thapsigargin and thapsigargin analogs. *The Journal of biological chemistry*, 285(37), 28883–92.

Witherden, D. a., Verdino, P., Rieder, S. E., Garijo, O., Mills, R. E., Teyton, L., Fischer, W. H., Wilson, I. a., & Havran, W. L. (2010). The junctional adhesion molecule JAML is a costimulatory receptor for epithelial gammadelta T cell activation. *Science (New York, N.Y.)*, 329(5996), 1205–10.

Wolska, B. M., Stojanovic, M. O., Luo, W., Kranias, E. G., & Solaro, R. J. (1996). Effect of ablation of phospholamban on dynamics of cardiac myocyte contraction and intracellular Ca2+. *The American journal of physiology*, 271(1 Pt 1), C391–7.

Xu, C., Ma, H., Inesi, G., Al-Shawi, M. K., & Toyoshima, C. (2004). Specific structural requirements for the inhibitory effect of thapsigargin on the Ca2+ ATPase SERCA. *The Journal of biological chemistry*, 279(17), 17973–9.

Yao, a., Su, Z., Nonaka, a., Zubair, I., Lu, L., Philipson, K. D., Bridge, J. H. B., & Barry, W. H. (1998). Effects of Overexpression of the Na+-Ca2+ Exchanger on [Ca2+]i Transients in Murine Ventricular Myocytes. *Circulation Research*, 82(6), 657–665.

Yasui, K., Liu, W., Opthof, T., Kada, K., Lee, J.-k., Kamiya, K., & Kodama, I. (2001). I f Current and Spontaneous Activity in Mouse Embryonic Ventricular Myocytes. *Circulation research*, 88, 536–542.

Yu, Z. W. & Quinn, P. J. (1994). Dimethyl sulphoxide: a review of its applications in cell biology. *Bioscience reports*, 14(6), 259–281.

Yuen, S., Smith, J., Caruso, L., Balan, M., & Opavsky, M. A. (2011). The coxsackie-adenovirus receptor induces an inflammatory cardiomyopathy independent of viral infection. *Journal of molecular and cellular cardiology*, 50(5), 826–40.

Zaccolo, M. & Pozzan, T. (2002). Discrete microdomains with high concentration of cAMP in stimulated rat neonatal cardiac myocytes. *Science (New York, N.Y.)*, 295(5560), 1711–5.

Zemljic-Harpf, A. E., Miller, J. C., Henderson, S. a., Wright, A. T., Manso, A. M., Elsherif, L., Dalton, N. D., Thor, A. K., Perkins, G. a., McCulloch, A. D., & Ross, R. S. (2007). Cardiac-myocyte-specific excision of the vinculin gene disrupts cellular junctions, causing sudden death or dilated cardiomyopathy. *Molecular and cellular biology*, 27(21), 7522–7537.

Zorzato, F., Fujii, J., Otsu, K., Phillips, M., Green, N. M., & MacLennan, D. H. (1990). Molecular cloning of cDNA encoding the Ca2+ release channel (ryanodine receptor) of rabbit cardiac muscle sarcoplasmic reticulum. *The Journal of biological chemistry*, 265(4), 2244–2256.

Acknowledgement

First and foremost, I would like to thank Prof. Dr. Fritz G. Rathjen for giving me, as a chemist, the chance to work in his group and to give me the opportunity to do my PhD in Biology during this time. Further I would like to thank him for his support and suggestions within the project.

I also would like to thank Prof. Dr. Michael Gotthardt for agreeing to be the second reviewer of my PhD thesis.

I am deeply grateful for the supervision by Dr. Rene Jüttner. Special thanks for all the support, suggestions, discussions and great ideas during the experimental procedures and the analysis of the results.

Further, I would like to thank Dr. Marcus Semtner for providing and helping me with the analysis software IgorPro.

Very special thanks also to Karola Bach and Mrs. Falcke for their competent work in the animal facility and their great help during the mouse breedings.

To my colleagues Florian and Philip - thank you for all the coffee breaks, jokes, support and encouragements, talks and discussions about science and the many non-scientific topics. I also want to deeply thank all other members of the Rathjen lab. Especially Anne, Mechthild and Madlen thank you for your help, support and suggestions during the lab work (particularly for my beloved western blots). Thank you Gohar, Hanna, Laura, Alex and Hannes for your help, encouragements and support.

Furthermore, I thank my friends for all the very needed and funny distractions, their patience to listen to my animal breeding problems and their support.

Last but not least, I am very grateful for all the help, support and love from my parents and sisters. They gave me great opportunities during my life to discover new places and things and to become the person who I am now.

Extreme love to Kay - thank you for everything.

Curriculum vitae

For reasons of data protection, the curriculum vitae is not included in the online version.

Eidesstattliche Erklärung

Hiermit erkläre ich, Christina Claudia Matthäus, dass die von mir vorgelegte Dissertation von mir selbstständig angefertigt wurde. Verwendete Hilfsmittel und Literatur wurden vollständig angegeben. Diese Dissertation wurde noch keiner anderen Fakultät oder Universität zur Prüfung vorgelegt. Die diesem Promotionsverfahren zu Grunde liegende Promotionsordnung habe ich zur Kenntnis genommen.

Berlin, den 29.09.2015